USE OF MEASUREMENT WHILE DRILLING TECHNIQUES FOR IMPROVED ROCK MASS CHARACTERIZATION IN OPEN-PIT MINES

by

Mohammad Babaei Khorzoughi

B.Sc., Sharif University of Technology, 2011

A THESIS SUBMITTED IN PARTIAL FULLFILEMT OF
THE REQUIRMENTS FOR THE DEGREE OF

MASTER OF APPLIED SCIENCE

in

The Faculty of Graduate Studies

(Mining Engineering)

UNIVERSITY OF BRITISH COLUMBIA
(Vancouver)

April 2013

Abstract

Rock mass properties for a mining area are generally determined based on information obtained from the ore-body model (based on exploration data), visual observations in combination with other indices obtained from physical sample testing or geophysical logging. One of these indices is the blastability index. Blastability is generally dependent upon the geological and geomechanical properties of a rock mass in terms of such factors as intact strength as well as the degree and extent of fractures. Accurate determination of the blastability is a critical element that can be used for mine planning towards achieving higher loading and hauling efficiency through more optimal fragmentation. Based on previous works, a reasonable estimate of the rock mass blastability has been shown to be derived from the performance monitoring of blasthole drills using tricone bits. The current work aims to build upon the previous efforts through the creation of a comprehensive model and approach that can predict a range of blastability results for a broad array of variables such as: operating conditions, structural features, etc.

More specifically, the research will evaluate and enhance an Alpha Blastability Index Algorithm (Compensated Blastability Index) originally defined by a mining technology company (Peck Tech Consulting Ltd.) in 2008. This Alpha CBI algorithm was never fully tested, validated nor verified in terms of its ability to consistently and repeatedly generate accurate blastability data. The Alpha CBI algorithm was based on Measurement While Drilling (MWD) data and an associated suite of geophysical logs for the same blastholes during comprehensive field studies in an open-pit copper operation in British Columbia, Canada.

The improved Alpha CBI algorithm that results from the current research has been designed to use drill monitored data to generate improved blastability indices that provide more detailed information on in-situ rock mass properties than the previous approach. It accomplishes this by

an enhanced ability to identify zones of fractured rock and subsequently compensating for their presence. The resulting blastability indices thus derived through this new method have been shown to more closely reflect the true in-situ rock mass conditions as validated when correlated to the geophysical logs.

Preface

This thesis is submitted in partial fulfillment of the requirements for the degree of Master of Applied Science (MASc) at University of British Columbia. The research described herein was conducted under supervision of Dr.Hall in the department of mining engineering.

The MWD data, geophysical logs and core tests referenced in this work were outcomes of work that was undertaken by Peck Tech Consulting Ltd. in 2008 on behalf of Teck Metals. In addition, a preliminary version of the CBI algorithm referenced within the present study was provided by Peck Tech Consulting Ltd. as part of the same project with Teck Metals.

The CBI Algorithm presented at this research was coded by author. Current work includes evaluating Alpha CBI Algorithm, processing the MWD data, revising proposed approach for detecting fracture and interpreting geophysical logs to provide a baseline for validating the results.

Table of Contents

List of Tables

List of Figures

Nomenclature

ANFO	Ammonium Nitrate-Fuel Oil
BI	Blastability Index
CBI	Compensated Blastability Index
DMS	Drill Management System
DT	Transit Time
DTH	Down The Hole Hammer
FMI	Formation Micro Image
FRF	Fracture Reduction Factor
GPS	Global Positioning System
GR	Gamma Ray
HCP	Hoist/Pulldown Motor
HVC	Highland Valley Copper Mine
LWD	Logging While Drilling
MWD	Measurement While Drilling
OF	Open Fracture
PLC	Programmable Logic Controller
POF	Partially Open Fracture
RCP	Rotary Motor
RQD	Rock Quality Designation
RMR	Rock Mass Rating
ROP	Rate of penetration

RQI	Rock Quality Index
SE	Specific Energy
SP	Sonic Porosity
SV	Sonic Velocity
WOB	Weight on bit

Acknowledgments

This research project would not have been possible without the support of many people. The author wishes to express his gratitude to all of them:

My supervisor, Dr. Robert Hall who opened new ways for me, trusted on my abilities and encouraged me throughout my graduate studies. Without his supervision, guidance and support this thesis would not have been possible. I will forever be thankful to him;

Dr. John Meech and Dr. Leslie Smith who kindly accepted to be in my committee. It was a great honor for me. Their time and efforts were greatly appreciated;

Dr. Jonathon Peck, former Head of the Mining Department at Queen's University, for his contributions to my learning experience, his time and his support throughout my research as well as his understanding and kindness. His technical and editorial advice was essential to the completion of this dissertation; Mr. Ted Bronscombe who developed the preliminary version of CBI Algorithm, Highland Valley Copper Mine and Teck ART for their support during the research;

Mr. Chris Lear who without his inputs definitely it was impossible to finish this thesis. Working with him was a great opportunity for me which has made me a much more complete engineer. He has been and continues to be a fantastic mentor. I hope that I could be as hardworking, knowledgeable, enthusiastic, and energetic as Chris. Now it is my ''mission'' to thank him for his support, patience and the time he spent for me.

My Dad who always supported me and showed me that nothing can stop a real man; My Mom who called me every day to just hear my voice and reminded me to take care of myself; My dearest uncle, Iraj, who continuously supported me and didn't let me to feel that I am not at

home; Dr. Anoush Ebrahimi who has been and continues to be a mentor from the beginning, and always encouraged.

Last, but certainly not least, my lovely wife, who endured me and encouraged me throughout my graduate studies. Without her, I never would have made it through my graduate program. She is an angel, and I am so lucky to have her as my wife forever.

Dedication

To Siamak and Behjat, my parents

And

To Shirin, Love of my life forever

1. Introduction

1.1. Problem Definition

Blasting is an inseparable and key component of the mining cycle in an open-pit mine, although there are some scenarios in mining whereby soft rock is present and alternatives to blasting can be efficiently and effectively used, for example, water jet cutting and free digging. However, in the case of hard rock mining, blasting is necessary to break up the material prior to being loaded and hauled away for dumping or processing purposes (Bhalchandra, 2011). A suitable blast design and its proper implementation are both crucial to the economic and technical success of open-pit mining operations. A poor design based on using the wrong type and amount of explosive or improper placement in a blast hole combined with an inefficient timing design can lead to poor results and thus significantly reduce the overall productivity of an operation.

Many factors affect the drill and blast operation efficiency including rock type, strength and density as well as the presence of water and natural discontinuities (i.e. fractures, voids etc.). Thus, the extent and degree of these factors need to be properly considered when developing the blast design for a particular mining area. Through a detailed understanding of the in-situ rock mass characteristics of the bench to be blasted, an optimal fragmentation and acceptable amount of material movement can be achieved. The combined impact of such outcomes is more efficient excavation as well as lower dilution of the ore and waste products to potentially result in higher productivity and lower cost per tonne.

Rock mass properties for the purposes of drilling and blasting activities are generally derived from a variety of sources including the ore-body model as well as field observations and sampling and testing based classifications. The basic definition of the Blastability Index (BI) is that it is a measure of how economical and easy it is to fragment a rock mass. In this manner, it is considered an important index for use in estimating the degree of blast energy that is needed to properly fragment a particular rock mass (Bhalchandra, 2011; Liu and Yin, 2001; Mozaffari, 2007; Dey and Sey, 2003).

Over the past 30 years, several methods with different accuracy, cost and characterizations have been developed for obtaining rock mass properties or in broader view geological information for both mining as well as oil and gas applications. Geophysical surveys, geochemistry surveys, drill core, measurements while drilling (MWD) along with computer based data processing, manipulation and visualization are the most commonly used methods for geological exploration.

Physical properties of rock through laboratory test as well as fracture frequency can be derived from drill cores. For economic and efficiency reasons, drill cores have limitations as they are generally few in number over large areas due to the expense and their interpretation can be highly subjective depending on the skills and experience of the personnel conducting the survey. On the other hand, geophysical logs can be taken in both core holes and production blastholes to provide a wide variety of in-situ geological information including the presence of discontinuities (fractures). However particular geophysical logs (e.g. the FMI log) are highly costly to obtain and thus cannot be used frequently or in routine production practice at most sites. As a result, researchers have attempted to develop new ways to regularly and rapidly obtain geological and geomechanical information with minimal additional cost or effort. One such method that has been demonstrated to provide meaningful and repeatable results related to rock mass characterization has been through the use of Measurements While Drilling (MWD) systems (Scoble et.al., 1989; Kadkhodaei-Ilkchi et.al., 2010; Schunnesson, 1998)

MWD is a technique that has been extensively developed and directly used routinely in open-pit mining production drilling as well as oil and gas deep well drilling over the past 20+ years. This method is used to record signals from sensors installed on the drilling machines whereby the converted data in terms of physical units can be used to guide the drilling operation through either manual or automated (controlled) means. The derived data can be displayed locally or remotely in real-time or stored on a central computer for further optimization, evaluation, and prediction of the variation in geology or geotechnical properties of rock mass being drilled. Since drilling is used in different stages of mining, using MWD can be a considerable tool for improving economics by reducing exploratory core drilling and geophysical logs. As well as leading to optimum fragmentation based on the ground characterization using MWD.

The context of this research is focused only on blasthole drilling in open-pit mining using large electrically powered drills. Based on a data acquisition system that was deployed on several blasthole drills, the drill variables of penetration rate, rotary torque, rotary speed, weight on bit, bailing air pressure and vibrations were acquired during field studies conducted in 2008 at an open-pit copper in British Columbia, Canada. In parallel to the drill data obtained from the monitoring of multiple blastholes at this site, several cored holes were also drilled in the same vicinity. The blastholes were subsequently logged by Schlumberger using a comprehensive suite of geophysical logs to provide a detailed assessment of the presence of natural fractures from which the new Blastability Index could be validated. Section 1.2 briefly discusses the specific objectives of this thesis.

1.2. Research Objectives

As discussed in section 1.1, having a good knowledge of the in-situ rock mass characteristics is a key factor that determines a successful drill and blast operation. Among in-situ rock mass properties, the presence of fractured zones has a noticeable influence not only on the quality and efficiency of drilling but also on generating an optimal muckpile fragmentation.

As previously mentioned several studies have been conducted that have clearly shown the influence of fractures on blasting and drilling quality. In addition, many studies have also indicated that MWD systems on blasthole drills can be used to routinely, quickly and accurately detect fracture zones within a blast pattern. Thus, the goal of the current study is to further build upon these outcomes to further support the use of MWD systems to detect fractures(natural or blast induced fractures.

Towards this objective, the research investigates the correlation between acquired MWD data and known fracture zones detected by geophysical logs to establish an enhanced approach to directly highlight such features within a blasthole. The research leverages previously collected blasthole drill, core and geophysical data from the Teck Highland Valley Copper Mine (HVC) in 2008. The work also analyzes the logic and premise underlying an Alpha algorithm defined by Peck Tech Consulting Ltd. as a result of this 2008 field study. The result of the current analysis is the definition, testing, validation and verification of a new algorithm to calculate compensated BI (or CBI) indices based on drill monitoring data when fractures are present. The proposed CBI approach is intended for use as part of a post processing tool that takes data acquired from the monitoring of blasthole drills to generate CBI values on a per blasthole and bench basis. The intent is that the new CBI indices thus determined through this process will lead to more efficient explosives loading designs resulting in improved fragmentation and consequently a reduction in the overall cost of mining.

1.3. Thesis Structure

A literature review composed of the different aspects of drilling and blasting is presented in Chapter 2. Chapter 3 discusses the methodology that was used in this thesis that consisted of data collection, data pre-processing, derivation of fracture logs, defining the fracture detection approach that was developed as well as results correlation and comparison. Chapter 4 provides an interpretation of the geophysical logs and their correlation to the responses from the MWD data in terms of fractures is investigated. In addition, this chapter verify and validates the developed Alpha CBI algorithm through a comparison to the interpreted geophysical logs.

In chapter 5, the developed CBI algorithm is discussed and results examined and assessed in terms of the accurate degree of correlation to known geological features at the test site. Finally Chapter 6 presents the conclusion and suggestions for future improvements and research studies that can build upon the outcomes of the current work.

2. Literature Review

The literature review is comprised of two major parts that focus on (1) an examination of drilling and blast operations in open-pit mines and (2) followed by further investigation of various technical aspects related to blasthole drilling in the mining industry.

2.1. Blasting

Blasting is the economical method of primary rock fragmentation (Bhalchandra, 2011). Rock is drilled in different patterns based on pre-blasting assessments then the holes are filled with explosives (charging) and finally the explosives are detonated. This detonation releases extremely high pressure and a large quantity of heat into the surrounding rock mass, which is referred to as detonation pressure or shock energy. The pressure caused by the released gases from the explosive detonation breaks apart the rock mass through expansion under containment by following fractures (natural and/or induced).

Towards developing an effective blast design, the rock mass characteristics are determined through previous drilling records, geophysical logs and geological surveys. Thus, the concept of a blast domain can be defined as a region where in encountering with blasting the entire region behaves similarly (Mohanty, 1996).

The objective of blasting is to break the in-situ rock mass into appropriate fragment sizes and looseness[1] to facilitate material loading and haulage to various destinations (waste or processing). Depending on the blast design, blasting can also create other less desirable outcomes such as ground vibrations, back break, mis-fire, fly rock and air blasts. The minimization of these outcomes is a key objective of correctly designing a blast for a particular rock mass with specific geological and geomechanical characteristics.

[1] A measure of how much the muck has bulked up volumetrically (air voids) and ease of digging (digability);

The optimization between the various blast design parameters such as burden, spacing, bench height and sub-drilling is necessary to effectively and efficiently distribute the explosive energy across the pattern to break the rock. An important consideration in designing a blast is the powder factor defined as the amount of explosive required to break a unit volume of rock as in the equation below.

$$PF=\frac{Charge\ amount}{Volume\ of\ rock\ blasted}\ \frac{1}{\rho} \quad \text{(Liu and Yin, 2001)} \qquad \textbf{(2.1)}$$

Where **ρ** is density of rock. In the mining industry the most common explosive is Ammonium Nitrate-Fuel Oil (ANFO).

The powder factor can serve as a relative indicator of the required explosive strength and related cost as well as rock hardness. Powder factor directly influences rock fragmentation since if the amount of explosive used in the blasthole is not optimized, the fragmentation will have a size distribution less or more than the desired (optimal). To account for these factors, the term optimum powder factor is introduced as the powder factor required to deliver optimum fragmentation while also minimizing the effects of ground vibration, air blast, fly rock as well as cost. Optimum powder factor is thus closely related to rock blastability.

In section 2.2.1 the rock fragmentation is discussed as an important factor in both operation and planning activities in open-pit mining.

2.1.1. Rock Fragmentation

The main objective of blasting is to create small enough fragments that can be easily excavated and removed from the blasting site. In ore extraction, the size distribution of fragmented rock after each blasting cycle is an important parameter affecting the performance and efficiency of downstream loading, hauling and crushing processes. Overall Mine to Mill (M2M) fragmentation is composed of drilling, blasting, loading, hauling, primary crushing, secondary crushing and grinding stages (Atlas Copco, 2009). The central premise behind M2M is that energy used to fragment the rock is examined at various stages across the operation with the goal of being able to ensure the optimal particle size for processing. Based on having feedback from each stage, changes can be made at different stages such as the blast pattern including timing and explosive designs (type, charging, stemming length, blasthole depth etc.) (Atlas Copco, 2009). The M2M concept clearly connects the parameters of drillability (ease of drilling), blastability and grindability (ease of grinding) as well as their importance in ensuring optimal fragmentation and thus mine to mill optimization.

Since the 1980's, several models such as Kuz-Ram have been used to predict the fragmentation of rock mass due to blasting. However, image analysis techniques are a widely used method to rapidly calculate the size distribution of fragmentized rock mass (Mozaffari, 2007). Mozaffari (2007) showed that for a selected bench there is a significant correlation between measured penetration rate (drilling performance and possibly "drillability") and monitored rock fragmentation based on image analysis results. These results further demonstrate that the data acquired from an MWD system can be used as a reliable indicator of fragmentation, which in turn can lead to a more efficient mining operation.

2.1.1.1. In-Situ Rock Mass Properties and Fragmentation

One of the most important features of rock mass is the presence of structural discontinuities such as fractures (joints, faults) and bedding planes. Faults and joints are naturally formed discontinuity planes in a rock mass based on its geological and structural origins[2]. These

[2] As far as blasting is concerned in large surface mining there is little difference between faults and joints as both will impact the blast results (Bhalchandra, 2011). Thus, for the purposes of this work they are referred to as fractures;

discontinuities can be local or regional in terms of their presence and extent within a rock mass. The spacing (distance between joint planes) can also vary significantly within a particular rock mass. The filling within a discontinuity can be solid and closed (sealed) of varying mineralogical composition or filled with unconsolidated material due to the effects of water ingress as well as weathering that occurs along these surfaces. They can also be open allowing for the flow of water as well as dissolved materials to be present.

The effect of these discontinuities on the blasting outcomes depends on their density, continuity, type (open, partially open or closed) and their spatial orientation. In blasting, the fragmentation process of a rock mass is initiated by setting off the explosive within the blasthole. This process results in the generation of high pressure/high temperature gases that propagate (follows the path of least resistance) laterally and vertically (depends on stemming) from the blasthole. Depending on the extent and nature of the rock mass, this energy will follow structural discontinuities like faults, joints, etc. that are in close proximity to or intersect the blasthole. Depending on how the energy is channelled and dissipated into the area around a blasthole, the presence of discontinuities can directly impact the resulting fragment size distribution. Most of the fracturing due to the blast energy occurs along these discontinuities rather than within the intact rock mass due their lower strength. Thus, a good and efficient blast design is aimed at taking full advantage of these pre-existing discontinuities to break the rock mass down rather than through the use of excessive explosives.

For example large open fractures parallel to the borehole can result in more extreme fragmentation of a rock mass in the vicinity of the blasthole due to the reflection of the blast shock wave before it reaches a free surface (Leighton, 1982). In contrast, partially open fractures may be too thin to reflect the shock wave.

The fracture density over the borehole length (or joint spacing) is an important factor that also affects blast quality. Fracture density is defined as the number of fractures per unit length which is given by:

$$fracture\ density = \frac{Number\ of\ fractures}{L} \tag{2.2}$$

Where L is the length. A high fracture density can cause a hard rock formation to behave like a weaker zone. Therefore, by knowing the fracture density over the target bench, better decisions regarding the explosive design can be made.

All these characteristics have a direct influence and thus impact on the blast quality for a particular rock mass. For example, a blast design with uniform borehole spacing will result in a wide ranging fragmentation size distribution when the joint characteristics vary significantly over the bench. As a result, there will be a higher cost for loading, haulage, crushing and grinding activities due to a larger fragmentation distribution (Branscombe, 2010). This situation further demonstrates the value of identifying and accommodating the presence of fractures in any blast design such that it more accurately reflects the true nature of the rock mass.

Over the past 30 years, numerous researchers have attempted to establish a definitive relationship between the rock mass properties and blasting results (Fraenkel, 1954; Hino, 1959; Lilly, 1986; Azimi et.al., 2010). Based on the observed results of blasting, these researchers defined a Blastability Index or BI. The BI is an important factor which appears in the Kuz-Ram equation and has been demonstrated to vary based on the in-situ rock mass properties. Section 2.1.2 provides a more detailed discussion on BI.

2.1.2. Blastability Index (BI)

As previously stated, the efficiency of the blasting process in an open-pit mine heavily depends on the rock mass properties. Rock mass properties are introduced through different types of classification based on different factors (Bhalchandra, 2011). These classifications are based on visual observations as well as physical characteristics and represented by a variety of different indices.

Researchers have attempted to develop different classifications and indices that provide a definitive means of readily categorizing a unit rock mass. Classifications schemes such as the Rock Quality Designation or RQD (Deere, 1963), Rock Mass Rating or RMR (Bieniawski, 1973) and Rock Tunnel Quality Index (Barton et.al., 1974) have been used extensively within the civil and mining engineering fields. However, the vast majority of these classification schemes were primarily developed for geotechnical purposes related to slope, foundation or tunneling design. Therefore, in terms of their relevance to surface open pits, these classifications are useful for estimating drilling performance but have little value for the evaluation of rock blastability for blast design purposes (Dey and Sen, 2003). Thus, as a means to provide a rock mass blastability classification specifically for open pit mines, the BI concept was introduced.

As previously discussed there is a close relationship between powder factor and BI which can be used to determine the amount of explosive. Several researchers have attempted to estimate BI based on laboratory tests of rock, blast design parameters, drilling records and pattern recognition and data processing methods such as fuzzy logic and artificial neural networks (Fraenkel, 1954; Lilly, 1986; Feng, 1995; Yin and Lui, 2001; Azimi et.al., 2010). In the current work, BI models are divided in two categories: geotechnical based BI and drilling based BI. It should be noted that BI derived from drill MWD provides an alternate rating and does not require technical staff to physically inspect bench walls or undertake classification ratings. Thus, only drilling based definitions will be explicitly described. Sections 2.1.2.1 and 2.1.2.2 present a summary of developed BI models.

2.1.2.1. Geotechnical based BI definitions

Fraenkel (1954) proposed an empirical equation for blastability based on height and diameter of the charge, hole depth and maximum burden. Hino (1959) subsequently introduced a blastability coefficient equal to the ratio of compressive over tensile strength of rock. Hansen (1968) developed an equation for direct calculation of explosive amount based on the burden, free face height and a rock constant to be estimated by tests. An empirical equation for powder factor was proposed by Ashby (1982) based on fracture frequency as density of fracturing and friction angle as joint shear strength. Lilly (1986) proposed an equation for BI based on a variety of parameters related to the site conditions including joint orientation, joint density, rock hardness and density. The index thus derived related powder factor and required energy by a site specific equation. Feng (1995) established a neural network approach for comprehensive classification of rock stability, blastability and drillability. Azimi et.al. (2010) used fuzzy sets to predict the blastability designation of rock masses.

2.1.2.2. Drilling based BI definitions

Leighton (1982) developed a correlation between rotary drill performance and powder factor based on empirical field based studies conducted in a copper open-pit mine in British Columbia. He proposed the following equation between rock quality index (RQI) and powder factor for a BE40R blasthole drill using tricone rock bits:

$$\ln(powder\ factor) = \frac{RQI-24.9}{7.1} \tag{2.3}$$

Where powder factor is in kg/tonne and RQI in MPa. min/meter. To enable a measurement of RQI he used drilling data in the following equation:

$$RQI = \frac{Weight\ on\ the\ Bit(WOB)}{Rate\ of\ Penetration} \tag{2.4}$$

Leighton (1982) clarified that the main problems associated with this approach was that the RQI values were not a good representative of rock masses and the approach was tested only for one type of drill.

Lopez (1995) combined rate of penetration, pulldown force, rotary speed and drilling diameter to eliminate RQI limitations and introduced a rock characterization index (Ip) as follows:

$$I_P = \frac{Rate\ of\ Penetration}{\frac{Pulldown\ Force \times Rotary\ Speed}{Drilling\ Diameter^2}} \tag{2.5}$$

He made the observation that since the rate of penetration depended upon the geomechanical properties of rock mass, I_p has a close relationship with the rock strength. Therefore Lopez (1995) was able to demonstrate that I_p can be correlated with powder factor in the following manner based on data he collected and analyzed from numerous mines:

$$Powder\ factor\left(\frac{Kg\ ANFO}{m3}\right) = 1.124 \times e^{-0.5727Ip} \tag{2.6}$$

Yin and Lui (2001) also used information extracted from monitored drill data to estimate rock blastability. They introduced a revised Rock Quality Index or RQI as a measure of blastability and defined it as the amount of force required per unit penetration rate in drilling. Using dimensional analysis and defining two groups of dimensionless parameters consisting of rate of penetration (u) in m/s, Pulldown force (F) in N, torque (T) in N.m and rotary speed (N) in 1/s, they proposed the following equation for RQI:

$$RQI = \frac{1}{a}\frac{u^{\frac{1}{n}}F^{2+\frac{1}{n}}}{(NT)^{1+\frac{1}{n}}} \qquad \textbf{(2.7)}$$

Where a and n are constant parameters that are calculated based on a set of restricted assumptions rather than a rigorous mathematical driven approach.

At the Phelps Dodge Sierrita Mine (Phelps Dodge Mining Company et.al., 2002), measurements while drilling were used to find a correlation between BI and bench geology. The data was acquired using Aquila Mining System (now called CAT Terrain™ Drills) installed on their blasthole drills that used tricone rock bits. They also defined the BI as the response of rock to high strain during the blasting. They compared BI and Specific Energy (SE)[3] and concluded that rock recognition and BI does not need to agree. There are many factors that affect this difference. The most common one is the existence of fractures, which can contribute to the differences in BI values along a column of the same rock type. In addition to rock type the presence of fractures was seen to have a crucial role in determining the derived BI values and thus should be taken into account for BI calculation prior to use for short range planning.

Mozaffari (2007) studied the data derived from Aquila Mining System MWD systems at the BOLIDEN Aitik mine in Sweden. He showed that there was a correlation between the BI values automatically generated by MWD and the Specific Energy (SE). He concluded that the formula used by the Aquila system to calculate BI is similar to the specific energy.

To further investigate the influence of fractures on generating a more prescriptive BI value, a project was initiated between Teck Metals and Peck Tech Consulting Ltd. in 2008 at the Highland Valley Copper (HVC) mine near Kamloops, British Columbia. During this project a

[3] Specific Energy is the energy required to excavate a unit volume of rock which will be discussed at section 2.2.2.1;

preliminary algorithm was defined by Peck Tech to calculate a new BI value that accounted for the presence of fractures.

The field studies conducted in 2008 resulted in the collection of a vast set of data acquired from monitoring instrumented Bucyrus 49-RIII and 49-HR blasthole drills using tricone bits. The drill data was then correlated to known geological and geotechnical rock properties as derived from geophysical logs taken in the same blastholes (Peck Tech, 2009). In addition, several core holes were drilled in the vicinity of the monitored blastholes for the collection of samples for subsequent laboratory testing. Based on a thorough analysis of the data from all sources, a preliminary algorithm was defined called the Alpha Compensated Blastability Index or CBI. This algorithm had the apparent ability to compensate the standard blastability index as derived from the specific energy calculation based on the presence of fractures.

The proposed algorithm was based on an empirically derived approach to detect the presence of fractures in the blasthole while drilling. In this approach two groups of parameters have been introduced which are as follow:

$$WORON = \frac{WOB}{\left(\frac{ROP}{Rotary\ Speed}\right)} \tag{2.8}$$

$$WOSE = \frac{WORON}{SE \times D} \tag{2.9}$$

Where D is bit diameter. WORON is the monitored weight on the bit (WOB) over penetration rate (ROP) per revolution. WOSE examines the ratio between WORON and SE and is supposed to highlight the location and extent of fractures when plotted against blasthole depth. Based on generated WOSE and SE values, BI data are compensated for the presence of fractures using a new factor called Fracture Reduction Factor (FRF) (Peck Tech, 2009). FRF was defined as a number between 0 and 1. Based on this approach, the following equation for CBI was derived:

$$CBI = FRF \times BI \tag{2.10}$$

If FRF=1 then CBI=BI which means that there are no fractures present. As a result, the value of FRF can be viewed as an indicator of fracture severity (open or partially open or resistive fractures).

Further work within this study (and based on the results from Mozaffari, 2007) showed that due to the direct correlation of BI to SE, the following equation can be derived:

$$BI = \frac{SE}{BInorm} \times 100 \tag{2.11}$$

Where BI_{norm} is a normalization constant to turn SE (in Pa) into a normalized "Rock Hardness" index (typically a value ranging from 0 to 100). The normalization constant should be chosen so that an index 100 represents the hardest rock likely encountered by drilling[4]. BI and CBI are dimensionless numbers.

For the purpose of calculating FRF, a moving average technique was used. Averaging windows of increasing size of 4cm, 20cm, 100cm and 500cm were applied to the WOSE signal to produce progressively smoother representations of data. After generating new signals, where the smoother signals pass through granular signals by a pre-set (10% in Alpha Algorithm) amount,

[4] For HVC BI_{norm} is set as 135MPa determined from geotechnical data available at HVC at the time the first Aquila DMS were installed, as being the strongest rock likely to be encountered by the drills(Peck Tech, 2009);

FRF is applied to BI to compensate for the presence of fractures. Furthermore, a fracture log is produced by the sum of the variances between smoothed WOSE signals (Peck Tech, 2009).

Through empirical studies performed over several years at HVC, blastability index values have been correlated to a relative index of whether the rock is good, fair, fair/poor and poor for purpose of describing the ease of blasting which determines the expected blasthole pattern spacing and powder factor requirements. Table 2.1 show this relative index values (Peck Tech, 2009). However there is no correlation between CBI values and blast domains at this time.

Table 2.1, Rock classification at HVC for blasting (Peck Tech, 2009, adapted by permission)

Blast Domain	BI range
good	Less than 35
fair	35-50
fair/poor	50-70
poor	Greater than 70

Therefore, the derived approach first determines the locations of fractures and then compensates or reduces the BI values when fractures are present. Although geophysical logs (more specifically the Fracture Micro-Imager or FMI log) were obtained at the same time to assist in verifying the method, the results from their correlation were inconclusive. Thus, further effort was required to fully assess and validate the reliability and accuracy of the developed approach. As a result, this thesis is aimed at verifying, validating as well as improving on the outcomes of this previous work.

The review provided in this section shows the feasibility and viability of using MWD for defining a comprehensive and reliable BI index in open-pit mines. However the determination of a reliable and consistent BI value based on MWD data that can also contend with different operational, geological and geomechanical conditions is still to be achieved. Section 2.2 presents a summary of the typical blasthole drilling process for open-pit mines as well as an overview of the different MWD systems commonly used.

2.2. Drilling

Drilling is used extensively in a variety of applications to investigate the subsurface rock mass conditions, including geotechnical surveys, civil and construction projects, underground and open-pit mining as well as in all aspects of the oil and gas industry. Drilling in the mining industry is done during exploration, production and mine development for the following purposes (Australian Drilling Industry Training Committee Ltd., 1997):

- Exploration
- Stratigraphic information
- Seismic surveying
- Gravity, magnetic or geochemical survey
- Grade Control
- Reserve estimation
- Blasthole Drilling

In open-pit mining operations, there are several types of drilling which are commonly used:

- Rotary Drilling
- Percussion Drilling
- Rotary Percussion Drilling

Rotary drilling is used in surface mining and rotary percussion is widely used in underground drilling as well as for some special applications in surface mining (Lucifora, 2012).

As previously mentioned when the rock mass is very competent with few naturally occurring discontinuities and direct (free digging) excavation is thus difficult, blasting is the most efficient fragmentation approach to be used in such instances (Bhalchandra, 2011). Blasthole drilling using either tricone bits or down the hole hammers (DTH) are used to drill vertical and inclined holes for the placement of explosives. Once the explosives are detonated in a controlled manner, the fragmented rocks are subsequently excavated for processing and/or disposal (as waste). This thesis only deals with rotary blasthole drilling using tricone bits and for vertical blastholes in an open pit mining operation. However, some of the developed results could be applied to other forms of drilling.

2.2.1. Rotary Blasthole Drilling

Rotary blasthole drilling is a very flexible method which can be used in excavation of a wide range of rocks such as coal, copper and iron. In addition to rock hardness (rock type), hole diameter is an important parameter to select a suitable type of drill. Rotary blasthole drilling is the dominant way of drilling 230mm (9in) diameter or more (Atlas Copco, 2009).

In rotary drilling the generated energy which breaks the rock is a combination of rotary force (torque that induces the generation of spalling due to tensile failure along developed fracture surfaces) and thrust (feed force/pulldown that aids in coupling the bit to the rock interface and thus inducing material failure due to crushing or compressive failure mechanisms). For example, when an axial force due to the pulldown pressure is exerted on a tricone bit, the tungsten-carbide inserts in the rotating cones penetrate into the rock. Due to the rotation of the bit, the inserts induce further crushing and scraping actions that create cuttings. These cuttings are then removed by air or fluid that is circulated through the central bore of the drill string components under high pressure (bailing pressure). It should be realized that axial force (WOB) applied through the bit to the rock face does not really cause the bit to move any distance. It is only the action of rotation that breaks the chips out and clears the way for the bit to move forward.

The rotation, pulldown and bailing air are transmitted to the rock interface at the bottom of a hole via a drill string that is composed of lengths of steel as well as shock absorbers (subs) that help to maintain efficient energy transmission. The drill bit at the end of the drill string is the major element that is used for the transfer of energy into the rock. There are several types of commonly used drilling methods and associated bits in open-pit mining such as DTH or down the hole hammers and tricone rotary. Tricone bits are the most common bits used in rotary blasthole drilling due to their ability to work across a wide range of rock mass conditions. Tricone bits have three cones with different shapes and spacing of tungsten-carbide inserts as determined by the rock properties (compressive strength) they are required to drill. These cones are usually made from hardened (tempered) steel and further enhanced for durability by rows of tungsten carbide buttons at areas of high wear.

Over the past 30+ years, blasthole drills in open-pit mines have been instrumented with monitoring systems to record performance variables for use in both real time and post processed applications. These applications have included detailed analysis of drilling performance and productivity as well as for rock recognition for use in blast design.

2.2.2. Measurements While Drilling

Measurement While Drilling (MWD) is a technique which aims to obtain data during drilling to increase available rock properties and rock mass characterizations in a real time basis. It is also known as Logging While Drilling (LWD) in the oil and gas industry. The most significant feature of MWD is to achieve such information more quickly and cheaply and in some cases more accurately in a real time basis than alternative approaches such as core tests and geophysical logging. This can increase the efficiency of operations and improve the reliability of short range planning since decisions affecting the efficiency of mining depend on the real time access to operations, geological information and other data.

Since the 1980's, a variety of drill monitoring systems have been developed. In the mining industry companies such as Aquila Mining Systems, Modular Mining, Thunderbird Mining Systems and others have supplied drill monitoring systems to the open-pit mining industry (Mozaffari, 2007). These systems include an on-board computer and operator interface which collects and processes a large amount of data in real time that help to manage as well as control the drill. Time, depth, pulldown, rate of penetration, rotary speed, and torque are the typical recorded MWD parameters. In addition, other parameters such as vertical and horizontal vibration, bailing pressure, flow rate are also recorded.

For these monitoring systems, some main challenges and limitations are their capabilities regarding recording frequency and data quality as well as on-line or post-processed algorithms to generate accurate information on rock strength, rock drillability and blastability, fracture zones, etc. down the hole. In more recent years, some of these companies have sought to overcome some of these limitations to improve the quality and reliability of the rock mass information that can be obtained from their on-machine systems.

2.2.2.1. Specific Energy

Teale (1965) introduced the concept of specific energy (SE) as the energy required to excavate a unit volume of rock using a tricone rock bit. He developed this parameter using mechanical variables measured from drills being used for oil well development. The intent was to define a parameter that reflected the downhole efficiency of the drilling processes. Based on SE calculations, adjustments to the drilling could be made to improve performance through better energy generation and transmission at the bit-rock interface. Based on his investigations, it was apparent that calculated SE was seen to be highly dependent on the nature of the rock mass. He also observed that under real drilling conditions, the amount of theoretical versus actual SE values were not the same whereby the difference was due to energy loss. This energy loss was seen in other studies to be due to component wear (bit, steel, bushing), cuttings regrinding as well as mechanical loss at the bit-rock interface and along the blasthole walls (Phelps Dodge Mining Company et.al. 2002). These losses depend on parameters such as bailing velocity, rock structure such as fractures, rotary speed, component quality and drill design.

For tricone rock drilling, the energy developed at the bit-rock interface is a function of the applied thrust (pulldown) and torque due to rotation. Where thrust is F (N), torque T (Nm), rotation speed N (rpm), the area of bit A (m^2) and the penetration rate μ(m/min), the SE is calculated (in Pa) by the following equation:

$$SE = \left(\frac{F}{A}\right) + \left(\frac{2\pi}{A}\right)\left(\frac{NT}{\mu}\right) \quad \text{(Teale, 1965)} \qquad \textbf{(2.12)}$$

The above equation can be divided into the following components:

$$SE_A = \left(\frac{F}{A}\right) \text{ - (thrust, axial or feed)} \qquad \textbf{(2.13)}$$

$$SE_R = \left(\frac{2\pi}{A}\right)\left(\frac{NT}{\mu}\right) \text{ - (rotary component)} \qquad \textbf{(2.14)}$$

As shown, SE has the same units as the rock strength i.e. Pascals or Pa. Therefore it can be concluded that calculated SE values can provide a representative reflection of rock strength[5]. It has also been shown that calculated SE is affected by variation in rock properties (intact strength & degree and extent of fractures), drill efficiency and bit wear. Section 2.2.2.2 provides further discussions of such observations.

2.2.2.2. MWD Response to Rock Mass Properties

The drill measurement monitoring undertaken by Leighton (1982) enabled improved blast design based on the use of rate of penetration peaks to identify weak zones in a rock mass. Lutz (1982) showed that the width of measured penetration rate peaks while drilling shallow geotechnical holes were a direct measure of fracture aperture. He recorded penetration rate as a function of depth to enable the correlation between logs from different holes at the same scale to validate this observation. Scoble & Peck (1987) derived the location of fractures based on instantaneous penetration rate responses monitored from small percussive drills in a limestone quarry. These data were then depth correlated to results generated from both a borehole camera and core log. It was shown that 90 percent of fractures detected by the borehole camera were compatible with located fractures by defined peaks on logs of penetration rate to depth (Scoble and Peck, 1987)

Schunnesson (1996) did a site investigation using an MWD system on a percussive drill to accurately record structural features surrounding a railway tunnel construction in northern Sweden. Based on the collected data, he interpreted the drill performance parameter variations to identify the presence of fracture zones as an input for RQD prediction. The presence of fracture zones had been previously determined as the baseline for the correlation he conducted. His results showed that rate of penetration and rotary pressure (torque)/RPM are highly influenced

[5] In this thesis, any reference to SE implies the value determined by Teale (1965);

by fractures. Typically ROP increases when encountering a fracture and exhibits a high degree of variability when drilling through extensively fractured areas. However there is a situation where the rate of penetration decreases with an increase in torque (Schunnesson, 1996).

The increase in torque can be rationalized due to the tendency of the bit to stall under such broken rock mass conditions. Rotary speed (RPM) shows the same response as torque. This result is to be expected given that torque is dependent on rotary speed as well as the material properties being drilled as well as the bit type and condition (Schunnesson, 1996).

There is another type of response of these parameters to the presence of fractures in which when drilling in the middle of the fracture zones the rate of penetration as well as torque and rotary speed decrease. Schunnesson suggested this is because the drill string tends to stall in zones that are highly fractured. However in this case the variability in the rate of penetration can act as an indicator of a fracture zone (Schunnesson, 1996).

Schunnesson (1996) concluded both torque and rate of penetration are affected by fractures. However he further stated that a definitive correlation between these variables and fractures is complicated by other site related conditions. Regardless, he concluded that MWD can increase available knowledge about in-situ rock mass properties towards an improved RQD prediction.

Peng et.al. (2005) proposed a method for generating a quantitative void/fracture detection method for use in underground mines. They used a drill control unit from the J.H. Fletcher & Co. to record the drilling variables for the tests performed in the field and laboratory. To clearly understand drill variables response to the presence of fractures they defined some test conditions in the laboratory. Concrete blocks based on different level of fractures (small, medium and large) were constructed and then drilled to record drill variables responses. Then to verify the laboratory test results while drilling in different rocks, underground tests were also conducted.

To determine the criteria to detect fractures, they plotted all the measured variables for each hole (test) and concluded that feed pressure tends to exhibit deep valleys in data plots when encountering fractures. However they found when encountering small voids or fractures, feed pressure did not exhibit similar data plot responses or generated more subtle variations that were difficult to detect. They subsequently defined a complimentary criterion for fracture identification based on the actual shape characteristics of the generated feed pressure data plot responses.

This literature review has demonstrated a good understanding of in-situ rock mass properties is crucial to the success of open pit mining operations. Fractures are also clearly one the most important features of the rock mass affecting the quality and efficiency of the drill and blast operation. Additional techniques such as geophysical logging and core tests are commonly used in some mines to further identify and characterize fractures within the selected bench. However due to economic issues (costs related to instrumentation or sample collection and data analysis) they are used infrequently in mines and only in situations where the geology is unknown or complex. Hence other tools such as MWD on blasthole drills have been demonstrated as a viable means to rapidly capture and process meaningful rock mass information without any need for additional techniques. Over the past 30 years, MWD use on blasthole drills has proven itself as a powerful technique for ground characterization. It has also been clearly established that drill variable responses from tricone rotary drilling provide unique signatures in the presence of intact rock strength variation as well as fractures. Therefore this thesis aims to clearly show the strong correlation between fractures and MWD responses upon which a tool to automatically locate fractures and compensate the blastability index has been developed.

3. Methodology

As discussed in the chapters 1 and 2 the context of this research is based on the MWD at Teck Highland Valley Copper Mine (HVC). At HVC, a commercial drill monitoring system and a GPS (Global Positioning System) guidance system from Aquila Mining Systems[6] were deployed on the fleet of three Bucyrus 49R model drills in 1997 (1x 49RII and 2x 49RIII). The drill operator uses GPS to accurately position the drill at the desired locations of holes in the blast pattern. The deployed drill monitoring system over a decade of operation showed an ability to precisely determine rock hardness (strength) variability based on rock strength variation. Furthermore, the Aquila Drill Management System (DMS) through drill variable monitoring and processing was able to generate a Blastability Index based on normalised Specific Energy.

In 2007, the Aquila DMS was replaced with the Leica DrillNav product at HVC. The new system has similar capabilities to the Aquila Mining System including providing high-precision GPS guidance as well as monitoring of the same drill variables and generation of a drillability coefficient instead of a BI value.

After deploying the new monitoring system, a new project for developing a more advanced BI value was conducted by Peck Tech Ltd. starting in 2008 on behalf of HVC. During that project a preliminary algorithm was defined with the capability to identify the presence of fractures while drilling whereby the base BI values could be subsequently compensated. However the validity and accuracy of this algorithm was not assessed. In this thesis another version of this algorithm named CBI Algorithm is developed based on the methodologies described in the following sections.

[6] Now owned by Caterpillar Inc.;

3.1. Field Data Collection

3.1.1. Mine Geology

As geology is the most significant parameter which influences the drill and blast operation, a good understating of geology of the place that the data is gathered is essential in studying drilling and blasting.

The data set used in this thesis was collected from an open pit mine 75km southwest of Kamloops in British Columbia, Canada. Highland Valley Copper (HVC) mine has three pits: Valley, Lornex and Highmont. At HVC copper/molybdenum minerals are mined through conventional drill and blast and truck and shovel techniques. Highland Valley is primarily a granodiorite body overlain by glacial tills. "Its deposits are within the Guichon Greek batholith, one of a series of plutons that are associated and comagmatic with the Nicola group, a succession of Late Triassic Islands of volcanic rocks within the southern portion of the Quesnel Trough in the intermontane belt''(Casselman, 2000, p.161).

The recorded data was collected from two benches at Valley pit: V0770 and V1115. Drills were positioned on these two benches as following:

- Drill11 on 1115 bench in ore just below the overburden contact, which was assumed to provide examples of weaker rock with some contrast possibly due to weathering.
- Drill13 at pit bottom on 0770 bench in what was considered harder rock conditions with less variability.

Thus the selected dataset covers a range of soft to hard rock which is reasonable for evaluating the use of MWD toward detection of fractures.

3.1.2. Monitored Parameters

The drills used for this project were a 49RIII (drill 11) and 49HR (drill 13). The 49-R drill series is a large scale electric blasthole crawler mounted drill, capable of drilling holes in a single-pass or muli-steel pass. The drills deployed at HVC are configured for single pass rotary drilling to a maximum depth of approximately 20m. Figure 3.1 shows Drill11 at HVC where its operation and control system were observed by the author in 2012.

Figure 3.1, Drill 11 - Bucyrus 49-RIII at HVC

These drills utilise two DC electric motors that provide the Pulldown/Hoist force and Rotary Torque to the bit and are mounted on a movable cross-beam in the drill mast. The motors are PLC controlled with the capability for both manual and automated drilling operations. Figure 3.2 is the schematic of the motors outputs.

Figure 3.2, Schematic of output from drilling motors (Peck Tech, 2011, adapted by permission)

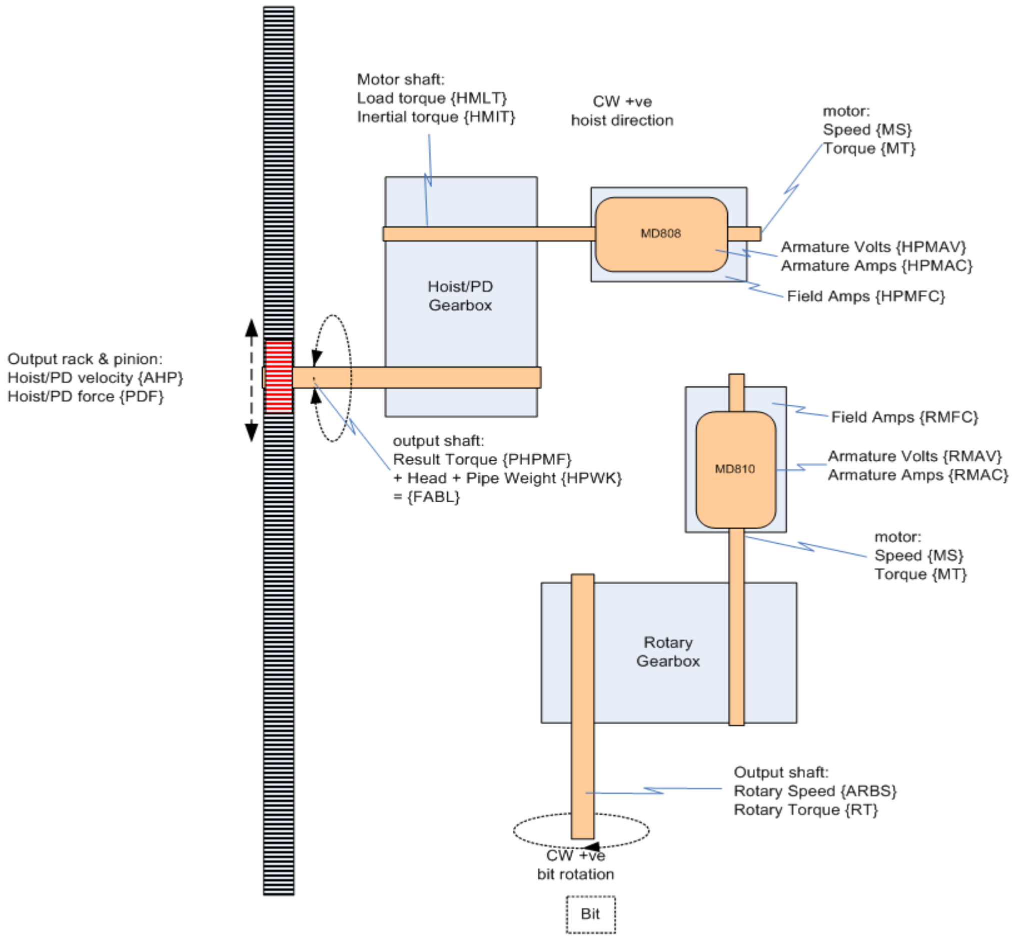

The armature shaft of the Rotary Motor (RCP) provides Rotary Torque and Speed and works through a reduction gearbox to the drive head & provides the rotary speed (RPM) and torque (TRQ) to the bit. The Hoist/pulldown Motor (HCP) works through a reduction gearbox onto a rack & pinion and provides the axial hoist/PD speed and force to the bit. When physically drilling in a downwards direction where the bit advances in depth, the axial speed is called the Rate of Penetration (ROP) and the applied force is the Active Pulldown Force. On this last point, the HCP drive applies the Active pulldown force and when combined with the static weight of the drill assembly, or the passive force, the two constitutes the total Weight on Bit (WOB). The static weight of the drill head, drill steel, bit, stabilizer and sub-assemblies is around 135-145 kN based on manufacturer's manual (Peck Tech, 2009).

Rotary torque and speed, rate of penetration and pulldown force are the desired mechanical variables which are measured indirectly on the drill while drilling. These variables in addition to the bit position (derived from a position encoder in the mast via the PLC) and other control and feedback measurements can be sourced either through a digital interface from the PLC or at the analog signal side of the PLC. Since the digital interface was utilised by the installed DMS and its sampling rate is fairly slow (< 10Hz), data measurements were undertaken on the analog side of the PLC using an Analog to Digital (A-D) sampling logger.

3.1.2.1. DataQ Data Logger

To record the data for the project, a DataQ DI-718Bx data logger was used which has been designed for general purpose Analog to Digital measurement and data recording for up to 16 channels. Each channel of input is sampled and converted by individual AD conversion modules selected based on the measurement type i.e. volts or amps and signal magnitude; the output from the modules is a digitally scaled voltage. The DI-718Bx collects the output of the individual AD modules and stores the data onto SD flash cards along with time and date. SD cards can be retrieved and read or data downloaded online through the loggers interface. The logger and its modules is capable of recording at a rate of up to 14400Hz therefore for 16 channels of data the maximum recording rate per channel is 900Hz. Sampling frequency configured in the DataQ device for this study was 400Hz or 0.0025 second sample intervals due to the limitation of 1GB SD cards providing recording capacity of just less than one day. Figure 3.3 depicts the DI-718Bx data logger.

Figure 3.3, DataQ DI-718Bx data logger showing individual A-D conversion modules (DataQ Instruments, 2007)

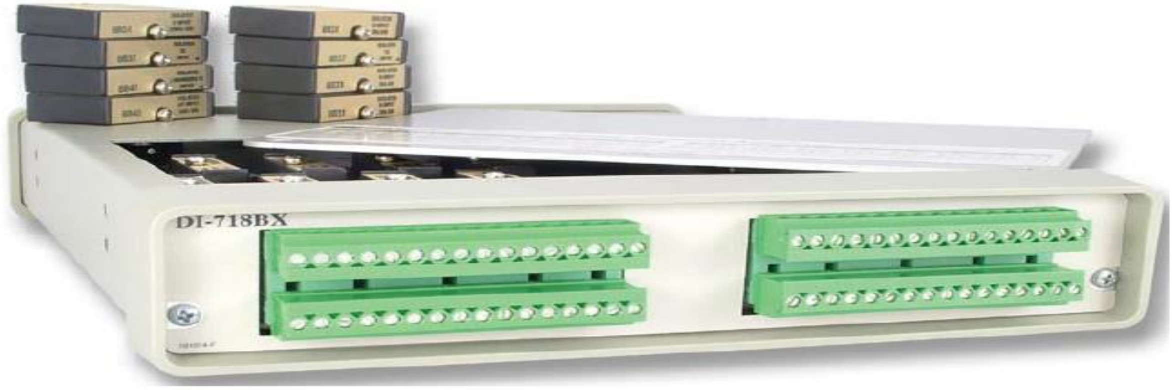

Regarding the MWD and rock classification, the 16 channels listed in the Table3.1 were collected. Some of the signals are compulsory for the project and others were collected as a reference to aid in interpretation of the data and the actions of the operator (manual control) and/or the drills auto control system.

Table 3.1, DataQ channels

Channel	Signal	Description	Project
1	Bit position	From PLC	Required
2	RCP Armature Voltage	~ Motor Rotary Speed -> Bit rotary speed	Required
3	RCP Armature Amps	~ Motor Rotary Torque -> Bit rotary torque	Required
4	RCP Field Current	~ Motor Field Strength	Required
5	RCP Speed Reference	RPM Control Signal	Reference
6	HCP Armature Voltage	~ Motor Rotary Speed -> Hoist/Rate of Penetration	Required

Channel	Signal	Description	Project
7	HCP Armature Amps	~ Motor Rotary Torque -> Pulldown Force	Required
8	HCP Field Current	~ Motor Field Strength	Required
9	HCP Speed Reference	ROP Control Signal	Reference
10	HCP Pulldown Current Limit	Maximum Pulldown Force Control Signal	Reference
11	Water Injection Valve Current	~ Water quantity	Reference
12	Rotary Master Switch Input	Non-zero when drill rotary motor under Manual control	Reference
13	Hoist/PD Master Switch Input	Non-zero when drill Hoist/PD motor under Manual control	Reference
14	Raw Vertical Vibration	Raw Vertical Acceleration	Reference
15	Raw Horizontal Vibration	Raw Horizontal Acceleration	Reference
16	Main Air Pressure	Bailing Air Pressure	Reference

General DC motor theory says that for a constant field flux the motor shaft torque is proportional to armature current and speed is proportional to armature voltage. For a given armature voltage & current, when the field strength (current) increases, the rotational speed will decrease and torque will increase. In the majority of Production Drilling the RCP & HCP motors operate in Strong Field. The operator may flip the HCP motor to Weak Field to get extra rotary speed when hoisting or lowering the drill assembly.

DATAQ data does not capture the field state of the motors but it can be interpolated from the magnitude of the field current in the motors.

To understand the source of recorded signals in the Table 3.1, layout of the DataQ Logger and the channel source points are shown in the Figure 3.4.

Figure 3.4, Layout of the DataQ logger and the channel source points (Peck Tech, 2011, adapted by permission)

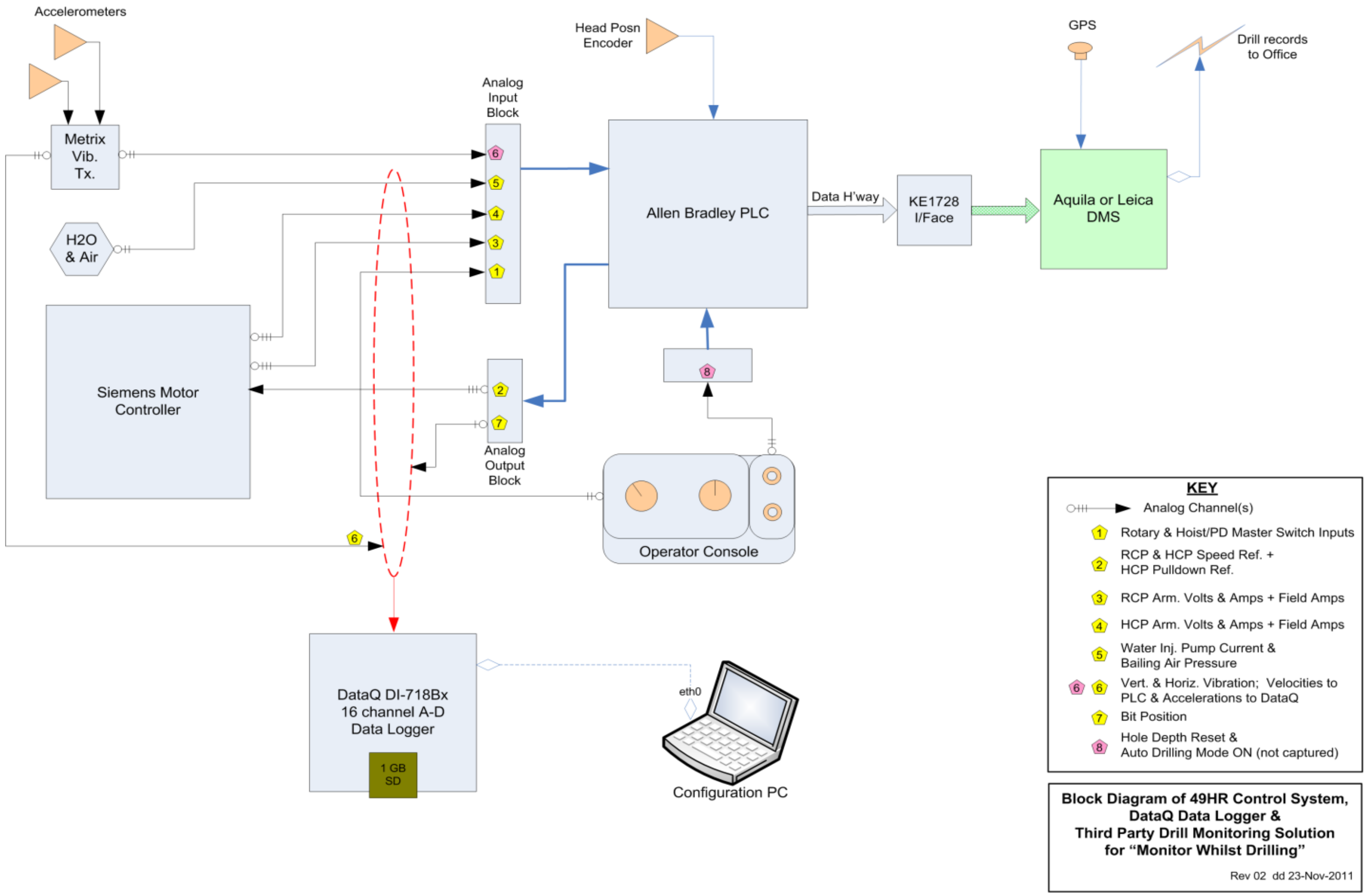

3.1.2.2. Selected Data Set

During the period of recording the data from May 13th to May 16th 2008, several sets of data from different blastholes were recorded but a few of them pertain to this research because of availability of geophysical logs and core tests. Table 3.2 briefly summarizes the selected test-holes.

Table 3.2, Selected data-set

DataQ File	Hole Number	Drill Number
D534003F	V0770-18-013	13
D534003F	V0770-18-018	13
D534003F	V0770-18-028	13
DB850018	V1115-260-022	11
DB85001B	V1115-260-030	11
DB850018	V1115-260-031	11
DB850018	V1115-260-032	11
DB85001F	V1115-260-044	11

In the Hole Numbers column in Table 3.2 the left part is the bench name, the middle number is the blast pattern ID and the right number is the hole number in the mentioned pattern and bench. For this study, on bench V0770, test-holes 13, 18 and 28 in pattern 18 and for bench V1115 test-holes 22,30,31,31 and 44 in pattern 260 were chosen as appropriate candidates for geophysical logging due to the stability of rock around the collar, re-measured depth compared to the reported drill depth and the least operator/manual intervention during drilling.

Figures 3.5 and 3.6 respectively show the test area of Drill 11 and Drill13. Five complete holes and one partial hole (10) were logged in test area 1 and three complete holes were logged in test area2.

Figure 3.5, Test area 1 (Peck Tech, 2009, adapted by permission)

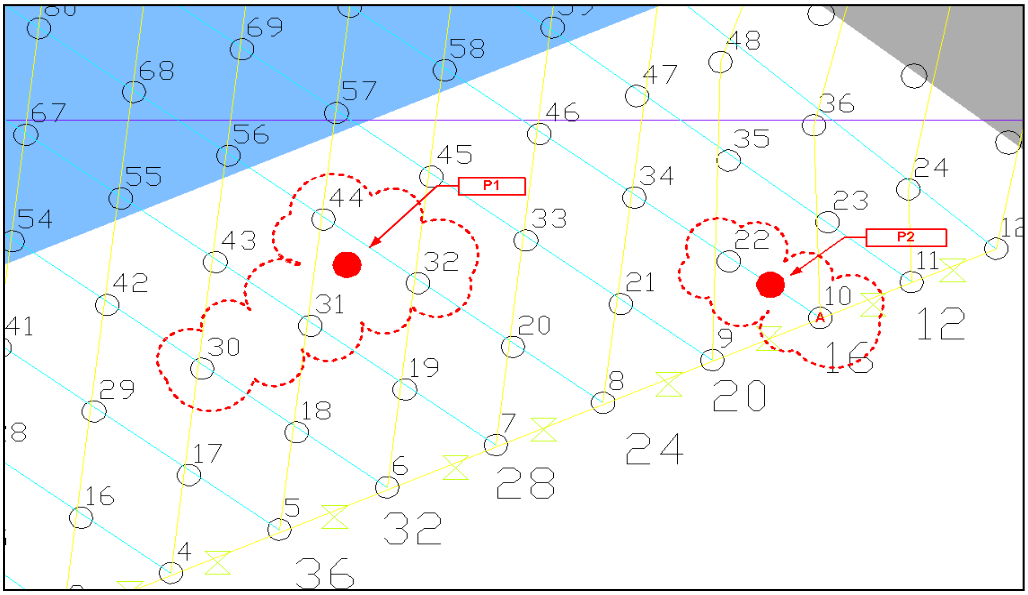

Figure 3.6, Test area 2 (Peck Tech, 2009, adapted by permission)

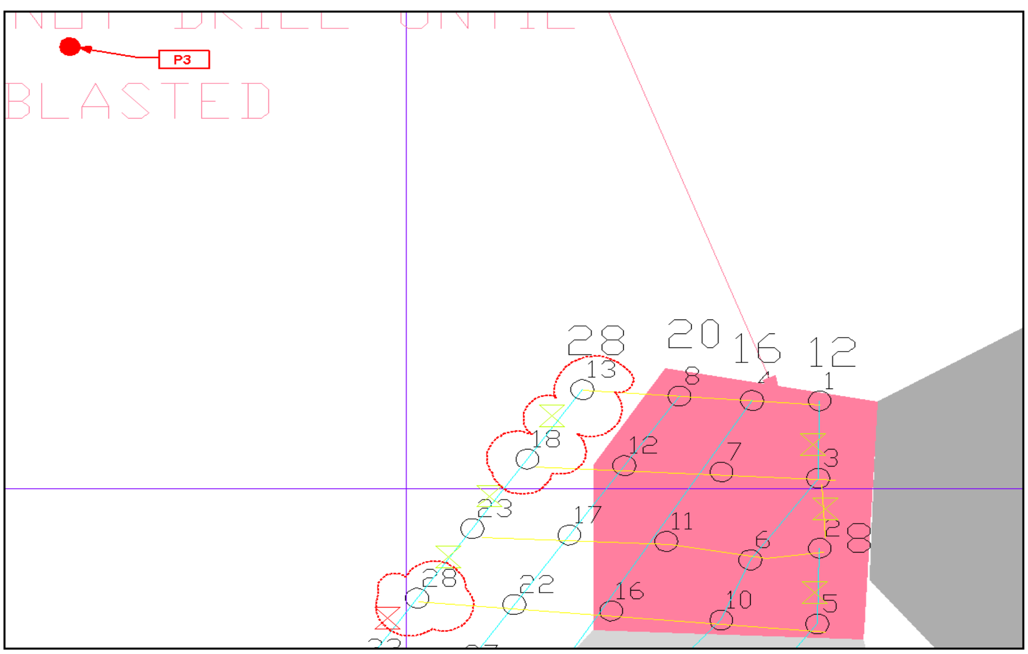

3.1.3. Geophysical Logs

‘’Measurement of physical, chemical and structural properties of the penetrated ground below the surface by a tool that moves in the borehole on wire line cable is named borehole geophysical logging’’ (Wonik and Olea, 2007). There are various logging methods such as radioactivity methods, optical methods and acoustic methods. Usually to have a better understanding of formation, different logs are taken to improve the results.

In this study the selected holes in Section 3.1.2.2 were identified for geophysical logging undertaken by a leading geophysical logging company. To fulfill this task, five tools were used as follows:

- Litho-density, Neutron and Caliper,
- Formation Micro Imaging(FMI)
- Sonic Velocity(SV)
- Elemental Capture (Mineral Analysis)
- Natural Gamma Spectroscopy

3.1.4. Core Tests

In addition to geophysical logs, core tests as another tool for geology correlation and identification is used. As shown in the Figures 3.5 and 3.6, three NQ diamond drill holes were drillied.P1 and P2 in test area 1 and P3 in the test area2. Holes P1 & P2 were drilled within the pattern in proximity to holes geophysically logged while P3 was drilled some distance from the test area due to pattern 018 being charged ready for blasting and the adjacent pattern being actively drilled. Issues with the retrieval and handling of the core as well as only double tube barrels available for the diamond drilling program resulted in a large number of induced fractures in the core that was recovered.

Possible intact samples were extracted and sent to the laboratory for strength and sonic tests. As samples from P2 were too small for strength testing, just the core data of P1 and P3 are available. The test dataset is composed of photographical records of specimens before and after tests and the result of rock strength tests consists of density, sigma3, sigma1, Young's Modulus, P-Wave Velocity and S-wave velocity. Since the rock at the bit pressure is slightly confined, conducted Tri-axial tests are not useful for this study but they are more useful in other aspects of geomechanics.

3.2.Data Pre-Processing

As the DataQ capture is continuous and captures data for both drilling and non-drilling time the data files need to be processed. This process includes partitioning of recorded data, signal conditioning, removing non-drilling events and finally filtering (de-noising) and interpolating signals to achieve the desired resolutions.

To conduct this part of the research, three software packages have been used:

a) WindDaq to view and extract the relevant hole drilling data from the DataQ native codas files and save the data in ASCII.csv format available for processing;
b) PDS View to view geophysical logs ;
c) MATLAB for all data processing, presentation and analysis (The pseudo-code is given in Appendix A).

3.2.1. Partitioning

The data recording by the DataQ Logger is continuous in time regardless of drill activity whilst the drill remains powered e.g. collaring, normal drilling, bit retracting, shift change, maintenance, drill movement onto other benches and tramming between holes. Thus since the data from different holes were recorded in time sequence, the data is segmented for marked test-holes and then is converted to a readable format for MATLAB.

Using records from the Aquila and Leica DMS systems the start and end drilling times for the target holes were retrieved and used to determine the appropriate DataQ file and location within the file for the drilling data associated with the target hole. This data including a buffer prior to commencement of and after completion of drilling is extracted. Figure 3.7 shows the data for 16 channels of a DataQ data file viewed in WinDaq with a number of holes. The Y axis is the voltage range for each channel and the X axis is relative time which the holes are extracted based on that.

Figure 3.7, WinDaq presentation of a DataQ file

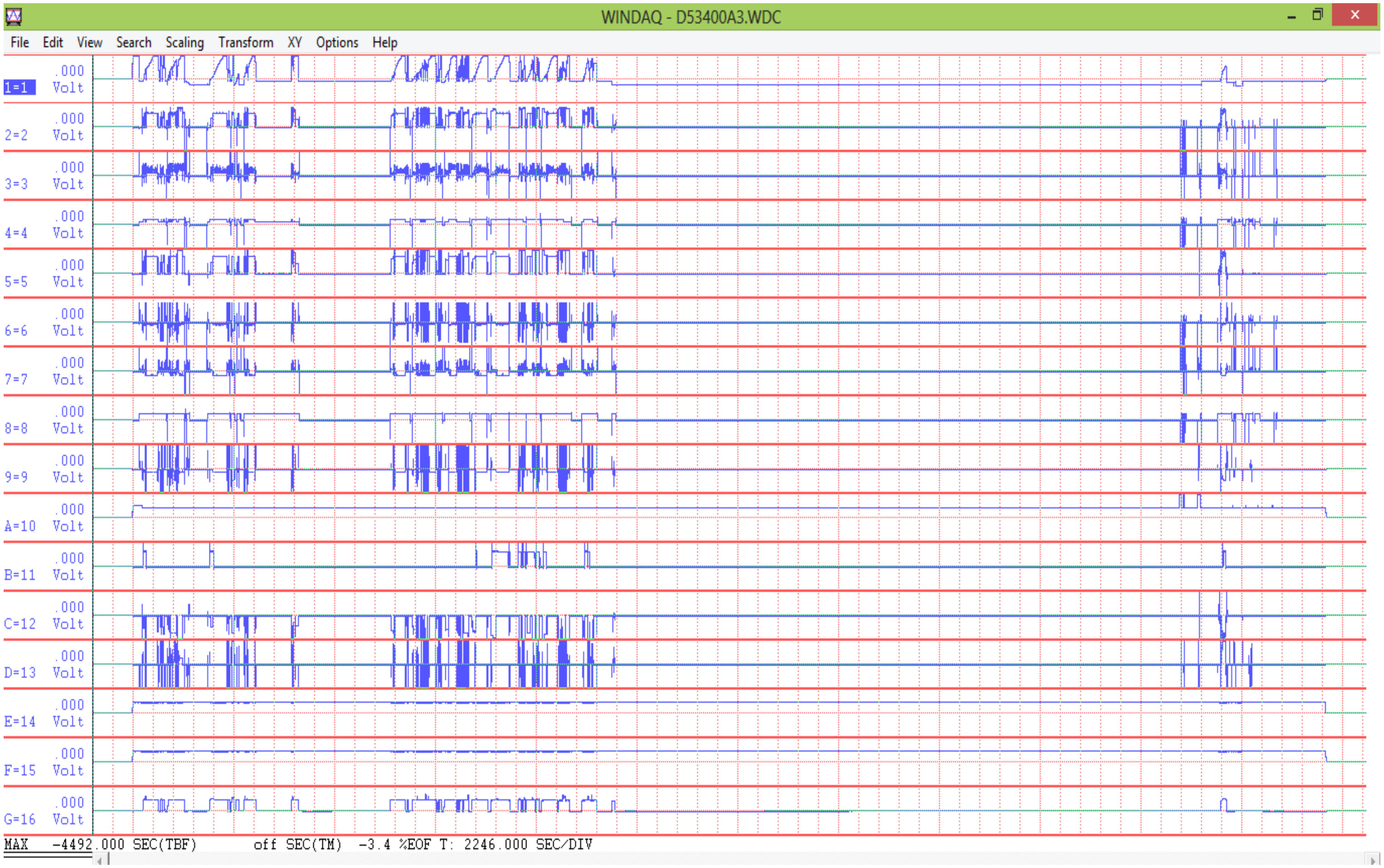

Due to different events that can arise during the drilling of a hole such as stopping (operator or auto-control intervention) or drill bit retraction it cannot be assumed that the extracted data represents a continuous drilling record over the depth of the hole. As it is only the drilling (bit breaking ground) portions of the record which can reflect ground characterization it is therefore a requirement to remove (filter) non-drilling events from the recorded data. Figures 3.8 and 3.9 shows the unfiltered voltage signals parsed from DATAQ for Hole13 against relative time from the start of the data record. In this study the duration of drilling is important however actual calendar time is not relevant. Therefore all the timelines are expressed in relative time.

Figure 3.8, Recorded signals for Hole13

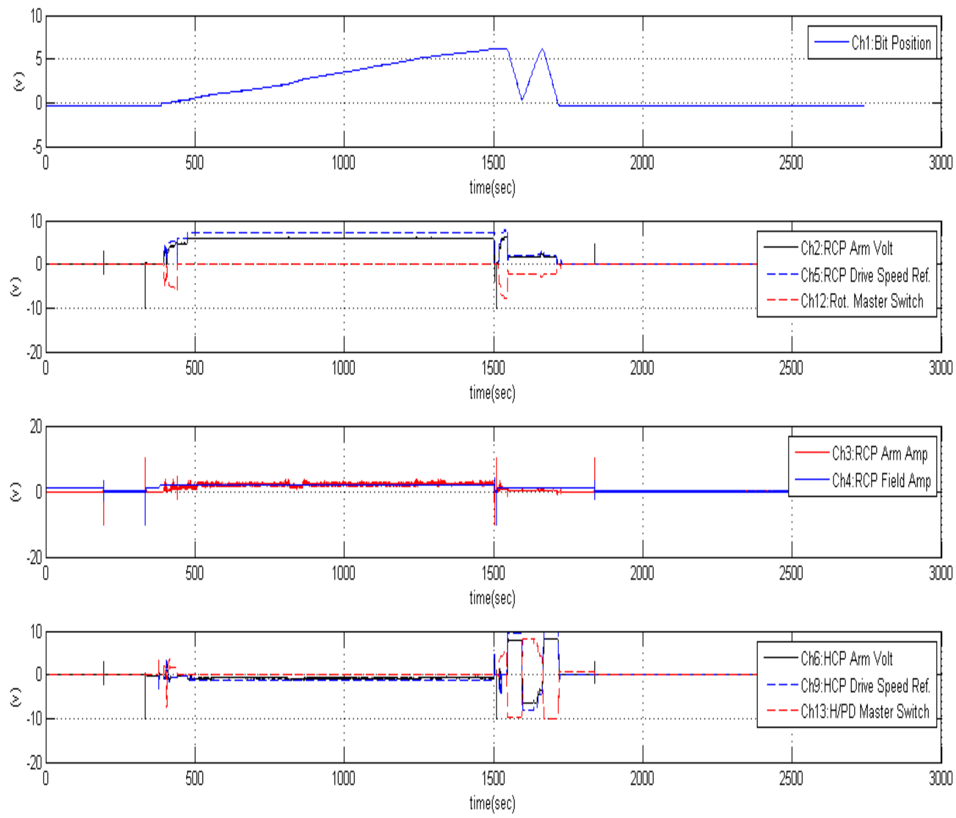

Figure 3.9, Recorded signals for Hole13

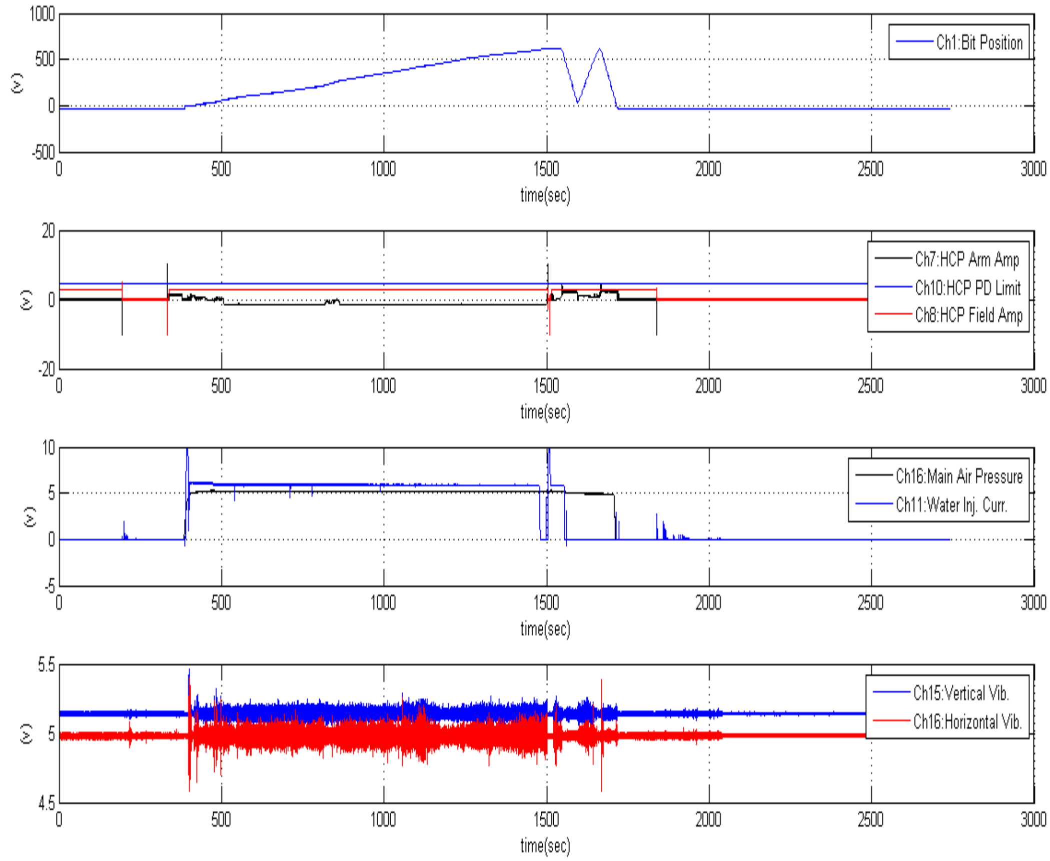

To interpret different events in the signals, the bit position (hole depth) channel is used as a reference signal in Figures 3.8 and 3.9. The bit position should have a value of zero when depth is zero i.e. the bit is resting on the ground and as the drilling progresses the voltage, and thus hole depth, increases.

Figure 3.10 shows a closer view of the bit position. The increase in the bit depth to zero at start of the hole is due to a Depth Reset done by the driller when the bit touches the ground. After completion of the blasthole, the drill bit is retracted back to the beginning of the hole and this may be followed by a cleaning pass to make sure that there is no loose rock material that may have come free from the sides of the hole remaining at the bottom of the hole. Finally the last step is drill assembly stowage which is why depth is negative.

Figure 3.10, Bit position while drilling of Hole13

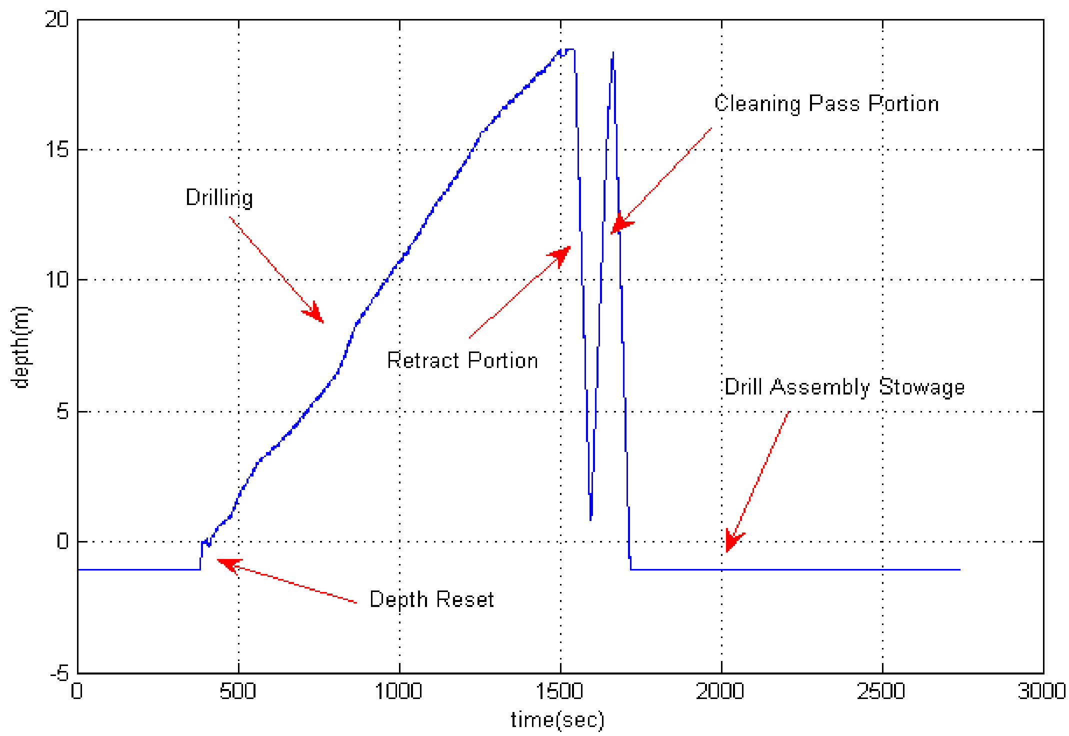

Consequently the bit position channel can help to determine the non-drilling events to remove them before beginning the analysis. In addition to the depth signal, other drill variables such as ROP and Rotary speed (and torque) can indicate non-drilling events. The DataQ data signals are filtered on the following rejection conditions:

- Zero or negative ROP (+ve hoist motor voltage)
- Zero or negative Torque(-ve rotary motor current)
- Stationary or negative rotational bit speed(-ve rotary motor voltage)

Figure 3.11 shows the original electrical rotary motor voltage signal and its filtered version for Hole13. The black zones are representative of the drilling portion of the recorded data while the blue zones are original data.

Figure 3.11, Filtered rotary speed for Hole13

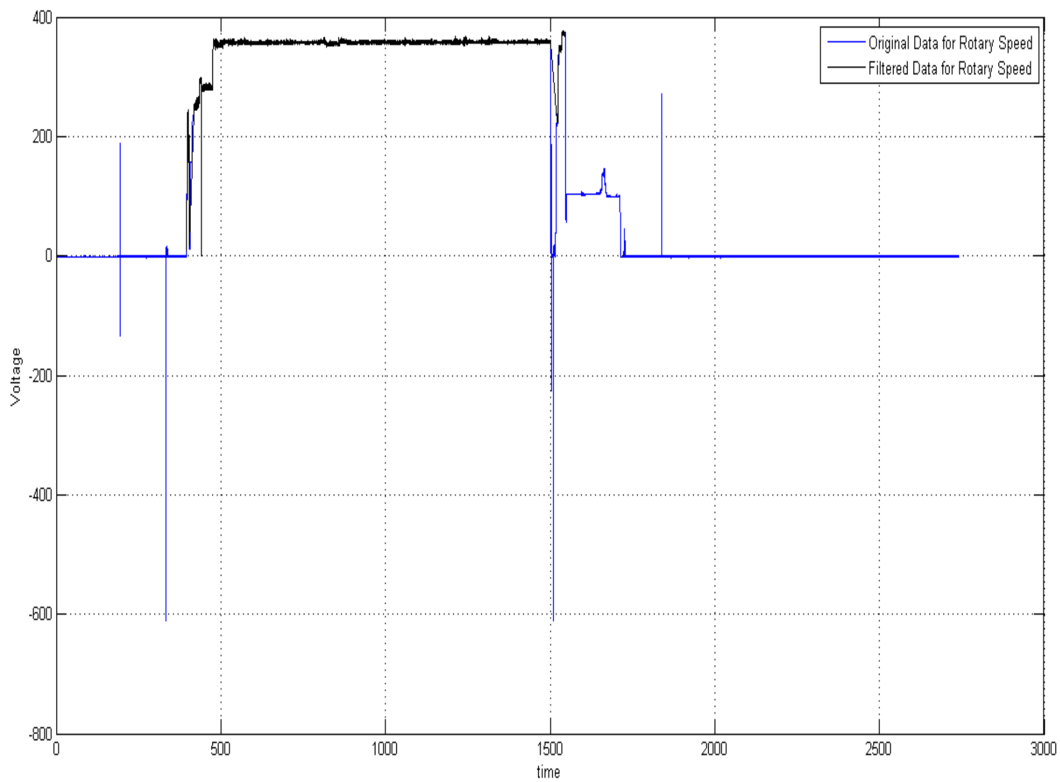

In addition to the 16 channels of data, the "relative "clock" time" (in seconds) for each sample is included in the DataQ data extract. Since the only relevant section of the data is the "drilling part", after filtering out the "non-drilling" data, it is necessary to re-index the timeline into a 'relative "drilling" time'which shows net drilling time at each sample point where the time increment is determined by the sampling rate. After re-indexing time zero represents the start of drilling (breaking ground) at the hole collar and the end time is the termination of drilling on completion of the hole (maximum depth).

3.2.2. Signal Conditioning

The 17 signals captured by DataQ must be scaled to represent the actual drill motors voltages, currents and other physical units. To fulfill this purpose a simple scaling matrix is constructed to scale the +/-10 volts signals into their electrical/physical units. Table 3.3 shows the scaling factors for each channel.

Table 3.3, DataQ scaling factors

Signal	Scaling Factor
Time	1
Bit position	3.048
RCP Armature Voltage	60
RCP Armature Amps	75
RCP Field Current	5
RCP Speed Reference	10
HCP Armature Voltage	60
HCP Armature Amps	75
HCP Field Current	5
HCP Speed Reference	1.6764
HCP Pulldown Current Limit	10
Water Injection Valve Current	10
Rotary Master Switch Input	10
Hoist/PD Master Switch Input	10
Raw Vertical Vibration	10
Raw Horizontal Vibration	10

Signal	Scaling Factor
Main Air Pressure	68.7

3.2.3. Bit Position Signal

In addition to time, the exact position of the bit down the hole is important to associate drill variables variations against depth in the rock mass and subsequently smooth them over the desired depth increments, to calculate ‘real’ rate of penetration based on bit position advancement and drilling time, to calculate SE for an interval and consequently to determine the location of fractures.

Bit Position is one of the DataQ Logger recorded channels by which was shown in the Figure 3.10. The bit position is derived from the head position on the drill mast which, at the time of the project, was measured with a 9 bit Grey code step encoder and processed by the PLC into a bit position. To better understand the nature of this signal (channel), Figure 3.12 shows the progress of the bit during the period of 770 to 800 sec in relative elapsed time.

Figure 3.12, Depth stepped signal

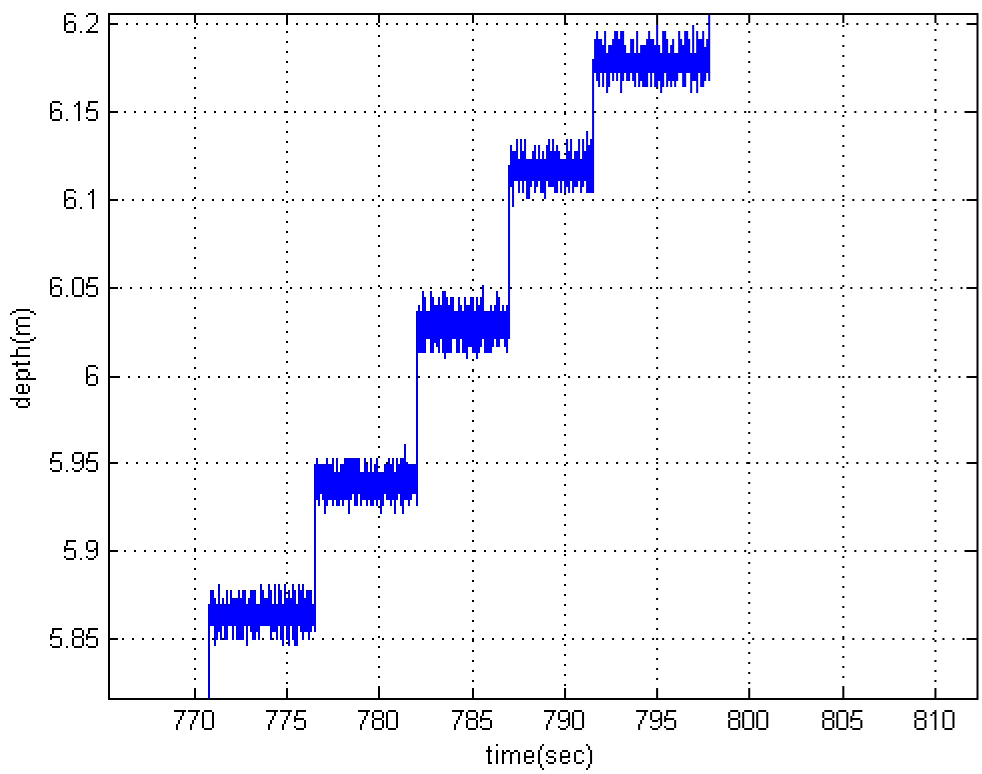

In the PLC, the bit position is resolved in 1/10th foot increments for purpose of drill control and display to the operator. The PLC digital values are passed and converted to a voltage signal by the D-A unit which is sampled and measured by the DataQ logger. The D-A scaling for bit position is 10Volts=100ft at a resolution of 1/10th of a foot (3.048cm). Figure 3.13 shows the block diagram of bit position recording system.

Figure 3.13, Bit position recording system

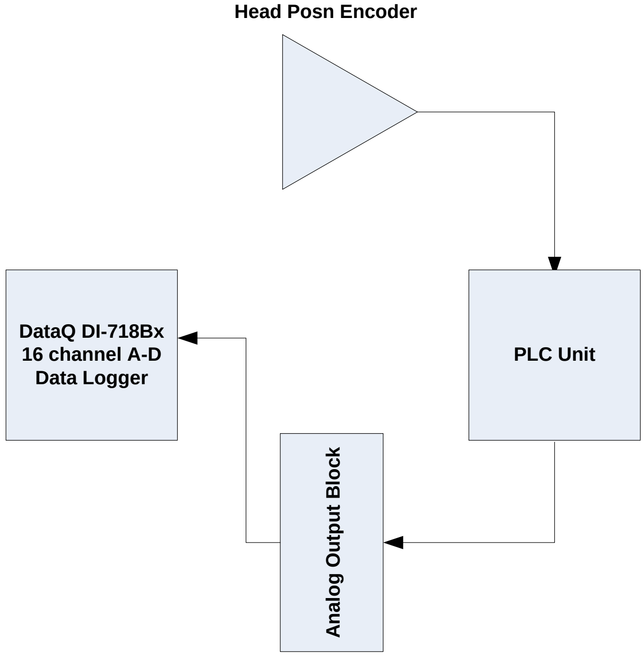

The depth encoder on both drills reports a digital step every 8.2669568 cm. The PLC conversion of this signal expresses the bit position in integer 1/10th foot (3.048 cm) units which is recorded by the DataQ. Referring to Figure 3.12 it can be seen that the average depth steps are not always regularly spaced in magnitude. In addition it can be seen the depth step is not perfectly straight but contains a “noise” component. This noise is due to the PLC D-A conversion error and resolution, the DATAQ A-D conversion error and resolution and possible induced noise in the wire connection from PLC to DATAQ. As the resolution of the step encoder and the resolution of the PLC converted value differ, this results steps of either about 6 and 9 cm. To determine encoder and PLC bit positions, a MATLAB code was written to interpret them. Figure 3.14 shows the difference between Encoder, PLC and DataQ bit positions for Hole13 over the 410 to 500 sec time interval. An assumption in this approach (code) is that the encoder and the PLC depth step are perfectly aligned at depth zero.

Figure 3.14, Bit position for Hole13

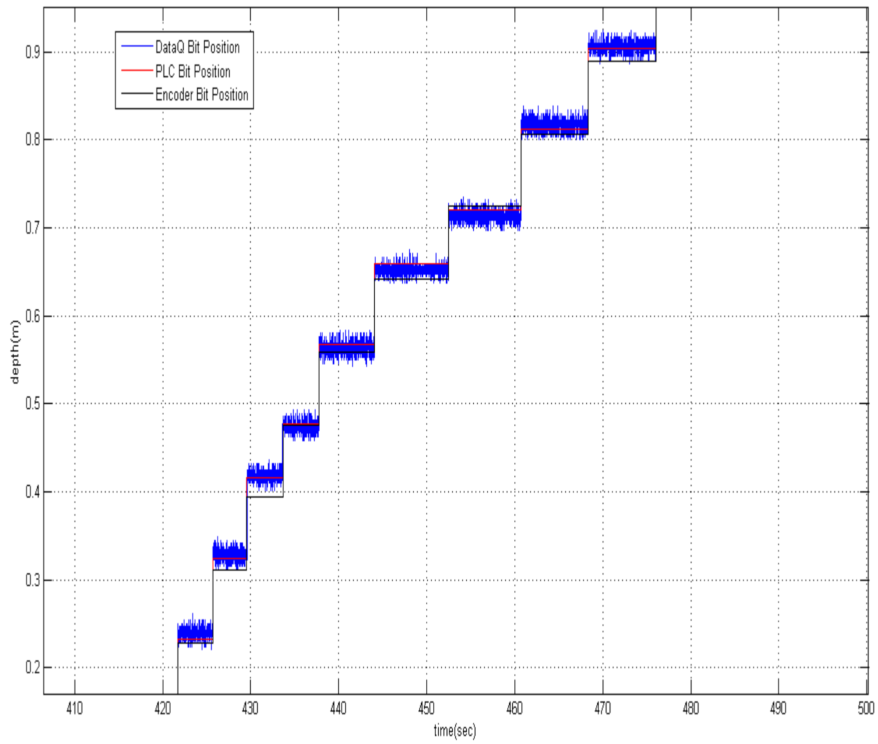

As Figure 3.14 shows the PLC bit position and consequently DATAQ bit position can be smaller or larger than the encoder bit position which is assumed to be the true position of the bit.

Now by understanding the process of bit position generation, after removing non-drilling events and recalculating new data set based on the relative "drilling" time, the time position of each DataQ depth step first needs to be found. Assuming the encoder step depth is zero at bit position zero, an encoder depth step profile can be synthesised with each encoder step at a constant depth increment (8.2669568cm) occurring at the same relative time as that for the DataQ bit position. It is assumed that PLC bit position zero occurs at Depth Reset time when the operator detects the bit engages the ground. However the driller sometimes presses the Depth Reset button too early or forgets until he has drilled part of the hole collar. In these cases the process needs to use the other signals to assert when real drilling (breaking ground) has started and determine a depth zero. The start of drill rotation above a particular threshold speed can be an indicator for when the drilling starts.

There are two questions left. The first is, given the noise profile on the bit position signal recorded by DataQ, what is the true magnitude of the step and where does the step change occur. The second question is whether the synthesised encoder profile can be used directly or needs to be processed.

To locate step changes in the DataQ bit position signal and to de-noise the depth signal, a Moving Mode technique is used which generates a statistical mode value for a number of samples defined by a moving window. The size of the sample window was determined on the average number of samples for a 0.5cm bit position movement based by the total number of samples in the “drilling” data set and the maximum depth. The moving window is applied around each sample point in the data set and the value of that point is substituted with the statistical mode of the window. The idea behind this approach for de-noising is that by calculating statistical mode in a desired window, the noise within each step is replaced with step mode (statistical mode).

To compare the results of this approach with the original data, Figure 3.15 shows the extracted step modes magnitude and timing from 590 to 670 sec for Hole13. It should be noted that in the CBI Algorithm, the step modes are calculated in the relative drilling time.

Figure 3.15, Step modes for Hole13

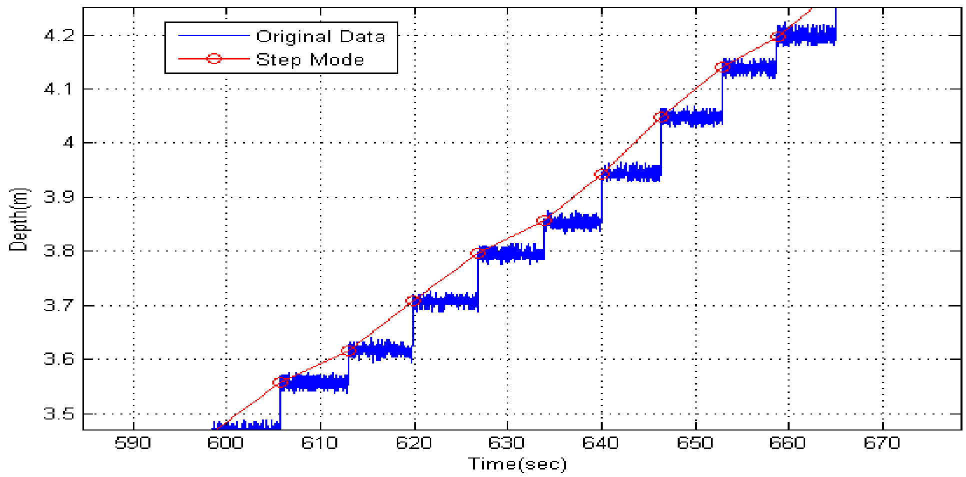

Given the step change times the true bit position signal based on encoder steps can be derived in relative drilling time. Figure 3.16 shows generated depth signal for Hole13.

Figure 3.16, True bit position from encoder for Hole13

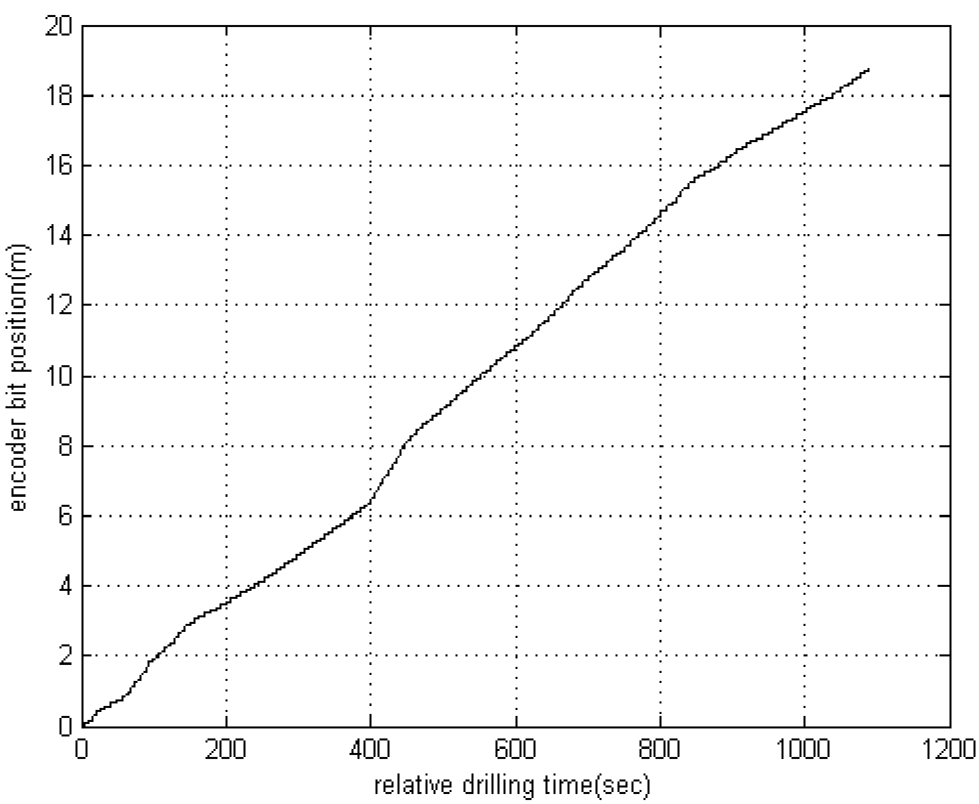

The generated depth signal is also a stepped signal. Obviously a drill does not drill the hole in steps. As all the other drill signals were recorded at an interval of 2.5 msec or a rate of 400Hz, it is necessary to interpolate the actual bit position progress between depth steps (encoder steps). To perform this task the following approaches can be used:

- **Linear Interpolation**: The following equation is used to interpolate depth between encoder increments.

$$\Delta x = 0.082669568 \times \frac{0.0025}{\Delta T} \tag{3.1}$$

  Where Δx is incremental depth per sample point and ΔT is time between two encoder steps. As the slope of depth against time reflects the ROP the assumption is ROP is constant between depth steps.

- **Weighted Interpolation based on the Hoist Motor Voltage**: Since the hoist motor controls the progress of the bit down the hole, the hoist voltage is used as the modifier of depth signal (Branscombe, 2010). In other words, the actual movement of the bit is seen in the motor ROP or hoist voltage signal. Consequently, to interpolate between two consecutive steps, the incremental depth is given by:

$$\Delta x = \frac{Hoist\ Voltage(i)}{ROPav(j)} \frac{L}{N.o.P} = \frac{Hoist\ V(i)}{\sum Hoist\ V(i)}\ L \text{ (Branscombe, 2010)} \tag{3.2}$$

  Where

  Δx= Incremental depth per sample point

  L=total depth of each step

  i=point counter in each step

  j=depth step counter for each hole

  N.o.P=number of drilling recorded points in each step

* **Weighted Interpolation based on the Mechanical ROP**: This approach is exactly the same as weighted interpolation based on the hoist voltage except using mechanical ROP instead of hoist voltage which is discussed later.

Figure 3.17 compares the result of weighted hoist voltage interpolation and linear interpolation depth for Hole13 during 27.94 to 28.06 sec time interval.

Figure 3.17, Depth signal for Hole13

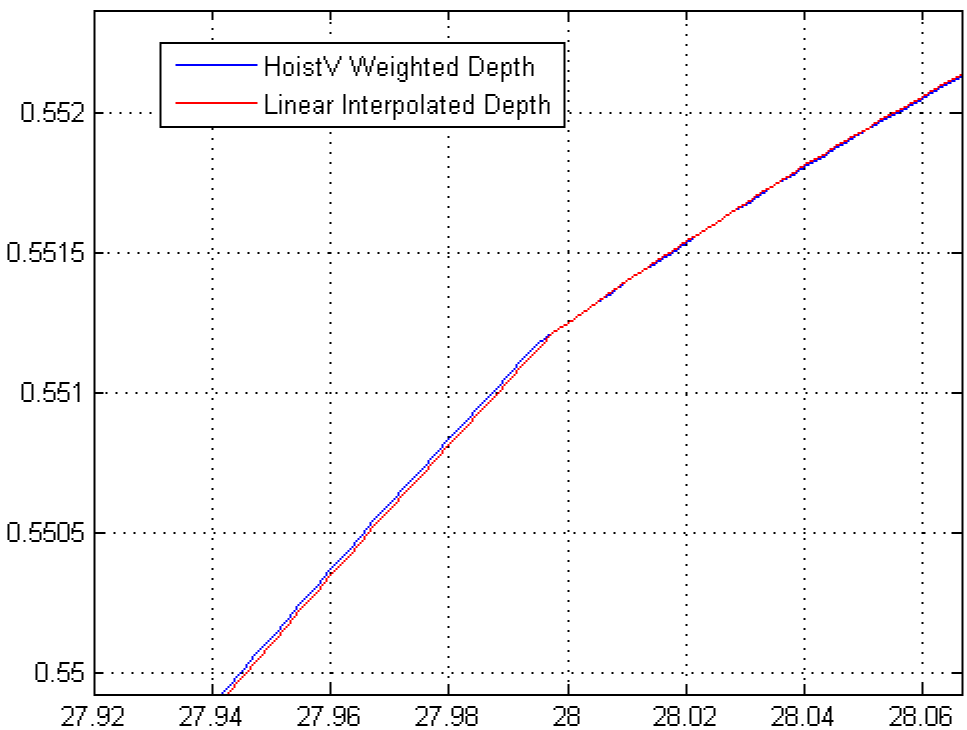

As Figure 3.17 shows and the final results of the CBI Algorithm will confirm, all the mentioned interpolation approaches yield about the same output. However in this thesis the weighted hoist voltage interpolation method is chosen for convenience.

3.2.4. Electrical and Physical Conversion and Signal Segmentation

All the performed analyses so far are based on the scaled electrical signals recorded by DATAQ Logger. But it is important to have drill variables like ROP, Rotary Speed, Rotary Torque and Pulldown Force expressed in their true physical units. Table 3.4 presents physical units for mentioned variables.

Table 3.4, Physical units

Variable	Physical Unit
ROP	m/min
Pulldown Force	N
Rotary Speed	rpm
Rotary Torque	N.m

As discussed previously the rotational speed of a DC motor is proportional to the voltage applied to it, and the torque is proportional to the current supplied to the motor armature. This simple relationship holds true if the field flux remains constant when the motor is in a steady state and in motoring mode (when current and voltage are of same sign forcing motor to work instead of generating):

$$\omega \propto V \tag{3.3}$$

$$\tau \propto I \tag{3.4}$$

Where ω is rotary speed, τ rotary torque, of the motor shaft and V voltage and I current in the motor armature

For the rotary drive the motor output is geared to the drill assembly and the resultant bit speed and torque are simple ratios of the motor output assuming no gearbox losses:

$$Rotary\ Speed \propto c_1 \times V_r \tag{3.5}$$

$$Rotary\ Torque \propto c_2 \times I_r \tag{3.6}$$

For the hoist/PD motor the motor speed and torque output is translated into a linear velocity and force via a rack & pinion as shown in Figure 3.2:

$$ROP \propto c_3 \times V_h \tag{3.7}$$

$$Pulldown\ Force \propto c_4 \times I_h \tag{3.8}$$

Where c1, c2, c3 and c4 are constant and dependent on the type of electrical motor. To undertake these calculations, in the CBI Algorithm a "Motor Calculator" processor is written based on emulating the DC Motor Characteristics and PLC ladder logic (PeckTech 2011). It is assumed that the conversion factors are the same for both drills since the electric motor models are identical.

In this thesis all of these physical drill variables are termed "Mechanical" for example Mechanical ROP. Figure 3.18 shows the mechanical signals including rate of penetration, rotary torque, rotary speed and pulldown force against depth for Hole13.

Figure 3.18, Hole13 Mechanical variables

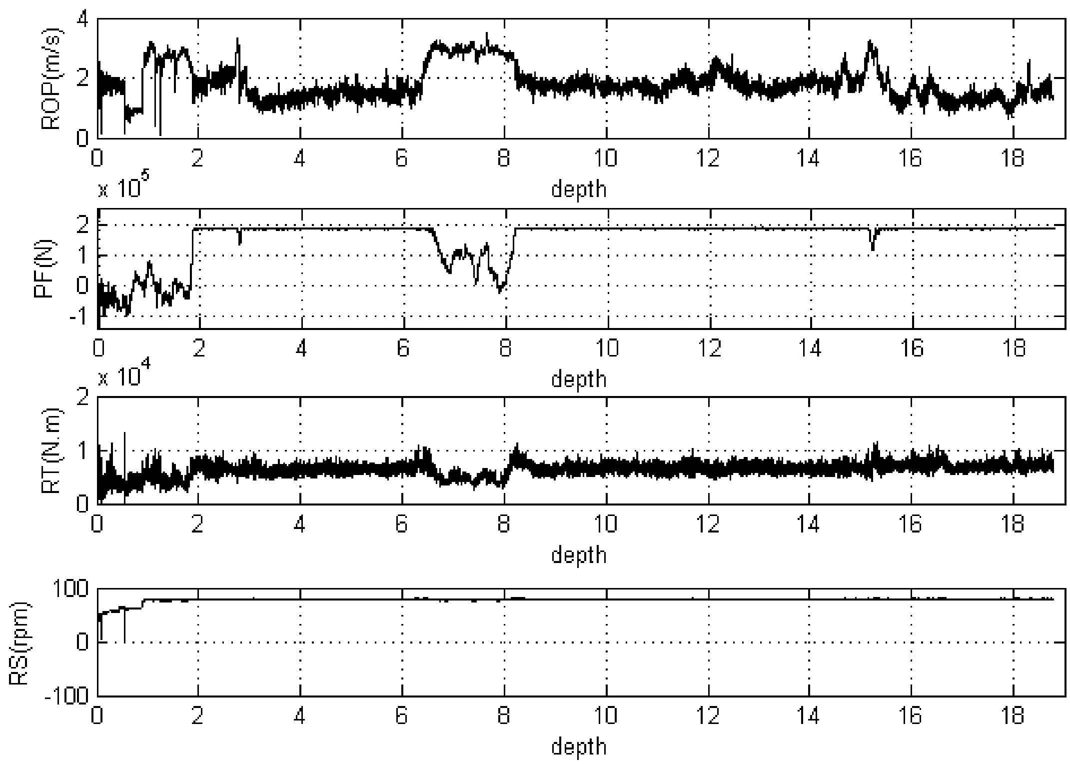

The extreme fluctuations in the beginning of the signals in Figure 3.18 are due to initial collaring of the hole which is done manually. As with the bit position signal the other signals also exhibit a degree of noise along with varying “sinusoidal” signal magnitude reflecting the response of the motor controller systems. As such it is difficult to interpret these sample by sample to determine occurrence & location of fractures. Therefore the entire electrical and mechanical signals are averaged over a variable window of depth which depends on the required resolution. In this research, in order to have sufficient sensitivity to the presence of fractures, 1cm depth resolution is desired. Figure 3.19 shows the averaged signals from Figure 3.18.

Figure 3.19, Averaged signals for Hole13

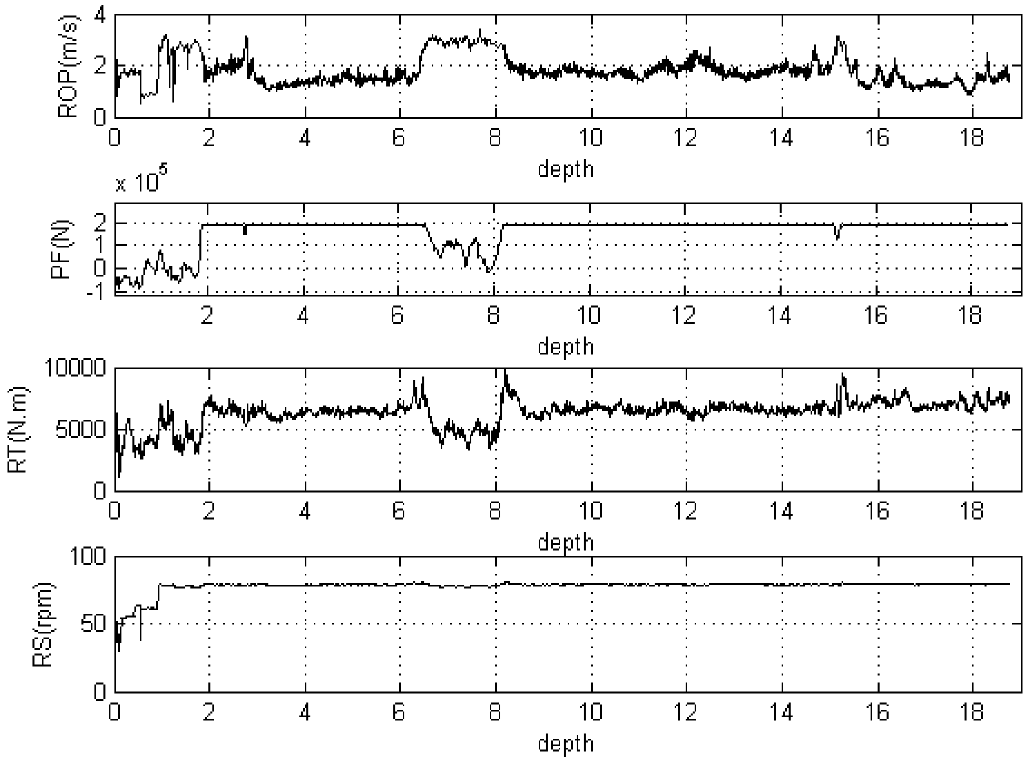

3.3.Specific Energy Calculation

Specific Energy is the measure of rock strength. SE values, or derivatives from it (e.g. Blastability Index or Rock Hardness) can be used as an input into the geological models in the mine to reflect the varying rock strength in the ore-body. The same data can also be used for drill performance and machine health monitoring through recording the consumed energy by the drill. Assuming the energy consumed in drilling is proportional to the required energy to fragment the rock, SE values can be used to design an efficient blast design. As discussed in Section 2.2.2.1, SE is comprised of two parts and can be expressed as:

$$SE_{tot} = SE_A + SE_R \qquad \textbf{(3.9)}$$

Where SE_A is Axial SE from applied weight on bit which determines the degree of indentation of the bit teeth into the hole face and SE_R is Rotational SE from bit rotation & rate of breaking rock.

Furthermore the axial SE can be decomposed since the weight on bit is the sum of two components as following:

$$SE_{A(tot)} = SE_{A(s)} + SE_{A(a)} \tag{3.10}$$

Where $SE_{A(s)}$ is Axial SE from the static (or dead) weight of the drill assembly and $SE_{A(a)}$ is Active Axial SE applied by the Hoist/PD motor .

The specific energy resulting from the static weight of the drill assembly is essentially the pressure of the static load applied onto the bit over the area of the hole.

$$SE_{A(s)} = \frac{W_s.g}{A} \tag{3.11}$$

Where W_s is the static (or dead) mass of the drill assembly and g is gravitational acceleration constant.

Depending on drilling machinery capability, rock mass condition & strength and drill operational procedures, the axial contribution varies from around 2-4% up to 10% of the total SE of drilling (Peck Tech, 2011).

There are three basic rules which have been considered in SE calculations:

- When the Hoist/PD motor is in pull-up or hoist mode it must first overcome the static weight of the drill assembly before the bit disengages from the hole face. At this point there can be no SE of drilling:

$$SE_{tot} = 0 \ \ when \ SE_A < 0 \ or \ SE_{A(a)} < -SE_{A(s)}$$

- When there is no rotation of the drill bit there cannot be any real rock breakage irrespective of the state of the applied axial load:

$SE_{tot} = 0 \; when \; SE_R = 0 \; (Rotary \; Speed = 0)$

- There is no ground breakage if there is zero rate of penetration:

$SE_{tot} = 0 \; when \; SE_R \rightarrow \infty \; as \; ROP \rightarrow 0$

The Teale equation defines the SE of drilling based on drilling inputs. Obviously the SE of drilling will vary over the length of hole so it can be reported as either:

- an instantaneous value for a specific depth in the hole;
- an average value for a defined depth segment in the hole; or
- An average value over the complete hole.

In this research "segment" average SE values are calculated for 1cm depth increments based on two approaches which are discussed in Sections 3.3.1 and 3.3.3.

3.3.1. Electrical power approach

The premise of this method is that the Specific Energy of drilling can be derived from the power applied by the Hoist/PD and Rotary drive motors to excavate a unit volume of rock. There are two key assumptions in this approach:

a) Power transfer from the rotary motor armature shaft to the bit is 100% efficient, i.e. there is no accounting for losses in the intermediate machinery such as the gearbox

b) Similar to (a), power transfer from the hoist/PD motor armature shaft to the drill assembly is 100% efficient and does not account for drill assembly inertial effects when the armature changes direction.

Now by reinstating the Specific Energy components:

$$SE_{tot} = SE_{A(s)} + SE_{A(a)} + SE_R \quad \textbf{(3.12)}$$

Examining the active components provided by way of the Hoist/PD and Rotary motors the mechanical power at the motor armature shaft is defined as:

$$Power = V \times I \quad \textbf{(3.13)}$$

The power is applied to a volume of broken rock for a specific period of time defined by the rate of penetration and bit area:

$$V_{rock} = ROP \times Area \quad \textbf{(3.14)}$$

On the other hand the motor specific energy applied to the unit volume of rock is given by:

$$SE = \frac{Power}{V_{rock}} \quad \textbf{(3.15)}$$

Then consequently the Specific Energy equation becomes:

$$Electrical\ SE(Pa) = \frac{V_h \times I_h}{Area \times ROP} + \frac{V_r \times I_r}{Area \times ROP} + \frac{W_s \times g}{Area} \quad \textbf{(3.16)}$$

Where V_h , I_h are armature voltage and current respectively for hoist/PD motor, V_r ,I_r are armature voltage and current for rotary motor and Area is bit area.

Still, there is a problem in the SE calculation and that is how to calculate rate of penetration. It is important to use true Rate of Penetration as the most significant parameter in ground characterization, drill performance monitoring and SE calculation. Section 3.3.2 discusses the possible approaches for calculation of rate of penetration.

3.3.2. Rate of Penetration

As discussed earlier, ROP is the most effective parameter in ground characterization by MWD. Thus it is important to have a true ROP profile down the hole. In this section two approaches for calculation of ROP are discussed.

Motor Based ROP: Motor based ROP is the rate of penetration extracted by motor calculations which after a filtering process convert Hoist Voltage and Current (V) to physical ROP (m/min). Figure 3.20 shows the motor based ROP.

Figure 3.20, Mechanical ROP for Hole13

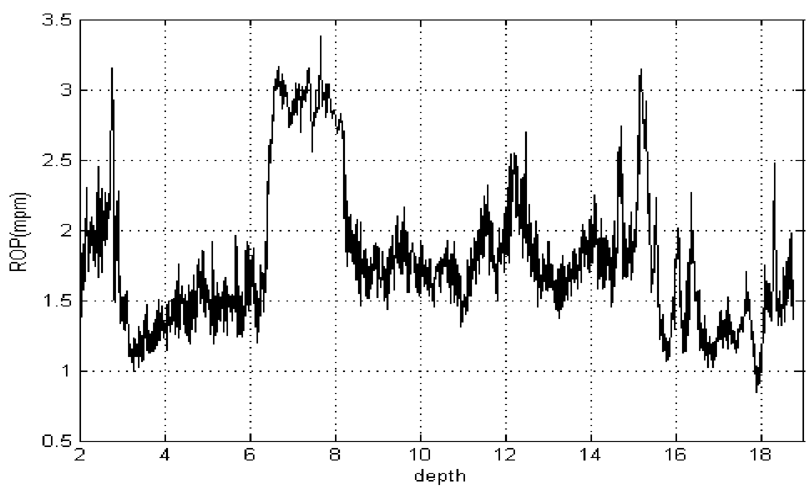

The motor based ROP (driven ROP) is not the true ROP as it is possible to put more voltage into the motor but if the ground is not broken there is no increase in ROP.

Depth and Time based ROP: To extract ROP from depth and time signal, three general approaches are proposed as follows:

1. (Hole) Averaged ROP

In this approach at each sample point ROP is calculated as the ratio of depth at each point to elapsed time from surface to that point:

$$ROP = \frac{Depth}{Time} \quad \textbf{(3.17)}$$

The Depth and Time values are coming from generated bit position signal in relative drilling time which can be based on linear interpolation, Hoist Voltage weighted interpolation or Mechanical ROP weighted interpolation. However at this section all the depth signals are based on the weighted Hoist Voltage interpolation. Figure 3.21 shows the derived average ROP.

Figure 3.21, Average ROP for Hole13

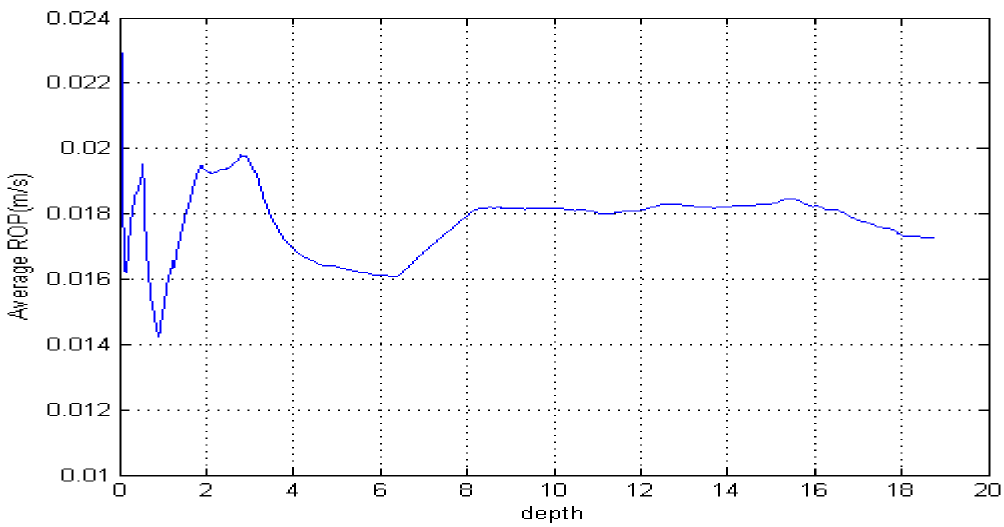

Using the above approach smooths out the rate of penetration with increasing hole depth so it cannot be a suitable representative of variation in rock hardness. Change of ground characterizations cannot be observed by this signal. Also at the collar of the hole, from 0 to 2 meter, where drilling performance through blast affected ground results in extreme fluctuations of ROP, the ROP values are not valid.

2. Instantaneous ROP

Instantaneous rate of penetration at a depth point in the hole is given by:

$$ROP = \frac{d(Depth)}{d(Time)} \qquad \textbf{(3.18)}$$

Where d is the symbol of first order differentiation. Figure 3.22 shows the derived ROP from the above definition for Hole13.

Figure 3.22, Instantaneous ROP for Hole13

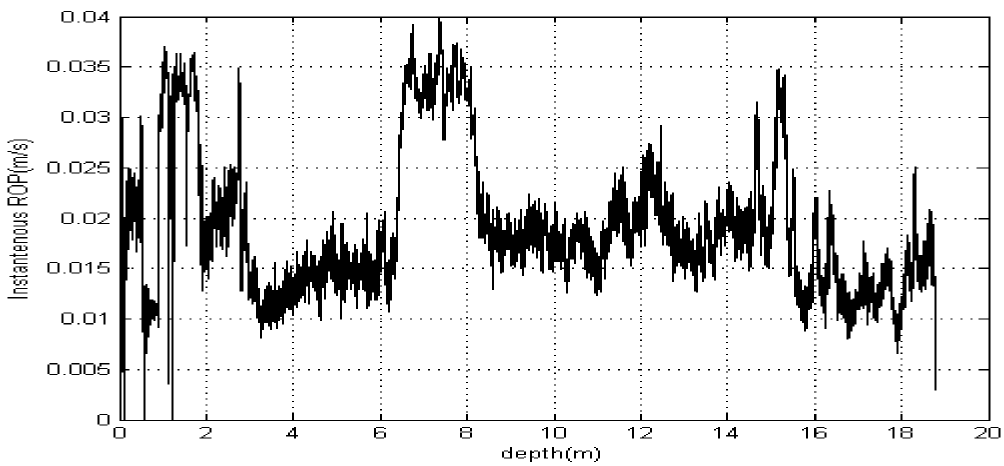

Figure 3.22 shows that due to a high rate of sampling, the instantaneous ROP has high variability. To smooth out the variation in ROP another approach is used in the CBI Algorithm.

3. Segmented ROP

This is an approach which is completed during segmentation of signals as discussed in Section 3.2.4. ROP is calculated for each 1cm increment as follows:

For a depth segment:

$$ROP_m = \frac{Segment\ Length}{Number\ of\ Sample\ Intervals \times sample\ time\ interval} \qquad \textbf{(3.19)}$$

In the above equation, sample time interval is equal to 0.0025. Figure 3.23 compares the instantaneous ROP with segmented ROP.

Figure 3.23, Depth based ROPs for Hole13

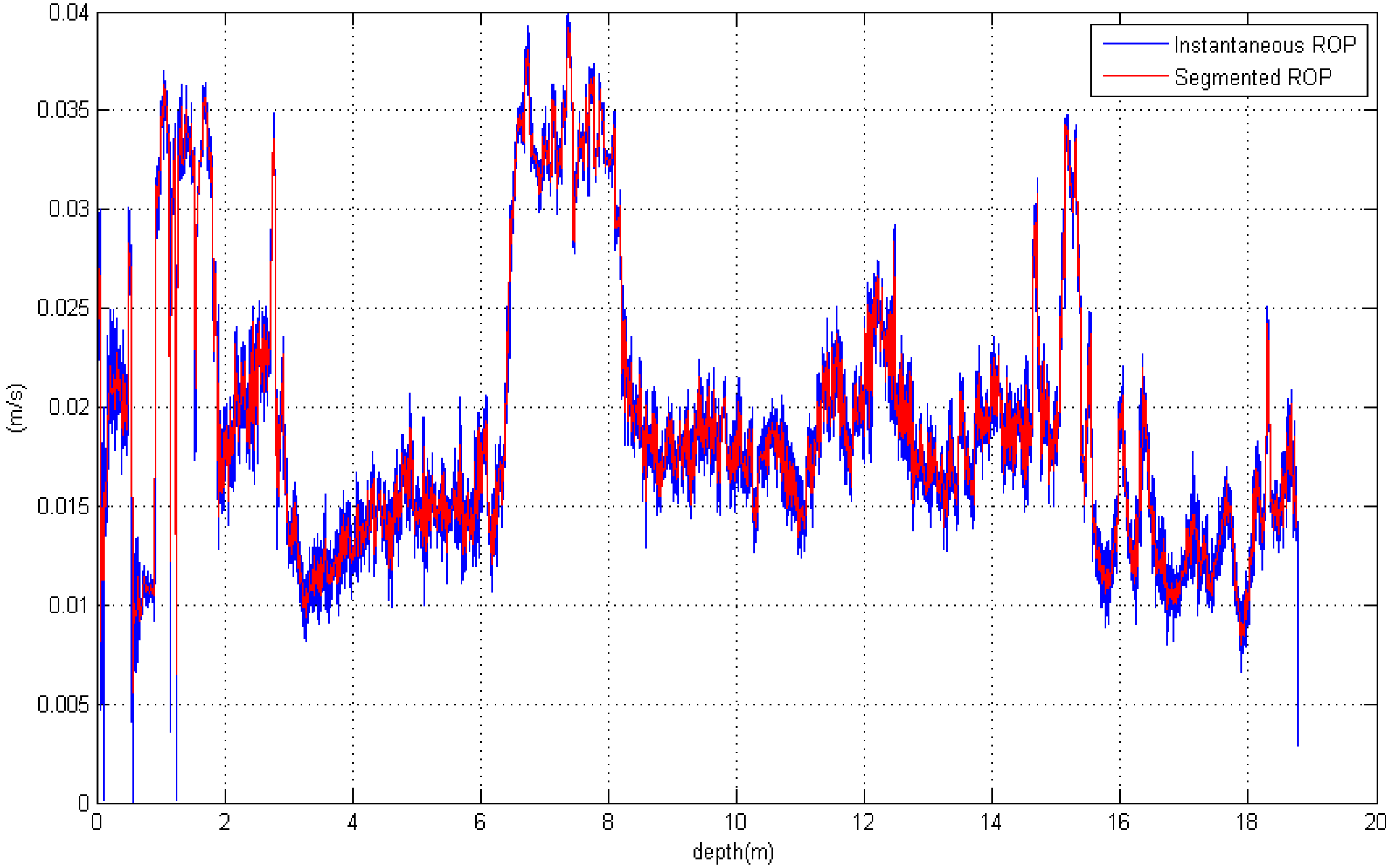

It should be considered that in the depth based ROPs when the depth has been interpolated based on Hoist Voltage, ROP does not necessarily follow Mechanical ROP since there is not a linear relationship between motor speed and Hoist Voltage based on DC motor properties. To have a ROP which follows Mechanical ROP, the depth should be interpolated based on the Mechanical ROP. Figure 3.24 compares Segmented ROP and Mechanical ROP.

Figure 3.24, Segmented ROP and mechanical ROP for Hole13

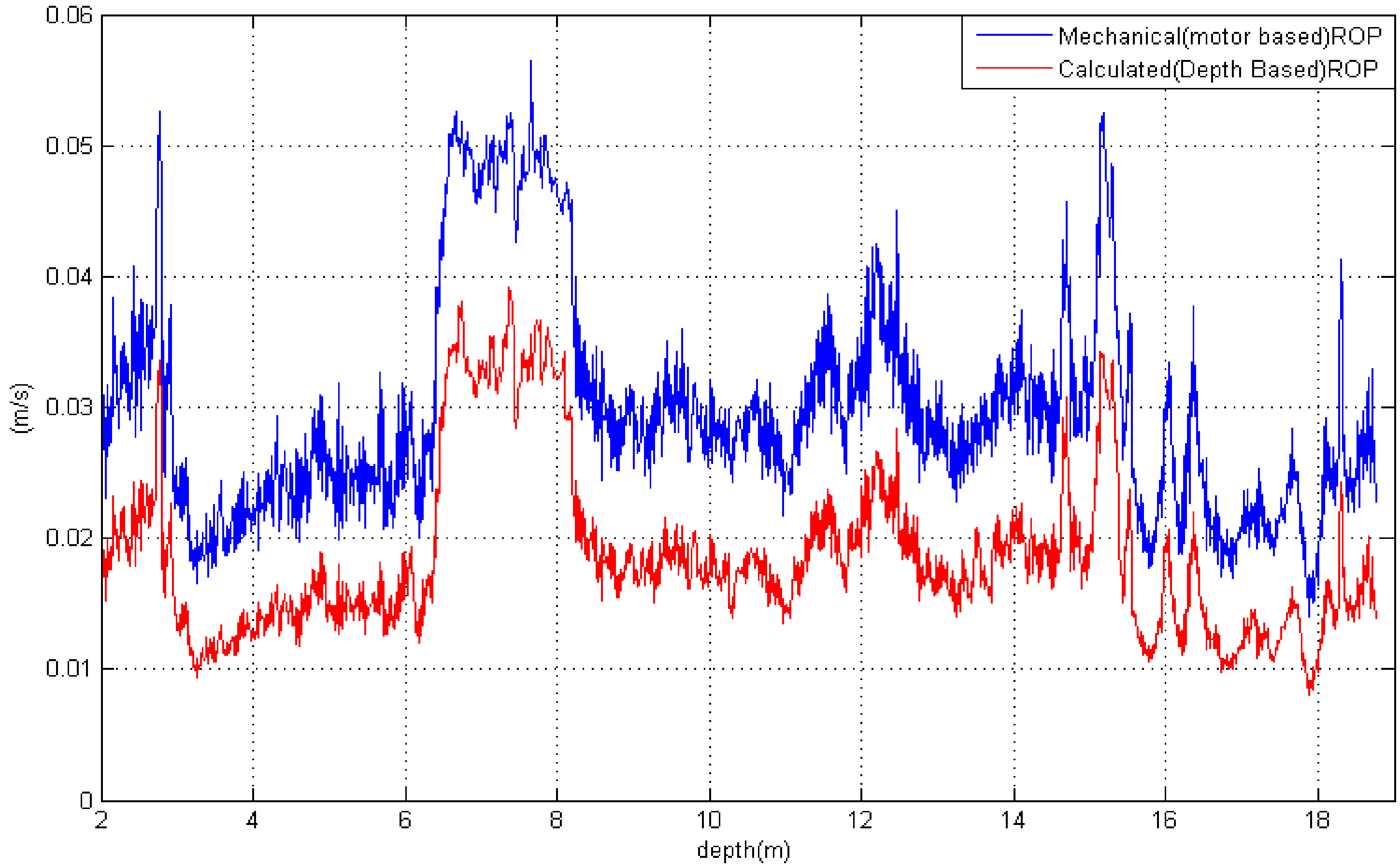

3.3.3. Mechanical Signal Approach

In the mechanical approach, mechanical SE is calculated based on mechanical drill signals. After converting the electrical signals to physical units, averaging them over 1cm depth intervals and calculating true ROP, mechanical SE is calculated by the equation below:

$$Mechanical\ SE(Pa) = \frac{WOB(N)}{Area(m^2)} + \frac{120\pi \times Rotary\ Speed(rpm) \times Rotary\ Torque(Nm)}{Area(m^2) \times ROP(\frac{m}{s})} \quad \textbf{(3.20)}$$

Figure 3.25 plots calculated electrical and mechanical SE for Hole13.

Figure 3.25, Electrical and mechanical SE for Hole13

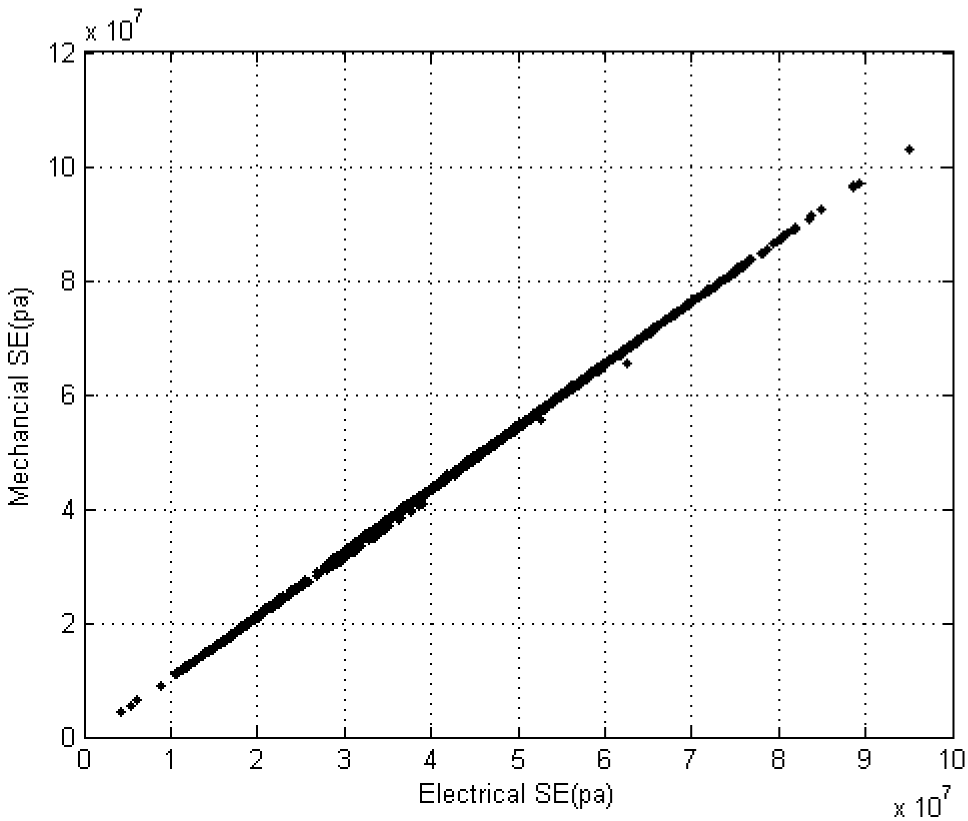

As the Figure 3.25 displays, the relationship between Mechanical and Electrical SE is linear. The correlation coefficient between these two sets is given by:

$$\mathrm{Pxy} = \frac{\mathrm{COV(X,Y)}}{\sigma x \sigma y} \quad \text{(Pearson product-moment correlation coefficient)} \quad \textbf{(3.21)}$$

Where COV is covariance and σ is standard deviation. Based on Equation 3.21, there is a strong correlation between Mechanical and Electrical SE with coefficient of 0.999. This strong correlation shows that Mechanical and Electrical SE demonstrate similar behaviour when they are plotted against depth. The performance of the Electrical Power approach compared to the Mechanical Signal approach can be quantified by calculating percent difference as follows:

$$percent\ difference = \left|\frac{Electrical\ SE - Mechanical\ SE}{Electrcial\ SE}\right| \quad \textbf{(3.22)}$$

Based on Equation 3.22, the percent difference of Electrical SE and Mechanical SE for all the test-holes are presented in the Table 3.5.

Table 3.5, Percent difference of specific energy values

Hole ID	**Percent difference (%)**
13	7.47
18	8.13
28	7.48
22	5.40
30	6.40
31	5.84
32	5.60
44	6.67

Based on Table 3.5, for Drill 13 the average percent difference is 7.69 % and while for Drill 11 is 5.98%. This shows that the accuracy of SE calculation depends on the drill performance (i.e. efficiency) and for each drill the difference between Mechanical and Electrical SE is almost constant.

3.4.Fracture Log Derivation

Having processed the MWD data into a set of segmented signal averages and derived SE by two methods the subsequent algorithmic process to determine fractures needs to be assessed against measured data. In this section geophysical logs are used to provide a tool for validation of results.

To use geophysical logs, first of all, it is important to have an understanding of the logs, their measurements and approach of measurements. Geophysical logs simply are done by lowering an instrument down the hole and correlating a feature of rock with depth. When geophysical logging is discussed it means a recording of any properties of rock formation against hole depth (Serra, 1988).

These recordings or measurements typically are categorized in two groups. In the first group, logs are based on the natural phenomena and in the second group logs are based on the induced phenomena. In the first group a detector is used to measure rock properties directly while in the second group an emitter is used to induce rocks to emit suitable response to receivers.

In this study, Formation Micro Imaging, Gamma Ray, Density, Sonic, Caliper and Neutron Logs are used for rock characterization. Among these geophysical logs, Gamma Logs and Caliper are in the natural phenomena group. In the following, each of mentioned logs is briefly discussed.

3.4.1. Formation Micro Image

FMI logs carry an array of electrodes on pads used to produce an electrical image of formation seen on the borehole wall. FMI gives micro-resistivity formation images with water as the conducting medium between the tool and hole wall. The colour of a FMI log changes based on the resistivity of formation along the borehole depth. For example in the grey scale, low resistance zones appear dark and high resistivity zone appear white and anomalies such as fractures appear on the images. They have been established as the most powerful tool in detection of fractured zones in the oil and gas industry (Schwartz, 2006). Schwartz (2006) explicitly described fracture characterization using FMI Logs in his thesis.

In general, electrical images are sensitive to variation in mineralogy, porosity and fluid content that highlights natural fractures (Gaillot et al, 2007).

3.4.2. Gamma Logs

Gamma logs measure natural gamma radiation which is produced from natural Potassium (^{40}K) in the rock along with isotopes of Uranium and Thorium. They are used to characterize rock in the borehole. Different types of rock emit different amounts and spectra (energies) of gamma radiation. Clay and shale usually have high levels of gamma radiation.

3.4.3. Density Logs

Density is one of the most useful ways to determine lithology and formation density. Density is the function of density of minerals forming the rock and the fluid in the pore spaces. These logs are a measure of back-scattering radiation by the atoms of surrounding rocks when energised by a source of gamma radiation (Wonik and Olea, 2007). The density log shows low density values in the presence of fractures, vugs (small cavities in the rock especially in the carbonate rocks) or rocks with high porosity.

3.4.4. Neutron Logs

The principal applications of neutron logs are porosity analysis, lithology identification and clay analysis. Neutrons are emitted from a source on the probe and the interactions of the neutrons with the rock in the borehole wall are measured by a detector (Wonik and Olea, 2007). Generally both the neutron log and the density log are run together to provide the best interpretation of the rock’s fabric in the hole.

3.4.5. Caliper Logs

The Caliper is a tool to measure the shape and diameter of the borehole. To measure the diameter, two sets of arms placed symmetrically on each side of logging tool are used (Serra, 1988). The diameter of the borehole depends on lithology and rock mass structure so it can be used as a contributory tool in assessment of lithology as well as detection of borehole breakout, cavities and presence of discontinuities.

3.4.6. Sonic Logs

The Sonic log shows the travel time of P-waves against depth. This log is a measurement of the capacity of the formation to transmit sounds, so based on this measurement, the type of formation and consequently its porosity can be determined. The sonic tool emits a sound wave which travels from a source into the formation and then back to receivers. Based on the pass taken by the transmitted wave, four types of waves (P, S, Reflected Fluid and Stoneley waves) are picked up by the receivers. These waves form a wave train which can be used to determine fractures. Sonic Velocity (SV), Sonic Porosity (SP) and transit time (DT) are the three measures of sonic logs that are used in this research study.

The next section presents a geometrical approach for derivation of fracture logs from FMI logs.

3.4.7. Fracture Logs

The extracted fracture zones from geophysical logs are used in both validation and interpretation of the results of the proposed approach for detection of fractures from MWD.

As discussed in the section 3.4.1, FMI logs are widely used to determine the place of fractures based on electrical resistivity differences. The interpretation process of the FMI log categorises the detected fractures as either a conductive or Open Fracture (OF), semi-conductive or Partially Open Fracture (POF) and resistive or Closed (C) Fracture. This classification is based on their resistivity which is proportional to their ability to transfer water. Open fractures are truly open (or in some cases filled with Clay) to flow and appear as low resistivity zones and partially open fractures may have been partially filled but still have some permeability. This study focuses on using the open and partially open fractures.

In the FMI logs fracture planes appear as a dark sinusoid trace (Conductive areas appear as dark zones). The available data from FMI logs are as follow:

- Hole Deviation
- Hole Dip Azimuth
- True Dip Angle
- Hole Azimuth
- Fracture depth

For all the test-holes in this research the hole deviation was less than 1 degree so all the blastholes are assumed vertical.

Fracture density is defined as the number of fractures per unit of length. To determine the fracture density the extent of each fracture within the blasthole needs to be determined. Then at each depth increment, the number of fractures intersecting the borehole can be calculated. Figure 3.26 shows how a fracture in the borehole is represented as a sinusoidal trace when the borehole wall trace is opened out onto a plane.

Figure 3.26, Planar fracture sinusoidal trace

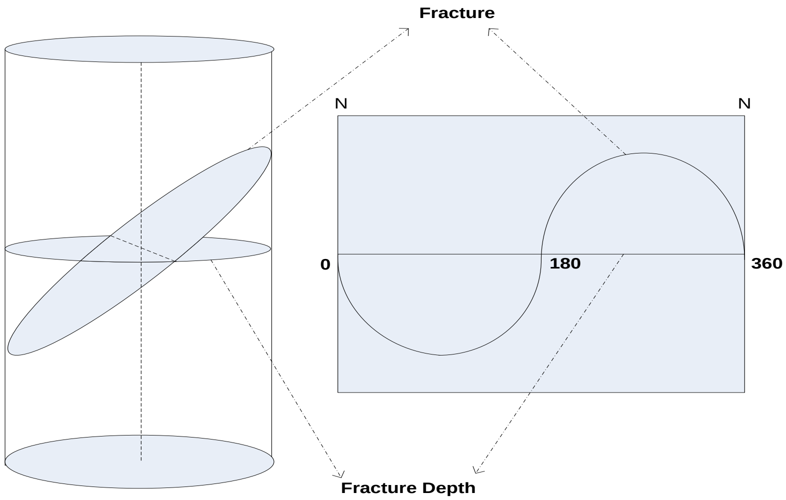

Here, the length of fracture over the borehole is defined as the peak to peak sinusoidal amplitude distance in the FMI sinusoid. Figure 3.27 shows the presence of a fracture in a FMI log.

Figure 3.27, FMI log for test-hole 13

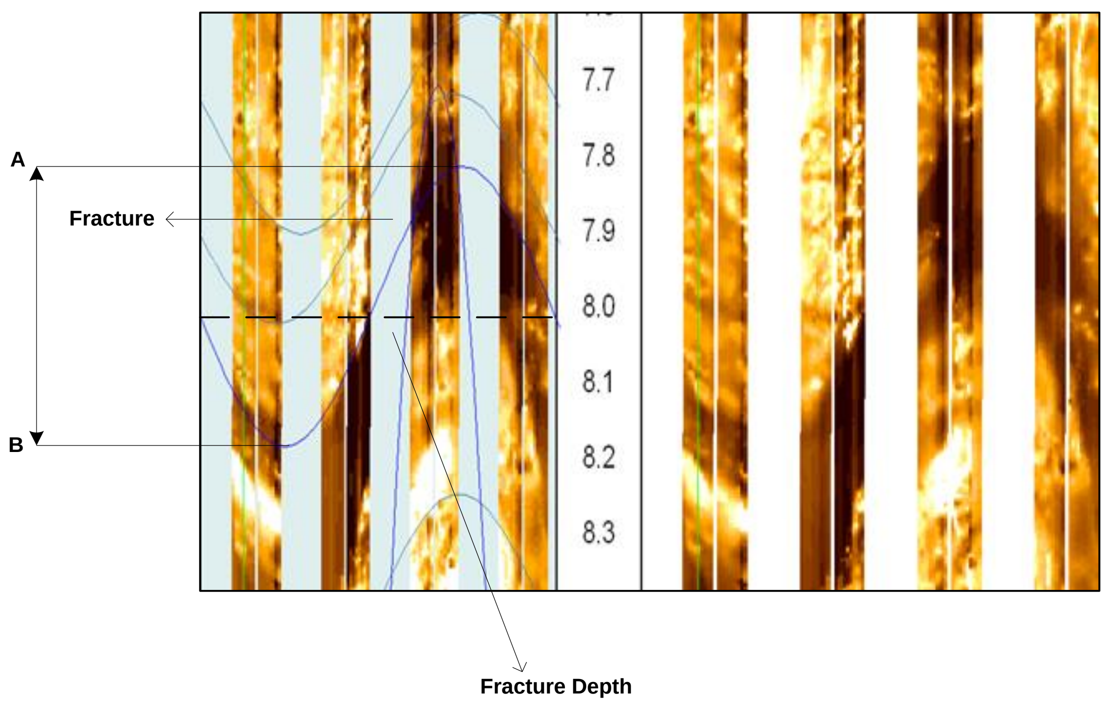

In Figure 3.27, the dark blue sinusoid is an open fracture extending over a depth 7.8 to 8.2 m from surface.

A and B are the peaks in the fracture sinusoid and the extent of fracture over borehole wall is defined as (B-A). So:

$$x = \frac{B-A}{2} \quad \textbf{(3.23)}$$

Based on geometrical analysis:

$$x = \left(\frac{D}{2}\right)\tan(\emptyset) \quad \textbf{(3.24)}$$

Where x is the half extent of fracture over borehole, D is borehole diameter and $\emptyset$ is the dip of fracture to a reference plane normal to the borehole. Since the holes are vertical, true dip and apparent dip are equal.

In using this approach it is assumed that fractures are fully intersected by the blasthole, i.e. they do not terminate within the blasthole. Also since the blasthole diameter is small in scale compared to the possible extent of the structural features, it is assumed that they are planar when intersected by the blasthole.

Based on the above terminology a computer program in MATLAB is developed to generate a Fracture Density Log (from the FMI Logs) for each test- hole.

3.5.Fracture Detection Approach from MWD

To determine possible fractures from drilling a parameter or group of parameters are sought which when plotted against depth are capable to highlight the location of fractures. Also it is important to distinguish fractures from soft zones which have an effect on ROP.

WORON is used as a measure of how it is difficult to achieve bit insert penetration. In encountering fractures there is reduced effort to achieve bit penetration. The ratio between WORON and SE, named WOSE, is plotted against depth and its peaks can reflect the location of fractures. SE as the rock strength is used to normalize WORON values for soft rock zones.

To implement this approach in the CBI Algorithm, WORON is first calculated based on the Mechanical drill signals. The following equations are used for calculating WORON and WOSE in the CBI Algorithm:

$$WORON = \frac{\frac{60 \times WOB}{ROP}}{Rotary\ Speed} \qquad \textbf{(3.25)}$$

Where WOB is in N, ROP in m/s, Rotary Speed in rpm, WORON in N/m.

$$WOSE = \frac{WORON}{SE \times D} \qquad \textbf{(3.26)}$$

Where SE (as a measure of rock strength) is in Pa and D is bit diameter in m. WOSE is a dimensionless parameter. It should be noted that WORON definition has a close relationship to that proposed definitions by Leighton (Equation 2.4) and Lopez (Equation 2.5) as rock characterization index.

After determining a fracture indicator (WOSE) based on the processed parameters, the next step is to automatically extract the location of the fractures and calculate a compensated BI values for them. In the CBI Algorithm an enhanced FRF value (Fracture Log) was developed to presents fractures over the blasthole.

For this purpose, in the CBI Algorithm smaller windows and threshold are substituted to extract the location of fractures. Window lengths of 4, 10, 80 and 150(cm) are applied on WOSE signal and 5 percent is used as threshold. These values have been chosen based on testing different scenarios using different combination of window lengths and threshold values. Then to calculate a factor which shows the presence and severity of fractures (FRF), The moving average window signals are divided by their adjacent signal (ratio: 4 cm/10 cm, 10 cm/80 cm, 80 cm/150 cm) and the data points below the threshold will keep their values, those above the threshold will not (i.e. receive a value of 1). Finally the FRF value at each data point in the CBI Algorithm is given by:

$$FRF_i = \left(\frac{WOSE_{4cm}(i)}{WOSE_{10}(i)}\right) \times \left(\frac{WOSE_{10cm}(i)}{WOSE_{80}(i)}\right) \times \left(\frac{WOSE_{80cm}(i)}{WOSE_{150}(i)}\right) \qquad \textbf{(3.27)}$$

Where ‘’i’’ is the sample index and $\frac{WOSE_{4cm}}{WOSE_{10}}, \frac{WOSE_{10cm}}{WOSE_{80}}, \frac{WOSE_{80cm}}{WOSE_{150}}$ are the ratios after applying threshold value.

This factor is an indicator of fracture localisation and ranges in values between 0 and 1. Figure 3.28 shows the smoothed WOSE signals using moving average technique for Hole13.

Figure 3.28, Moving average WOSE signals for Hole13

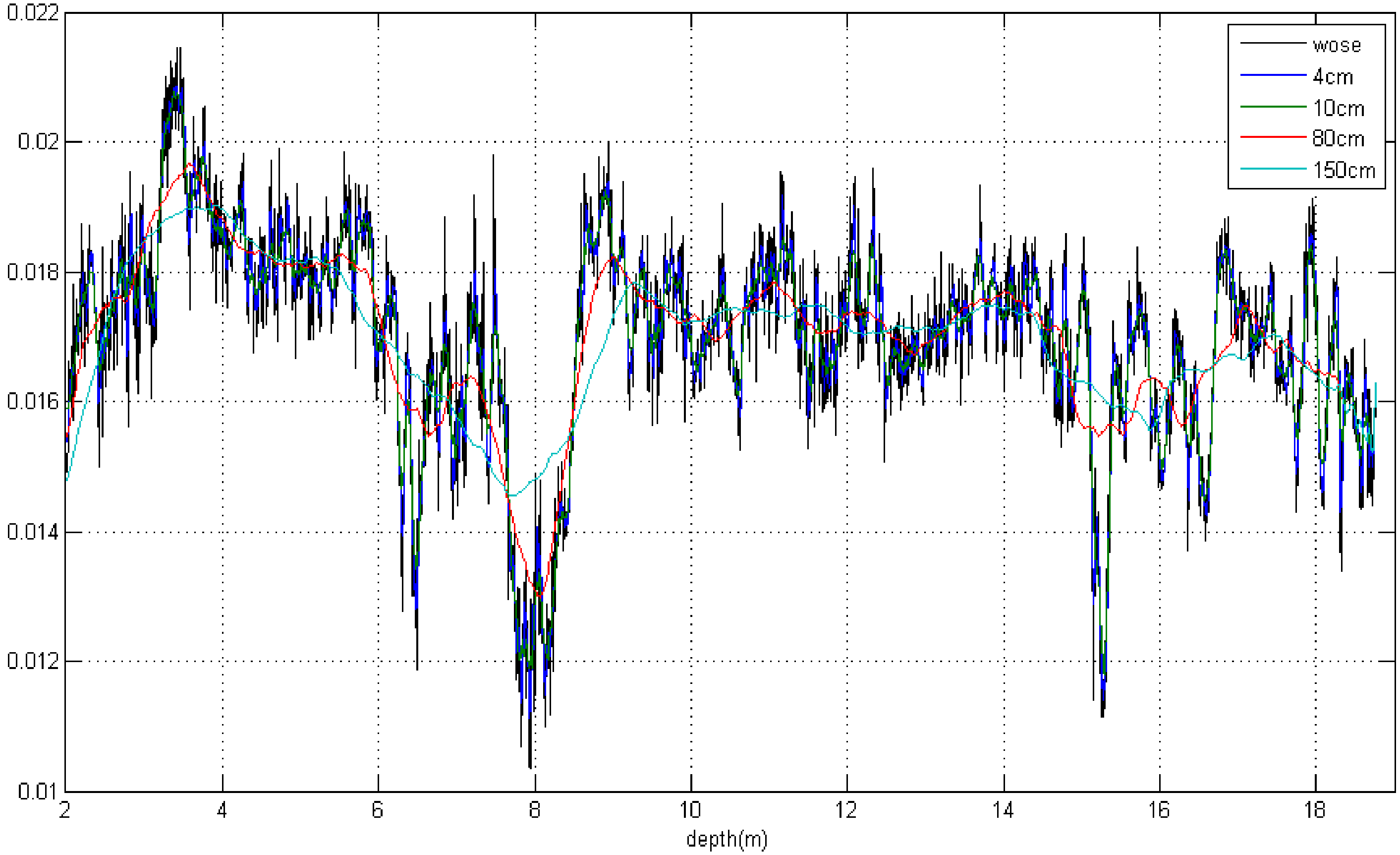

Consequently The Compensated Blastability Index (CBI) values as well as BI values are given by equations 2.10 and 2.11 respectively. These equations are repeated here for the ease of reader.

$$CBI = FRF \times BI \tag{3.28}$$

Where

$$BI = \frac{SE}{BInorm} \times 100 \tag{3.29}$$

To summarize the proposed approach for detection of fractures, Figure 3.29 shows algorithm flowchart.

Figure 3.29, CBI algorithm flowchart

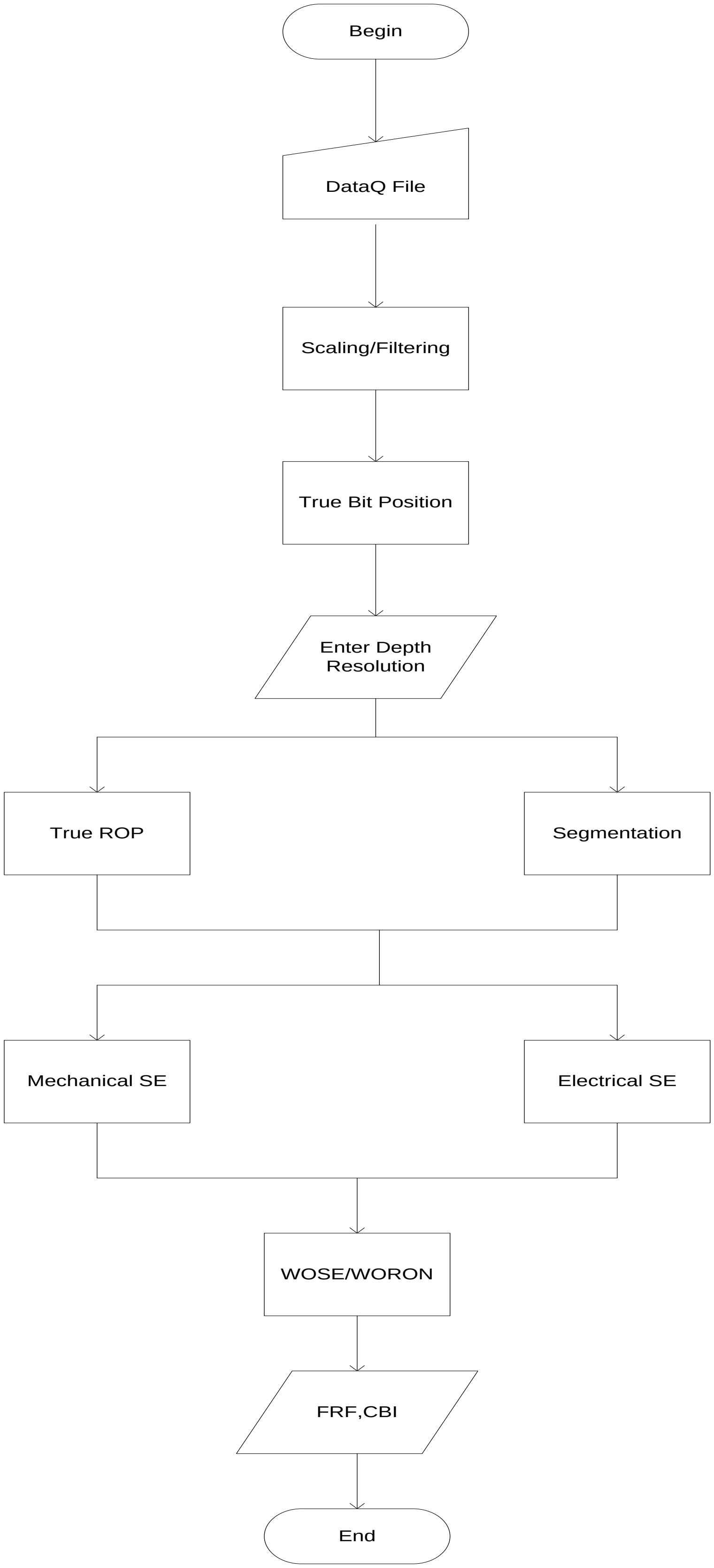

4. Data Interpretation and Analysis

After understanding the characteristics of the data sets, processing requirements, and calculating the SE, the next step is to interpret geophysical logs, examine the Alpha CBI Algorithm and to investigate the validity of proposed definitions for detection of fractures based on the response of MWD to them. Firstly geophysical logs are interpreted followed by validation of the Alpha CBI Algorithm and subsequently the relationship between natural fractures and MWD is explored.

4.1. Geophysical Logs Interpretation

As discussed in section 3.4.7, FMI logs are commonly used for detection of structural features such as fractures. A geometrical approach in the section 3.4.7 was used to derive fracture density logs.

Figures 4.1 and 4.2 show the derived fracture density logs from FMI logs for holes drilled by Drill13 (Holes: 13, 18, 28) and Drill 11(Holes: 22, 30, 31, 32, 44) respectively. In these Figures OF denotes Open Fracture and POF denotes Partially Open Fracture. The Y axis is the scaled index of fracture count which shows the numbers of fractures at each depth segment based on the following rules:

- 100 means that there is no fracture,
- Every 10 grades are equal to the presence of one fracture at each depth. For example 110 means there is one fracture, 120 means there are 2 and so on.

With respect to geophysical logs the following issues are important considerations:

- Due to the FMI tool geometry and limited blasthole depth the FMI logs are limited to the specific period of length. Table 4.1 shows the FMI range for all the test-holes.

- In this thesis the top portion of the hole (2meters) is not considered due to blast effects from the bench above and the sub-drill and is truncated from the plot
- The geophysical logs zero depth is not assured to exactly align with blasthole depth zero thus allowing latitude to shift the trace by a small amount (< 0.3m).
- There is a possibility that FMI logs overstate what actually is in the ground.

Figure 4.1, Fracture density logs derived from FMI log for Drill13

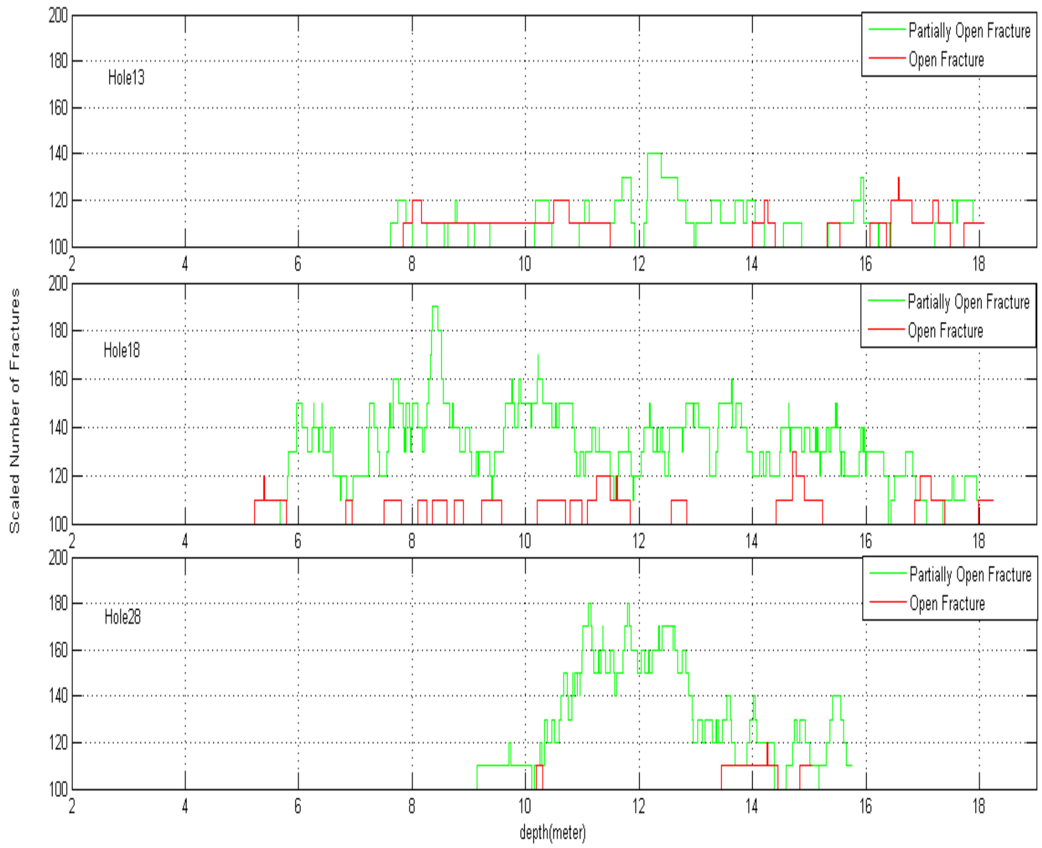

Figure 4.2, Fracture density logs derived from FMI log for Drill11

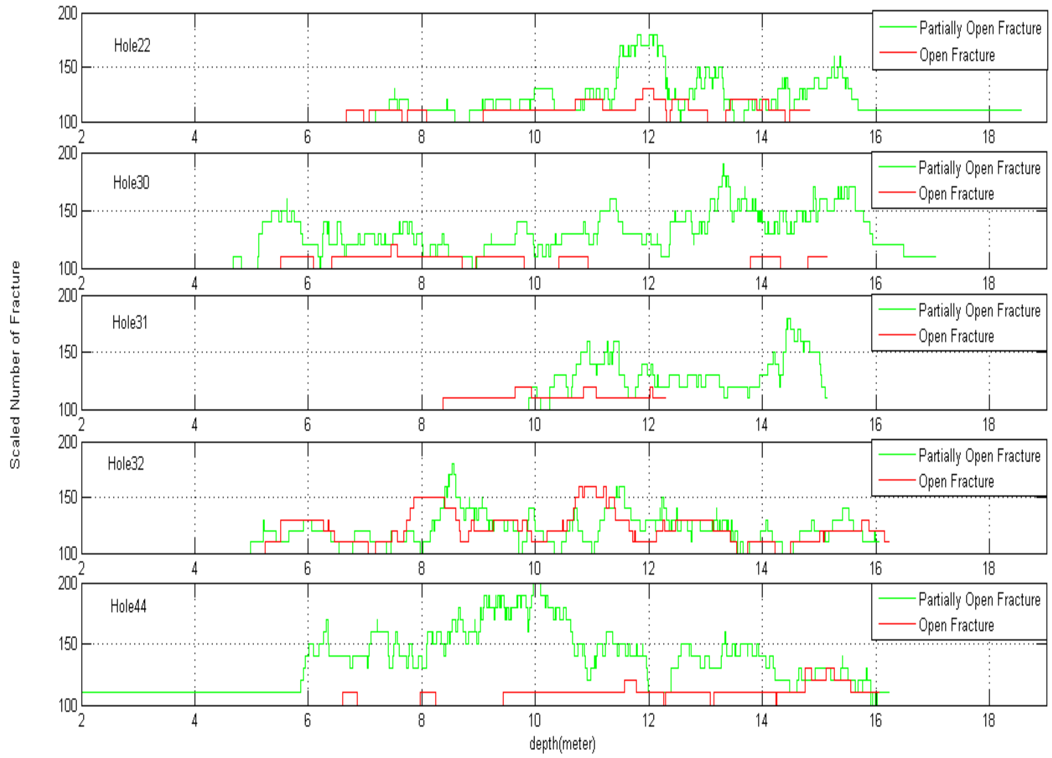

Table 4.1, FMI range in the blasthole

Hole ID	FMI Range(m)
13	7.1-18.1
18	5.1-18.3
28	9.1-16.1
22	4.4-16.8
30	4.4-16.8
31	8.4-15.1
32	4.4-16.5
44	5.3-16.4

In addition to fracture density, fracture dip angle can be an indicator for categorizing the fractures in terms of likely response of MWD to the presence of the fracture. For example it can be challenged whether high dip fractures can be detected by MWD. Figures 4.3 and 4.4 show histogram distributions of open and partially open fracture dips as determined from FMI Logs respectively for Hole13.

Figure 4.3, Open fracture dip angle distribution for Hole13

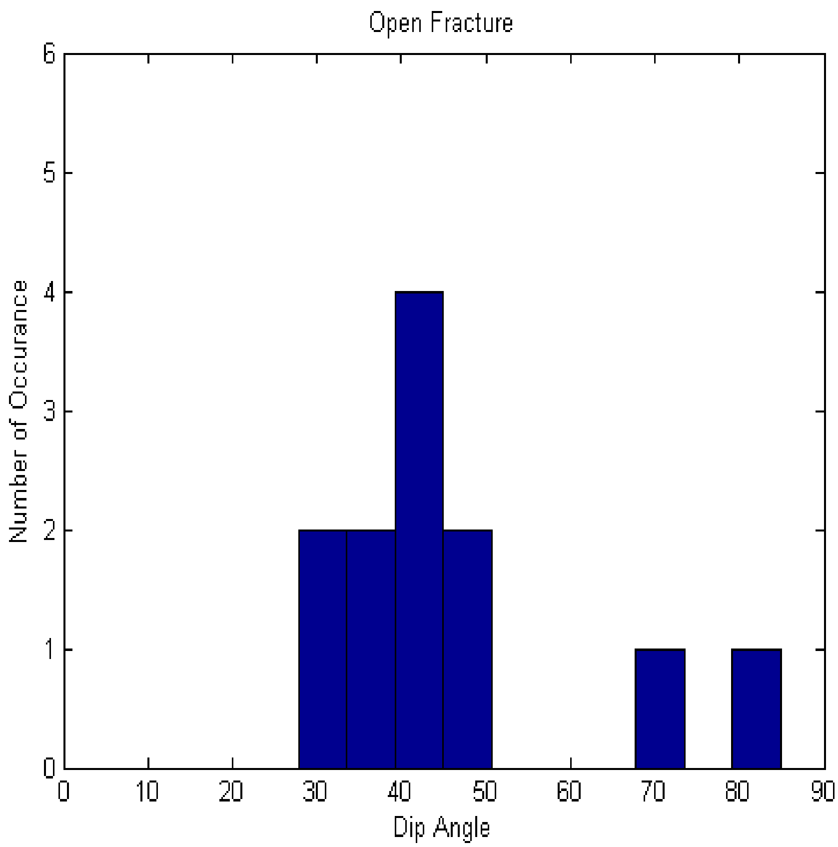

Figure 4.4, Partially open fracture dip angle distribution for Hole13

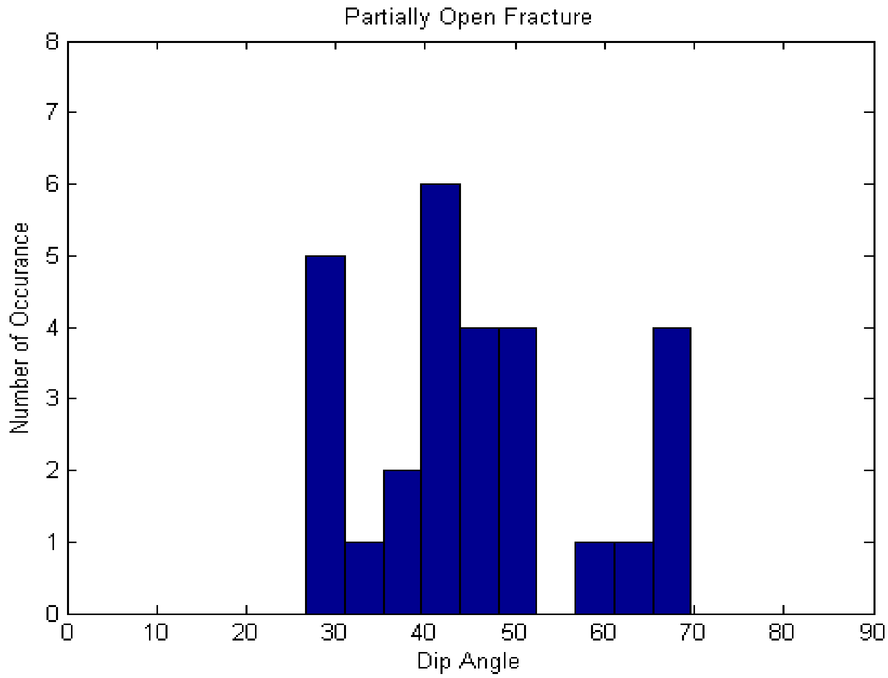

As Figures 4.3 and 4.4 show two primary fracture sets exist in both open and partially open cases. One is from 30 to 50 degree as a moderate dip and the other one is approximately from 60 to 80 degree as high dip planes.

To classify the probability of detecting fractures (Open, Partially open and Closed) by CBI algorithm, they are grouped based on their dip angle shown in the Table 4.2.

Table 4.2, Fracture classification based on the fracture dip angle

Fracture Classification	**Dip Angle**
Low dip	0-30
Moderate dip	30-60
High dip	60-90

In addition to FMI Logs and caliper, other logs such as Sonic Porosity, Neutron Porosity and Formation Density can be used to detect some fractures. The difference between sonic and neutron porosity represents secondary porosity consisting of fractures but this is not accurate in the case of heterogeneity of formation. In addition to sonic porosity, the sonic transient time (DT) value increases and sonic velocity decreases while sound wave passes through a fracture. However all of these statements are simple rules and they can change based on different circumstances.

Due to the presence of fractures, vugs or in broader view, secondary porosity through different phenomena such as dolomitization, the density of bulk formation decreases so the density logs can be used to determine the fracture zones but it highly depends on the size of fractures and presence of other discontinuities. Figure 4.5 shows a modest relationship in that large fracture densities align with Neutron/Density porosity peaks. Figure 4.6 shows that high sonic porosity peaks can correlate with large fracture densities. These results can be checked on FMI as well.

Figure 4.5, Correlation between neutron/density porosity and fractures

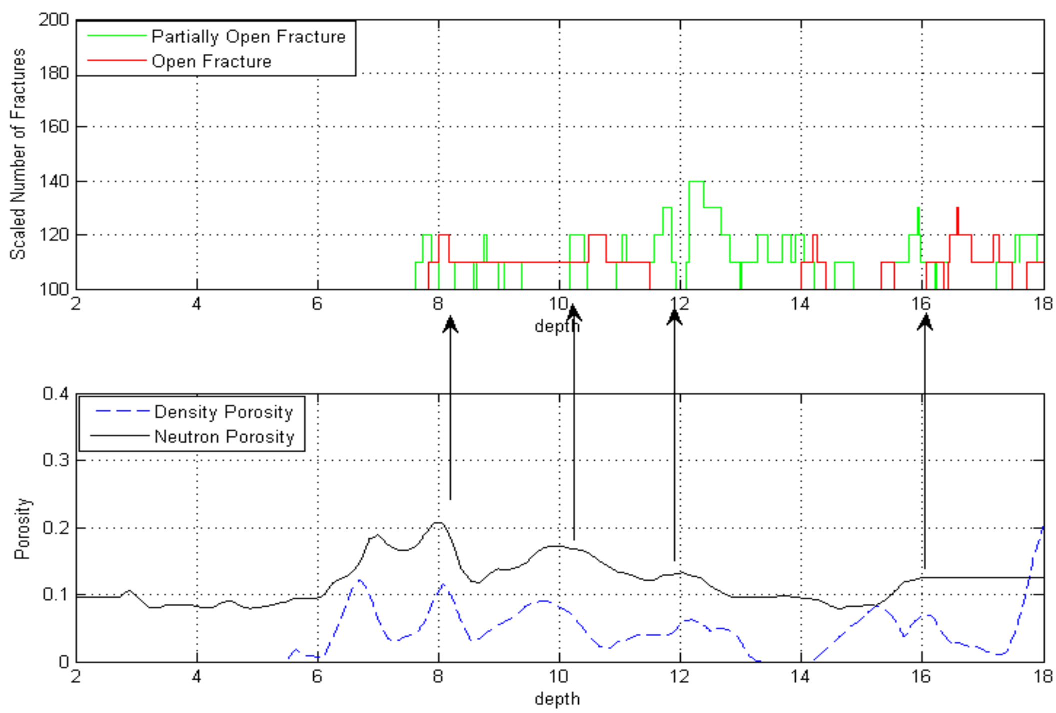

Figure 4.6, Correlation between sonic porosity and fractures

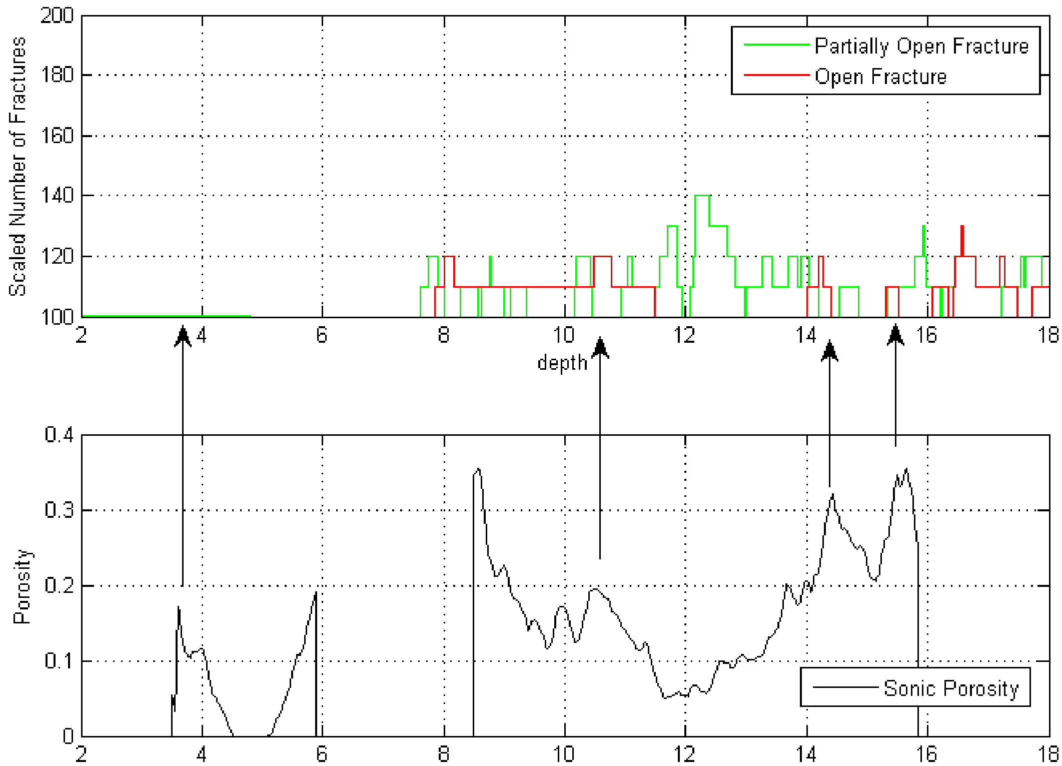

Therefore it can be concluded that Neutron and Sonic logs can be used as a backup tool for validation of fracture logs derived from FMI especially during the period where FMI Logs were not taken.

4.2.Evaluation of Alpha Algorithm

By deriving fracture logs from FMI Logs in Section 3.4 and then interpreting them based on other logs such as caliper, sonic porosity, neutron porosity and formation density, the results of Alpha CBI Algorithm for detection of fractures was investigated. In the first iteration the Alpha CBI Algorithm is run and the FRF (%) results and fracture density logs are plotted to compare them. As a representative of both benches, Hole13 and Hole32, in Figures 4.7 and 4.8, demonstrate moderate and weak correlation between Alpha CBI Algorithm FRF results (Fracture Zones) and derived fractures from FMI log.

Figure 4.7, Alpha CBI algorithm results versus OF and POF logs for Hole13

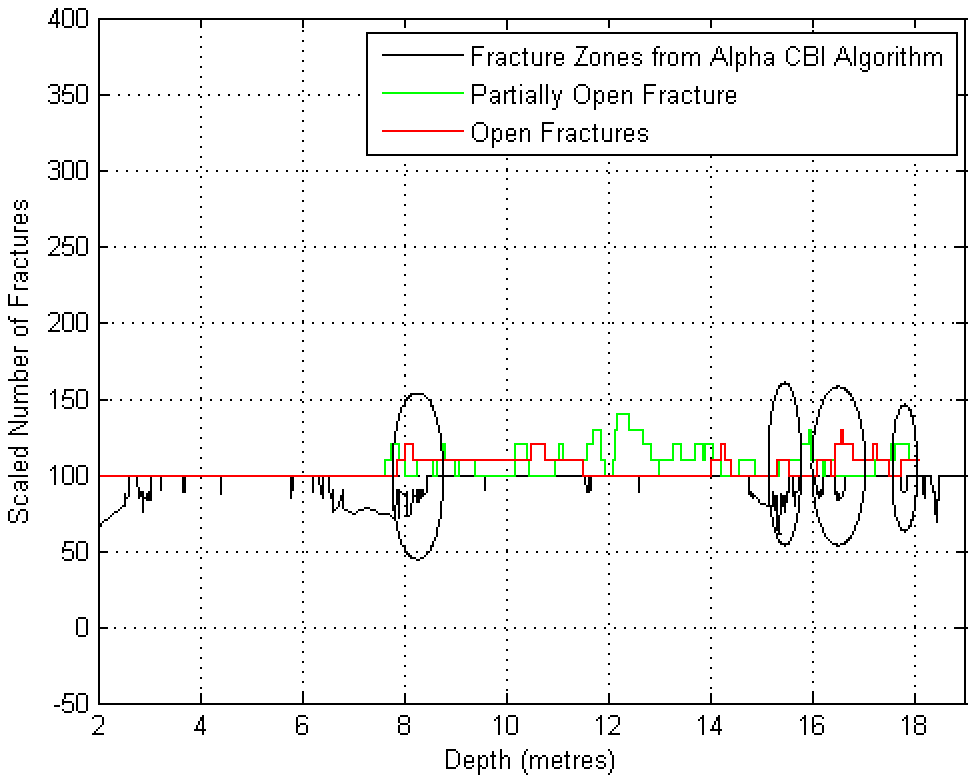

Figure 4.8, Alpha CBI algorithm results versus OF and POF logs for Hole32

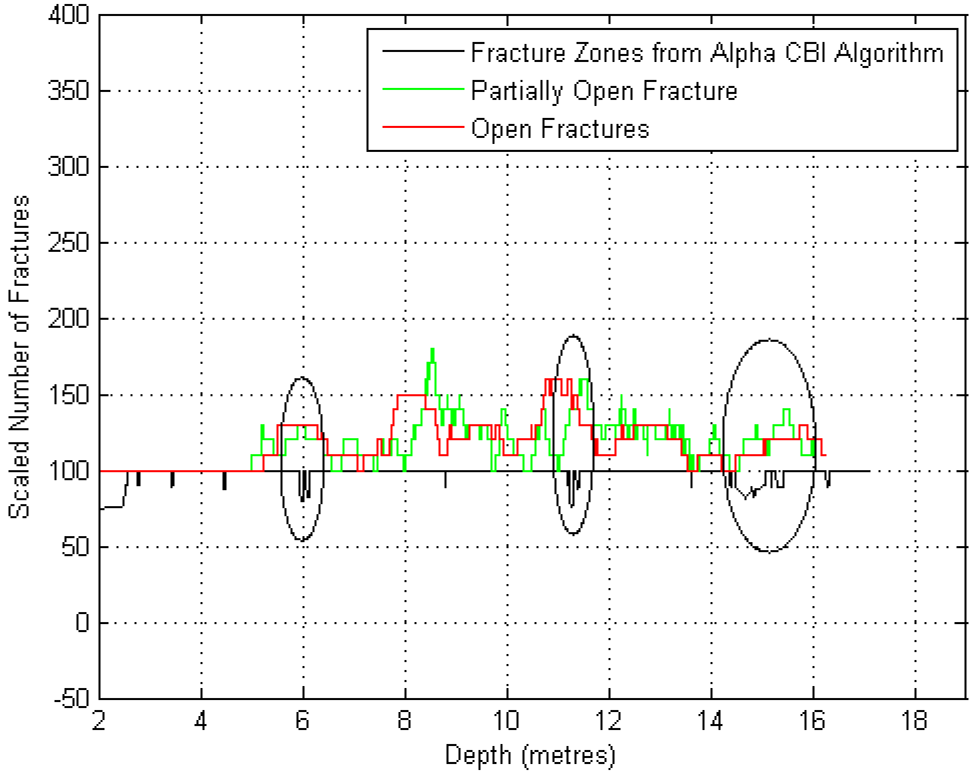

As the black ellipses in Figures 4.7 and 4.8 illustrates, the Alpha CBI Algorithm can determine some open fracture zones. However there are some open or partially open fractures that it did not detect. As previously mentioned It should be considered that the FMI Logs (OF &POF) were taken for specific period of blasthole so the observed mismatches at the beginning part of the hole are not because of wrong detection by Alpha CBI Algorithm. In this case other logs such as sonic can be used. The results of Alpha CBI Algorithm for other holes are presented in Appendix B.

After comparing the results of Alpha CBI Algorithm with geophysical logs, it can be concluded that Alpha CBI Algorithm (Data Processing and Fracture Detection) needs to be revised since it cannot reliably locate fractures.

4.3. Response of MWD to Fractures

To demonstrate the ability of proposed definitions in Section 3.5 for locating the fractures, it is important to have a good understanding of rock breakage process while drilling in either a rock mass without any fractures or in a fractured rock mass.

As discussed in the Section 2.2.1, rock fragmentation in the rock-bit interaction starts with abrasion where inserts are engaging to the rock face under small WOB. This causes small cracks on the rocks. By increasing WOB, the bit inserts will penetrate more in the rock and the cracks will propagate. WOB will increases till deep cracks get connected. Now with a heavy rotary torque, the rock is crushed.

To investigate the response of MWD signals to the presence of fractures, the processed signals are examined for their response to open or partially open fractures in either hard or soft rock conditions

As an example, for Hole13, Figures 4.9, 4.10, 4.11, 4.12 and 4.13 show ROP, Pulldown Force, Rotary Speed, Rotary Torque and Bailing Air Pressure respectively and corresponding open and partially open fracture logs. It is recognised that there is an option to shift fracture logs a little bit[7] since geophysical logs zero may not align exactly with blasthole zero depth.

[7] The geophysics zero can be lowered a little bit as geophysics depth zero is based on some timber placed over cuttings which is higher than hole collar.

Figure 4.9, ROP and open and partially open fractures for Hole13

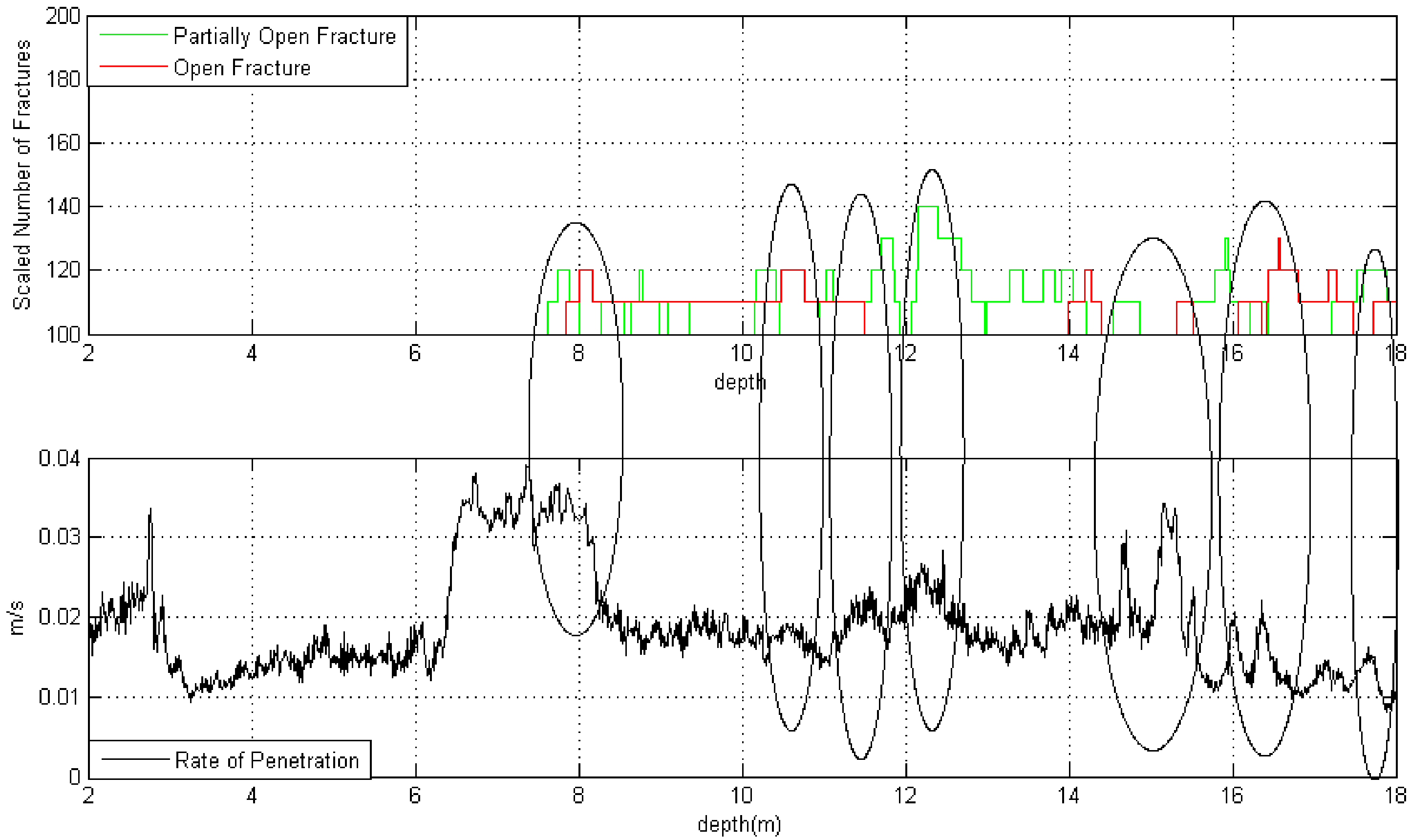

Figure 4.10, Pulldown force and open and partially open fractures for Hole13

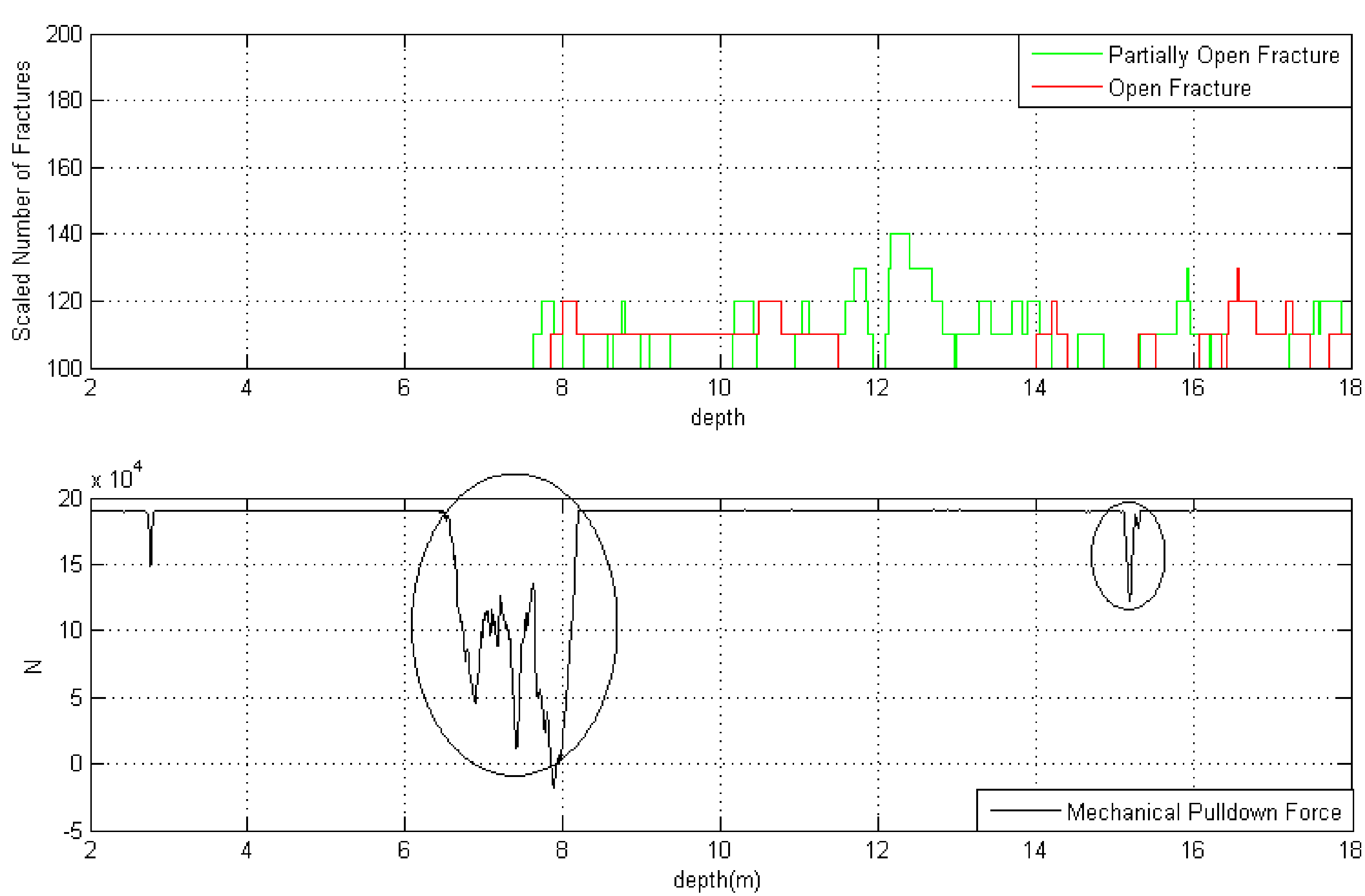

Figure 4.11, Rotary speed and open and partially open fractures for Hole13

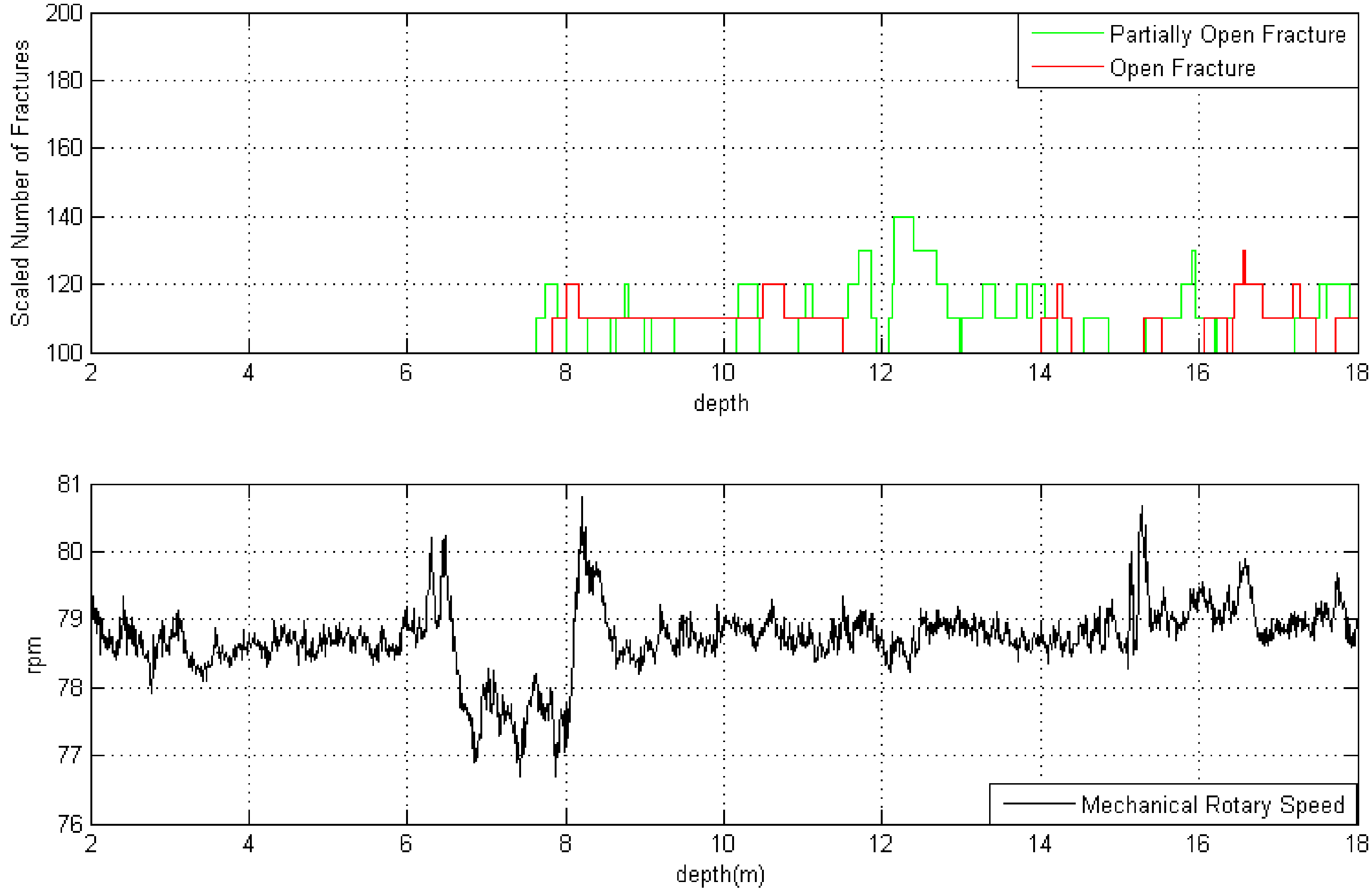

Figure 4.12, Rotary torque and open and partially open fractures for Hole13

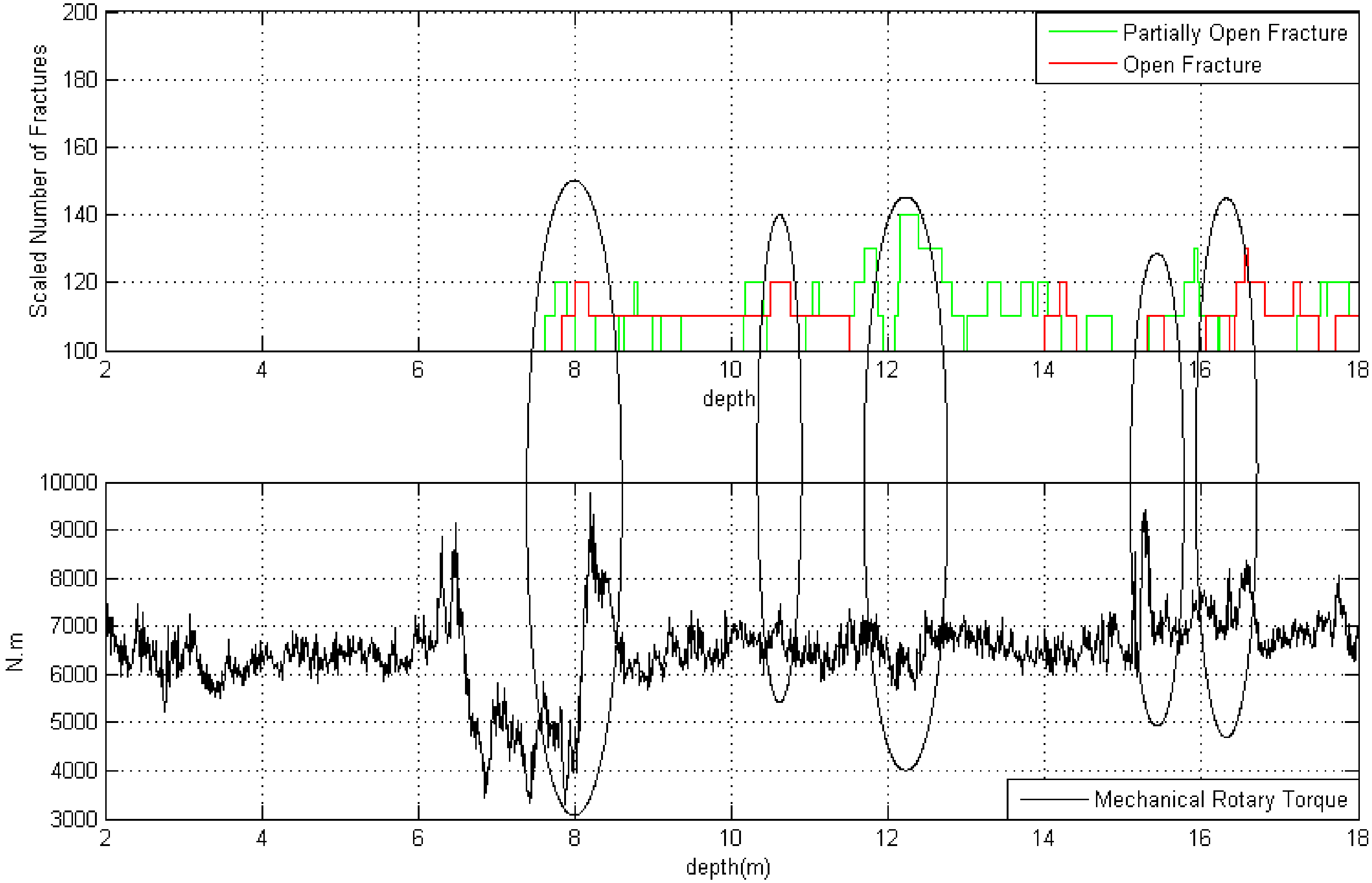

Figure 4.13, Air pressure and open and partially open fractures for Hole13

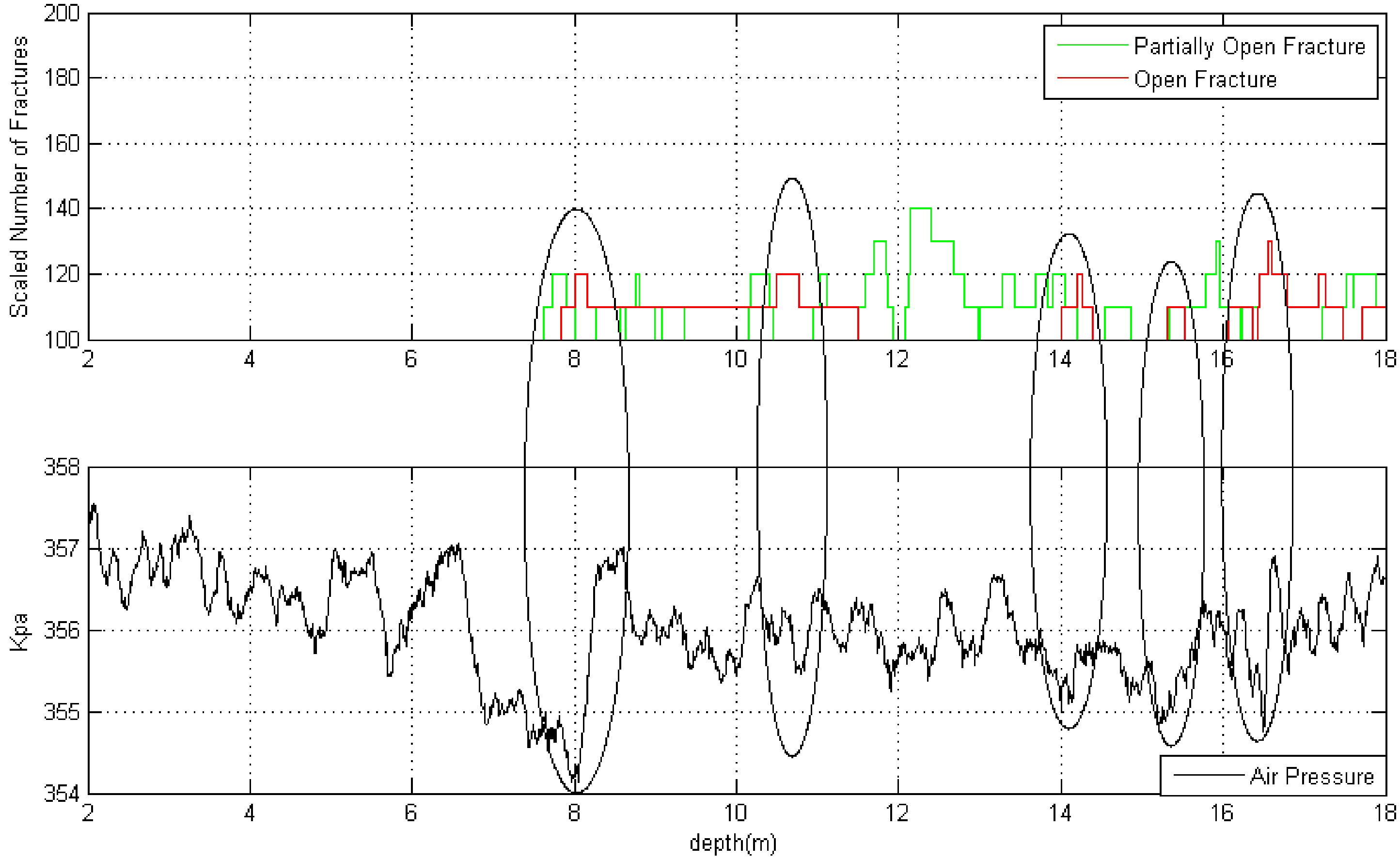

In encountering an open fracture, ROP increases because there is no resistance. Ellipses on Figure 4.9 show that ROP peaks occur at almost all the fractures density peaks. When the bit is traversing an open fracture since it is not engaged with rock, the rotary torque decreases (approaches zero based on the size of fractures) but when the bit hits the rock a rapid increase is observed. Ellipses in the Figure 4.12 demonstrate this statement. The rapid traversing of the bit causes the inserts to be buried quickly once the bit is engaged again to the rock face. Furthermore because of no engagement with rock, theoretically pulldown forces decreases as well when the bit is traversing the large fractures. In addition to all of these observations a slight drop off in the air pressure due to loss in the fractures can be observed as Figure 4.13 shows. The issue for 49R drills is that the compressor has very large capacity for the required flow rate to clear cuttings and it is hard to see much variation in bailing pressure.

However, all of these observations are not always true and they depend on several factors. WOB and rotary speed are controlled drill parameters and are almost constant in auto-drilling mode while ROP and Rotary Torque are responses. If ROP exceeds ROP threshold when it encounters the fracture then auto-drill intervenes by reducing WOB. Figure 4.14 compare ROP and HCP speed reference for Hole13.

Figure 4.14, ROP and HCP drive speed reference for Hole13

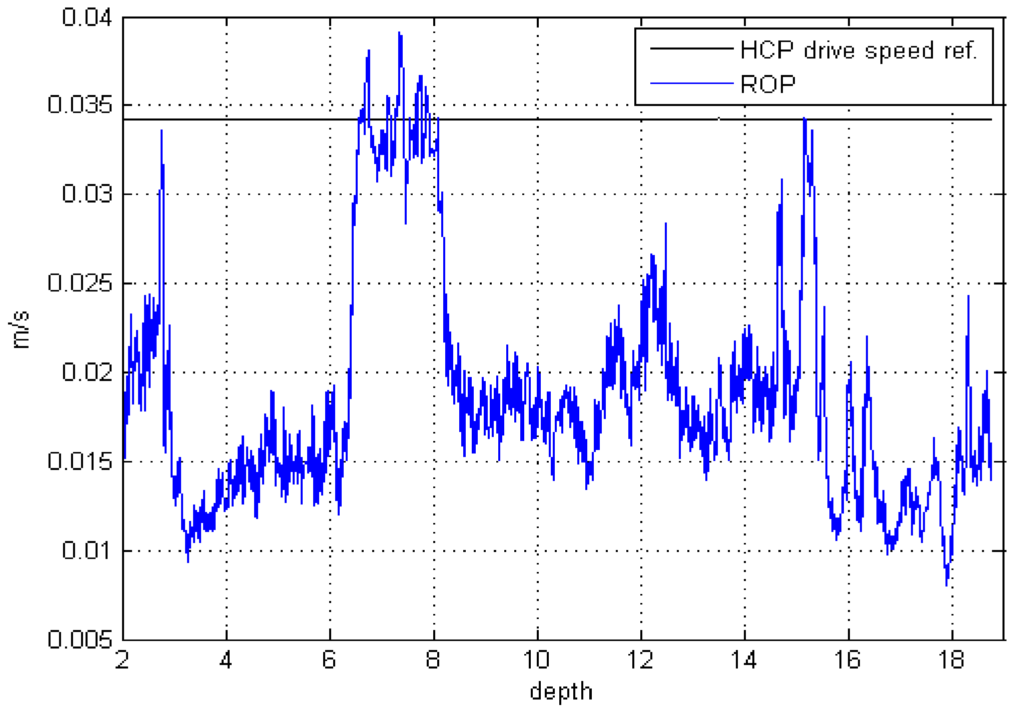

Figure 4.14 show that from 6 to 8 m depth interval, ROP has exceeded the Auto-drill ROP Threshold. To compensate for this, Auto-drill control decreases WOB as shown in Figure 4.19.

On the other hand ROP and rotary torque reflect the geology. In soft rock drilling ROP is high and rotary torque is low while in the hard rock drilling ROP is low and rotary torque is high. Furthermore ROP and Rotary Torque are affected by bit wear and variation in WOB and Rotary Speed which in some cases has a great impact on the results.

In addition, for some blastholes the ROP, Rotary Speed and even Rotary Torque show some large spikes which are believed to be the result of reference signal perturbations caused by autodrill as a response to excessive vibrations. These fluctuations can affect the interpretations and even feature in the CBI Algorithm results. Figure 4.15 shows an example of these perturbations for Hole32.

Figure 4.15, Drive speed references influence on ROP and rotary speed for Hole32

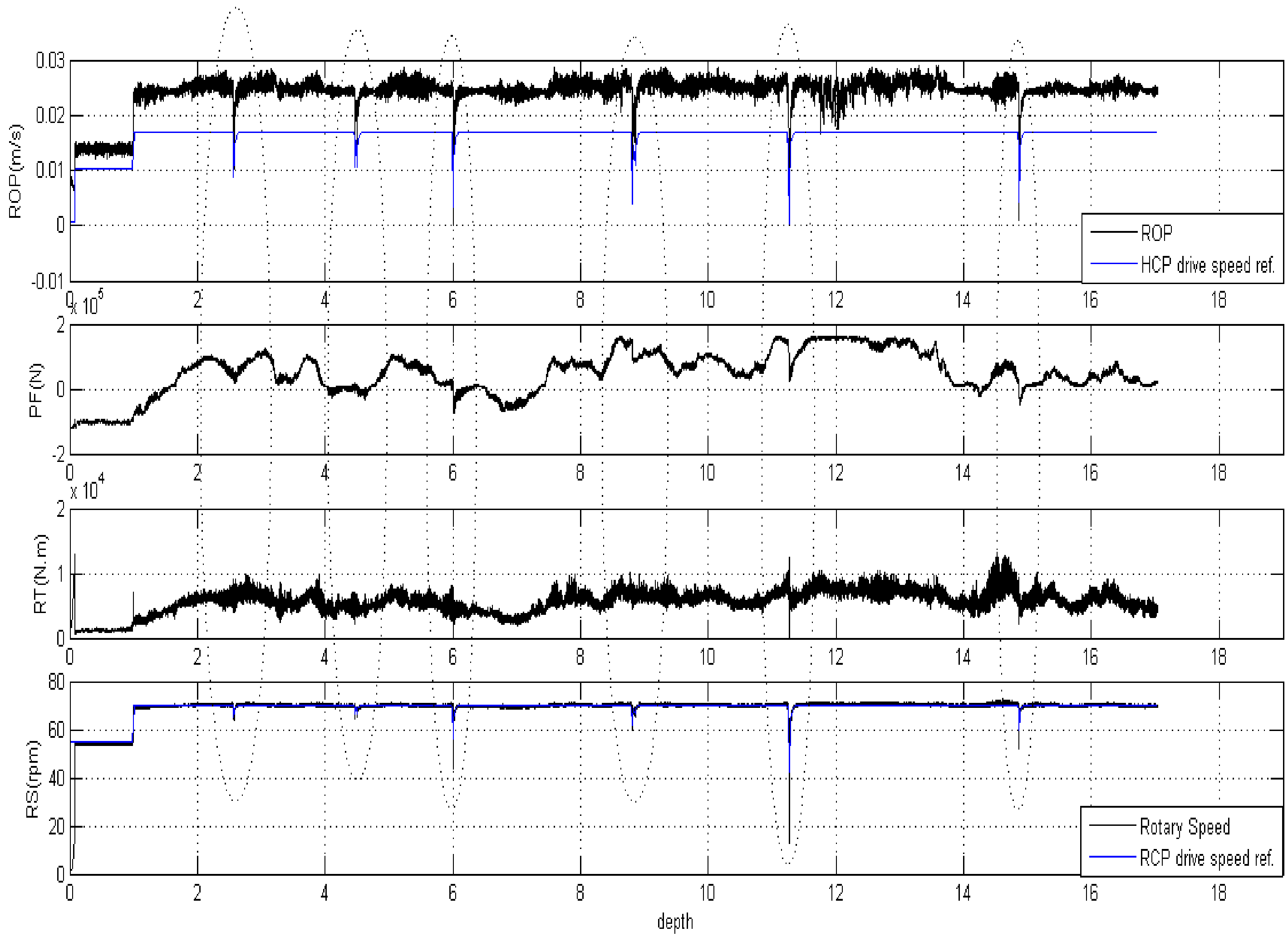

As ellipses in Figure 4.15 show, RCP drive speed reference and Hoist drive speed reference which are required speeds and set by technician (operator), can cause confusion in interpreting MWD by affecting drill mechanical variables. Thus cognizance of these situations through reading of reference signals needs to be taken in to account when using MWD for ground characterization.

Consequently, the above discussion demonstrates that ROP can locate either fractures or soft zones. In the auto-drilling mode, WOB and Rotary Speed are almost constant so it is expected that WORON shows inverse behavior to ROP to the presence of fractures. Figure 4.16 compares WORON and ROP for Hole13.

Figure 4.16, WORON and ROP for Hole 13

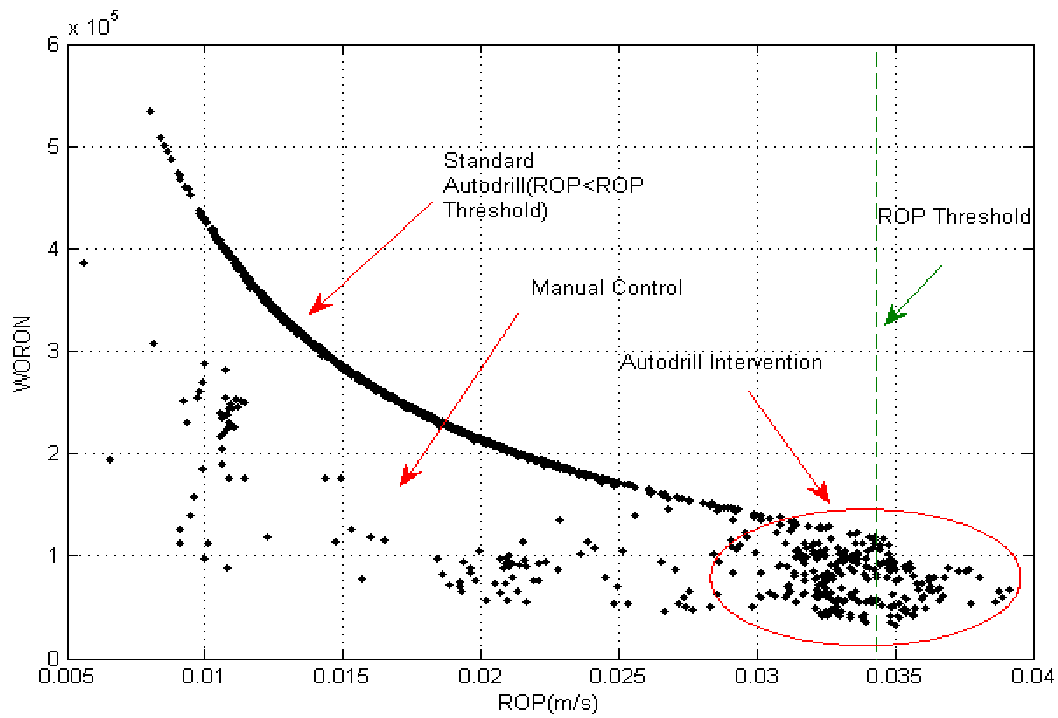

Figure 4.16 shows that in the auto-drilling mode where WOB & RPM are constant, WORON has an inverse relationship with ROP. Then when ROP approaches to auto control ROP threshold

there is a clustered scatter. The remaining scatter points under the curve are due to manual drilling.

As discussed in Section 3.5, to distinguish fractures from soft zones WOSE is introduced. Based on WOSE definition, SE is used to normalize WORON values.

The final question is whether the WOSE definition is to be defined based on Electrical or Mechanical SE. To investigate this issue, for all the test holes, WOSE is computed based on both definitions and then the calculated fracture logs (FRF Values) by CBI Algorithm are compared to open and partially open fracture logs form FMI Logs. Figure 4.17 displays the results of CBI Algorithm based on these two definitions for Hole13.

Figure 4.17, CBI algorithm results for electrical and mechanical SE definitions

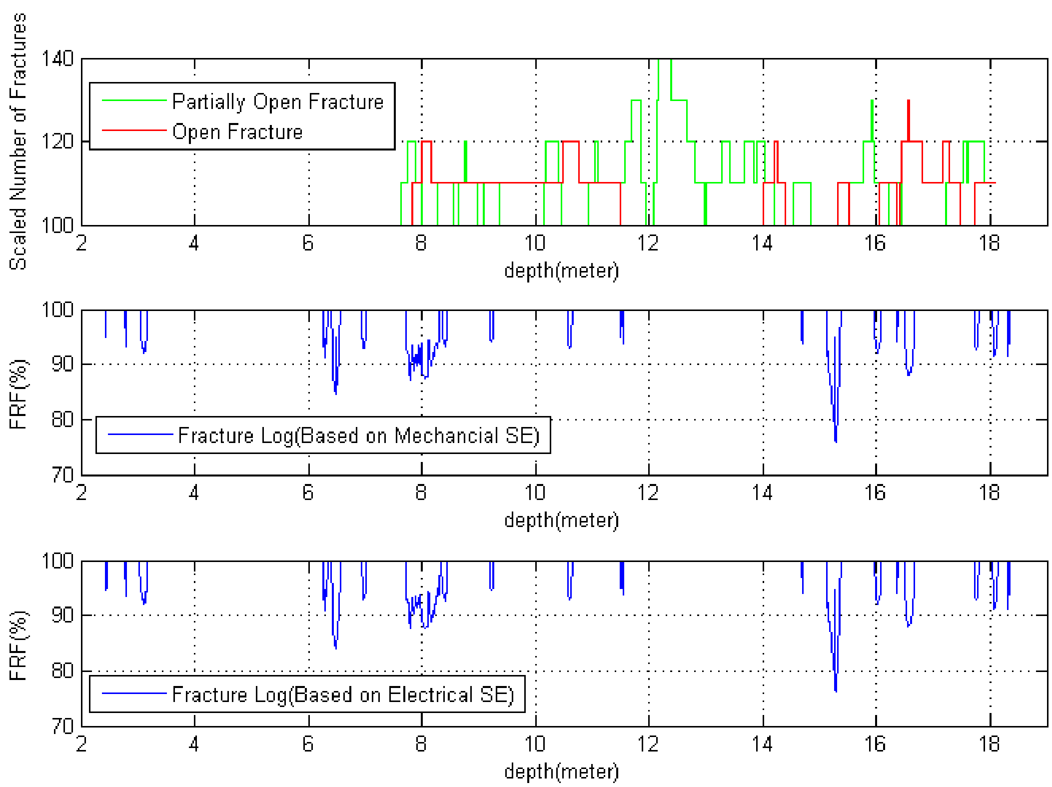

As Figure 4.17 shows in encountering fractures they have the same response in the final results of CBI Algorithm. For convenience in this thesis all of the algorithm calculations are based on the mechanically derived SE.

Through interpretation of the geophysical logs and exploring the response of MWD to occurrence of fractures and demonstrating the ability of WOSE as an indicator of fractures, the CBI Algorithm is a process with revised features to Alpha CBI Algorithm. Therefore in the next chapter CBI Algorithm results are examined by comparison to fracture logs.

5. Case Study Results

To evaluate the CBI Algorithm, the data, after conversion, filtering, segmentation and SE calculation is input into the algorithm. The algorithm output of a fracture indicator (the FRF) is plotted against the fracture density log derived from the FMI log as described in section 4.1. At the same time the blastability index along with the compensated index are plotted.

5.1. Drill 13 Test-Holes

Figures 5.1, 5.2, 5.3 present the calculated fracture and blastability logs for test-holes 13, 18 and 28 respectively. The top plot shows the fracture density logs from FMI and the bottom shows fracture signal from CBI Algorithm.

Figure 5.1, CBI Algorithm results for Hole13

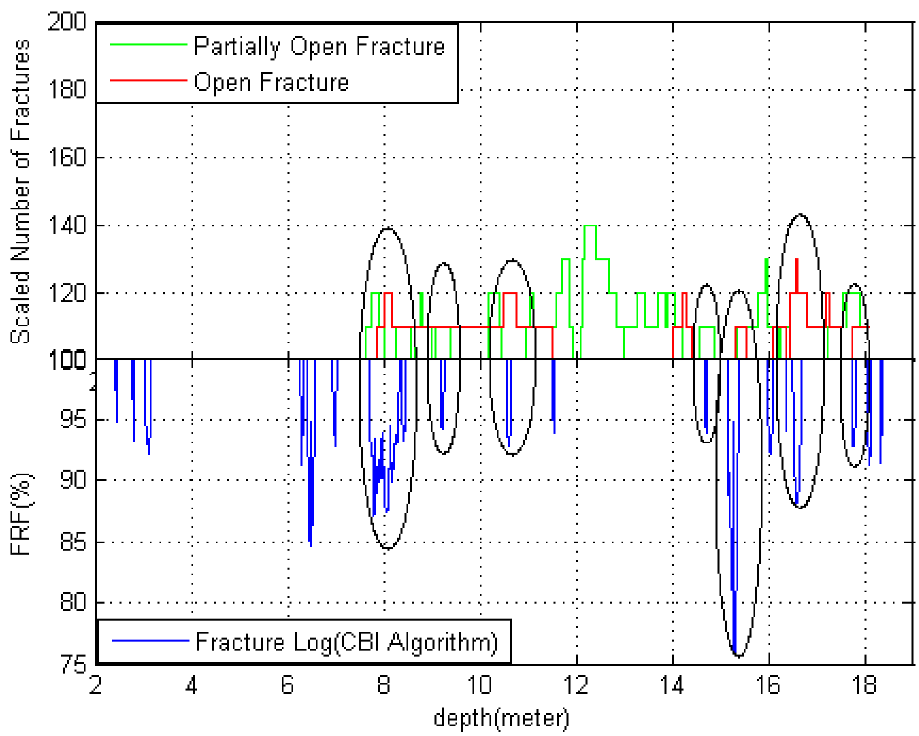

Figure 5.2, CBI Algorithm results for Hole18[8]

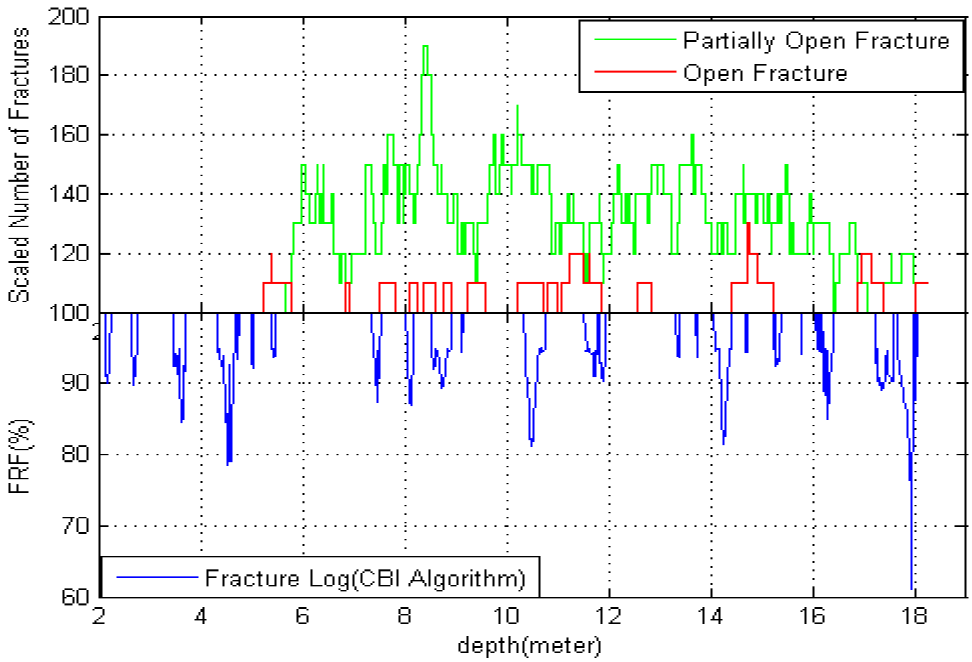

Figure 5.3, CBI Algorithm results for Hole28

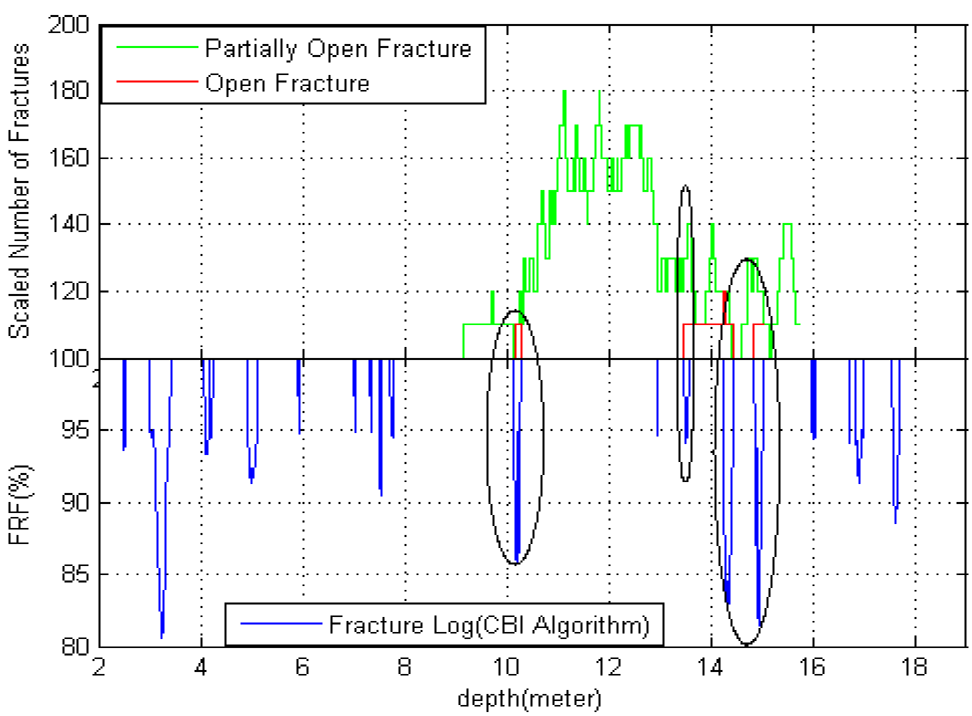

[8] Due to the data processing problem which will be discussed later in pages 109-111, the results of Hole18 are not valid

The ellipses in Figures 5.1 to 5.3 show that the CBI Algorithm can locate most of the Open Fractures and a few of the Partially Open Fractures. Based on the calculated FRF values for the presence of fractures, BI values are compensated. As an example Figure 5.4 compares CBI and BI values for Hole13 and for the rest of blastholes the results have been presented in the Appendix C.

Figure 5.4, CBI and BI values for Hole13

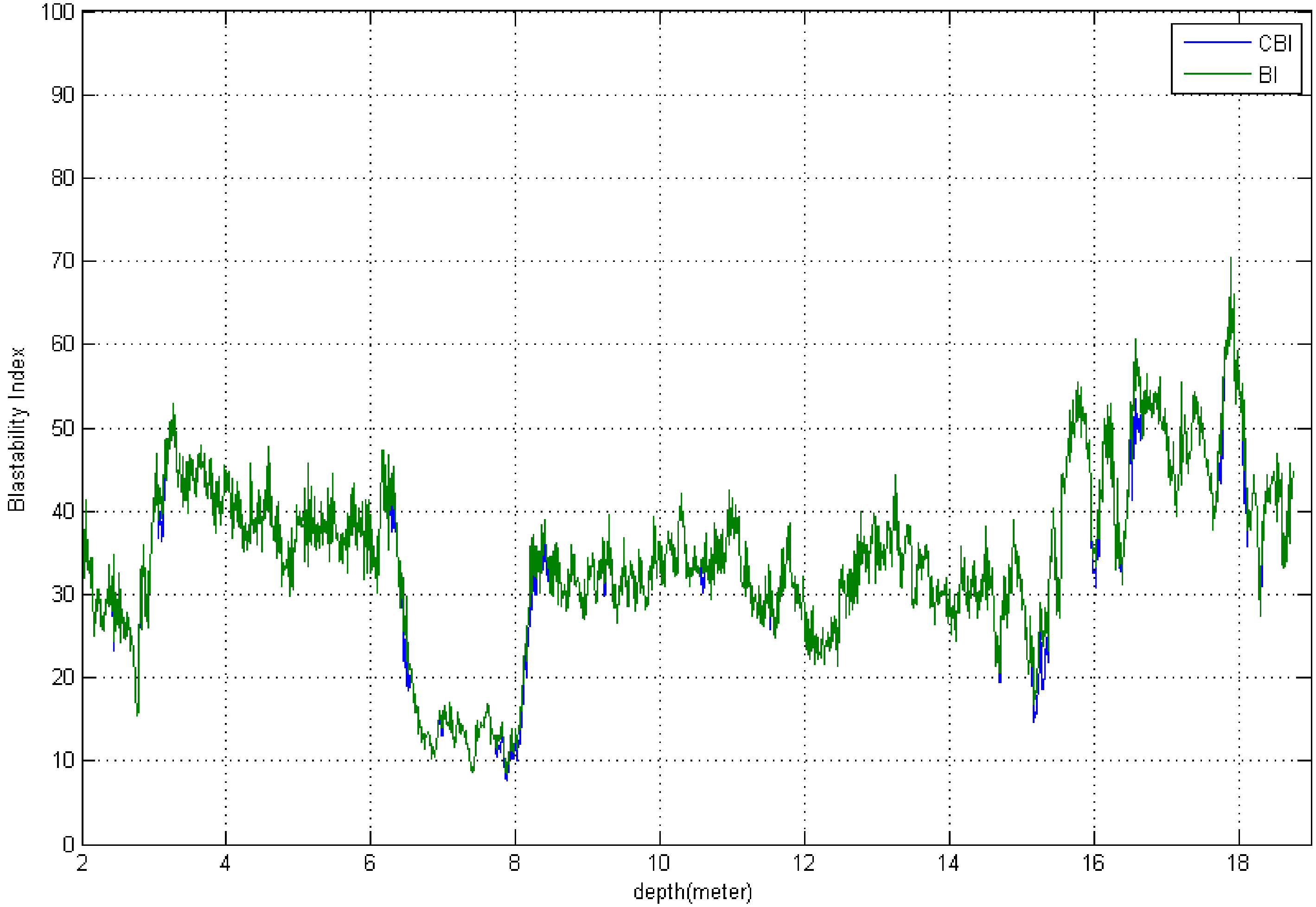

In Figure 5.4, the blue zones are the representative of fractures which BI values have been compensated by FRF values for their presence.

To determine which kind of fractures are more likely to be detected by CBI Algorithm it is important to know how open the fractures are and what their dip to the bit is. It should be noted that the extent of derived fractures are not exactly the same as fractures extents from FMI logs. It depends on the fracture features such as length and aperture.

As a first step, cumulative probability distributions of open and partially open fractures for each test-hole are plotted to see their distribution and most frequent values. As an example for Hole28, cumulative probability distribution of open and partially open fractures in Figures 5.5 and 5.6 are shown respectively.

Figure 5.5, Cumulative probability distribution of open fractures dip angles for Hole28

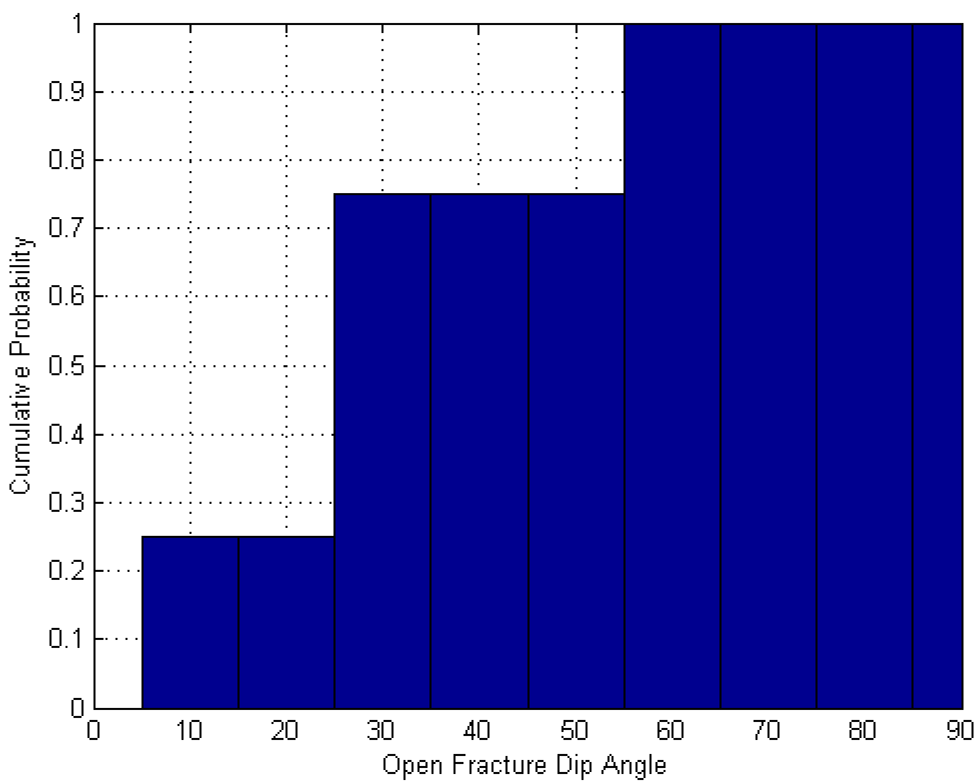

Figure 5.6, Cumulative probability distribution of partially open fractures dip angles for Hole28

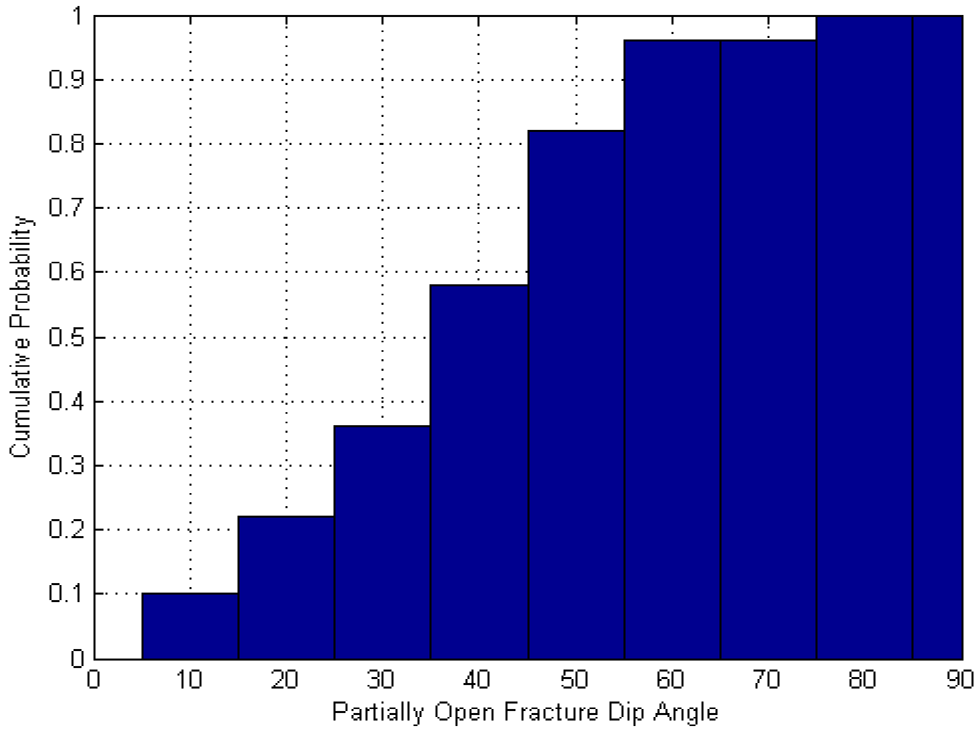

From these Figures, it is seen that more than 70 percent of the fractures intercept borehole at a dip angle of less than 50 degree for both open and partially open fractures. Figure 5.7 compares the FMI and algorithm fracture logs with the FMI dip angles for Open fractures.

Figure 5.7, Dip angles and open fracture logs for Hole 28

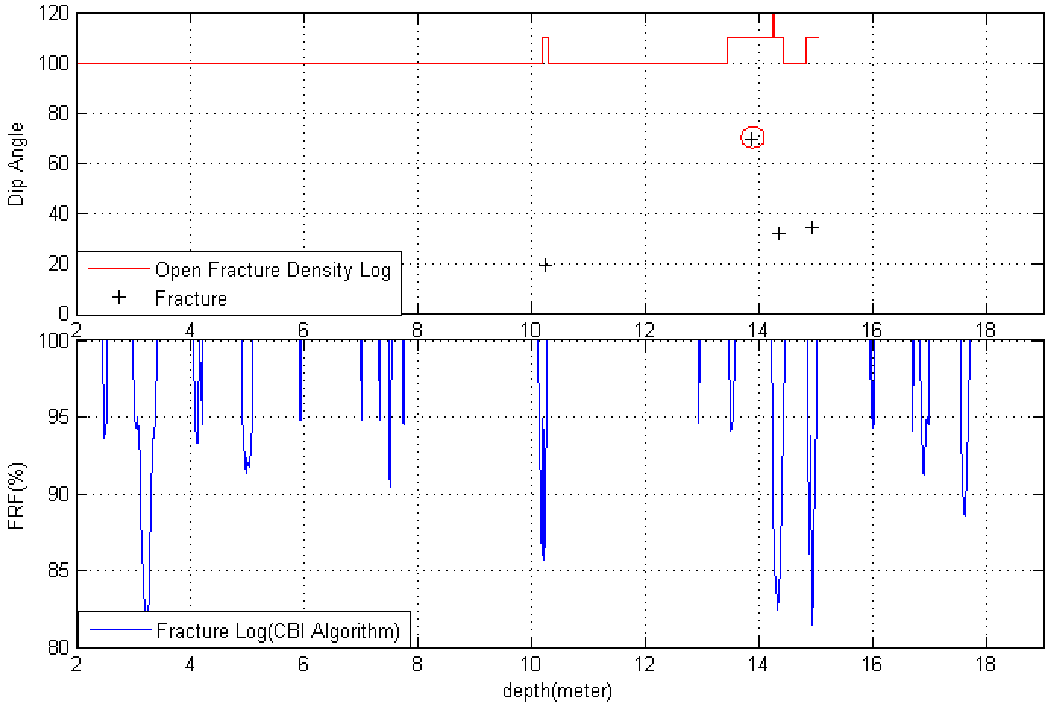

The red circled fracture in the Figure demonstrates that CBI Algorithm cannot locate the fracture within 60 to 80 degree dip angle as shown by the lack of spike on the FRF graph. Numerically CBI Algorithm can locate 100 percent (3 out of 3) of low to moderate open fractures for Hole28. The related diagrams for other holes are shown in Appendix D. Also the dip angles of partially open fractures for all the test-holes have been shown in the Appendix E.

To validate CBI Algorithm results for other holes, Figure 5.8 compares the FMI and algorithm fracture logs with the FMI dip angles for Open fractures.

Figure 5.8, Open fractures dip angles for Hole13

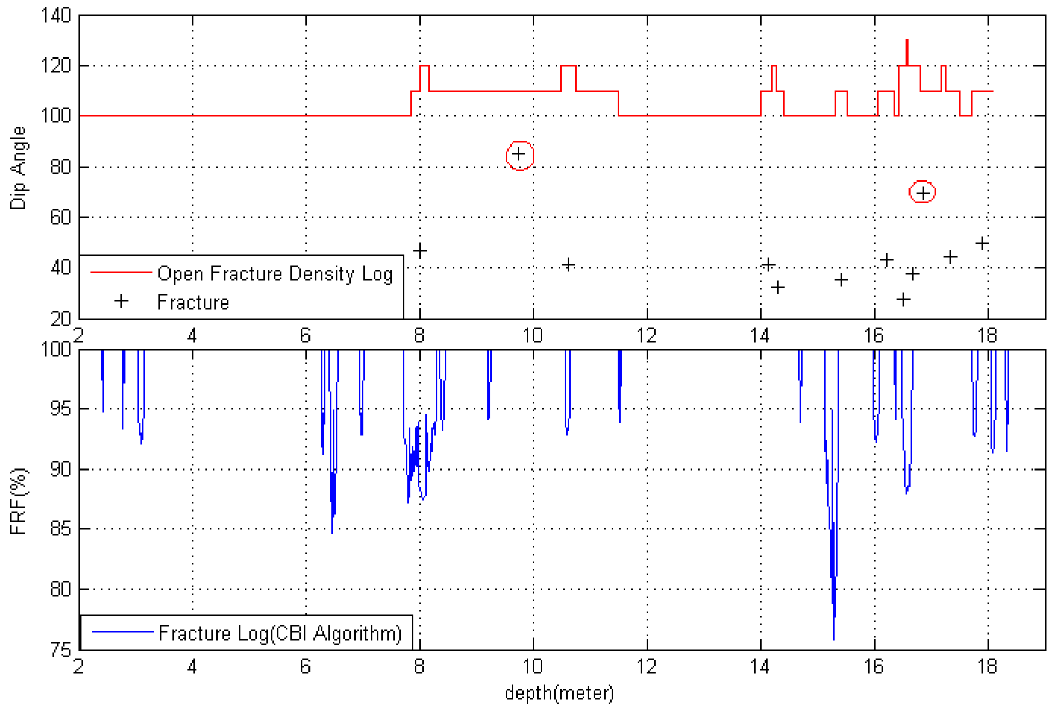

As with Hole 28, Figure 5.8 demonstrates that CBI Algorithm cannot detect high dip fractures highlighted by red ellipses. Also as the Figure shows there are two moderate dip fractures near 14 meter deep which the algorithm does not detect. This can be due ROP interpolation. Also as previously mentioned there is a possibility that FMI logs overstate what actually is in the ground. Numerically it can be declared that CBI Algorithm locates 70 percent (7 out of 10) low to moderate dip open fractures in Hole13.

As discussed in Section 4.3, to make sure that fracture log from CBI Algorithm is not affected by auto-drill control , they are plotted to check whether there is any perturbation or not. Figure 5.9 presents these signals for Hole28.

Figure 5.9, Hole28 speed reference signals

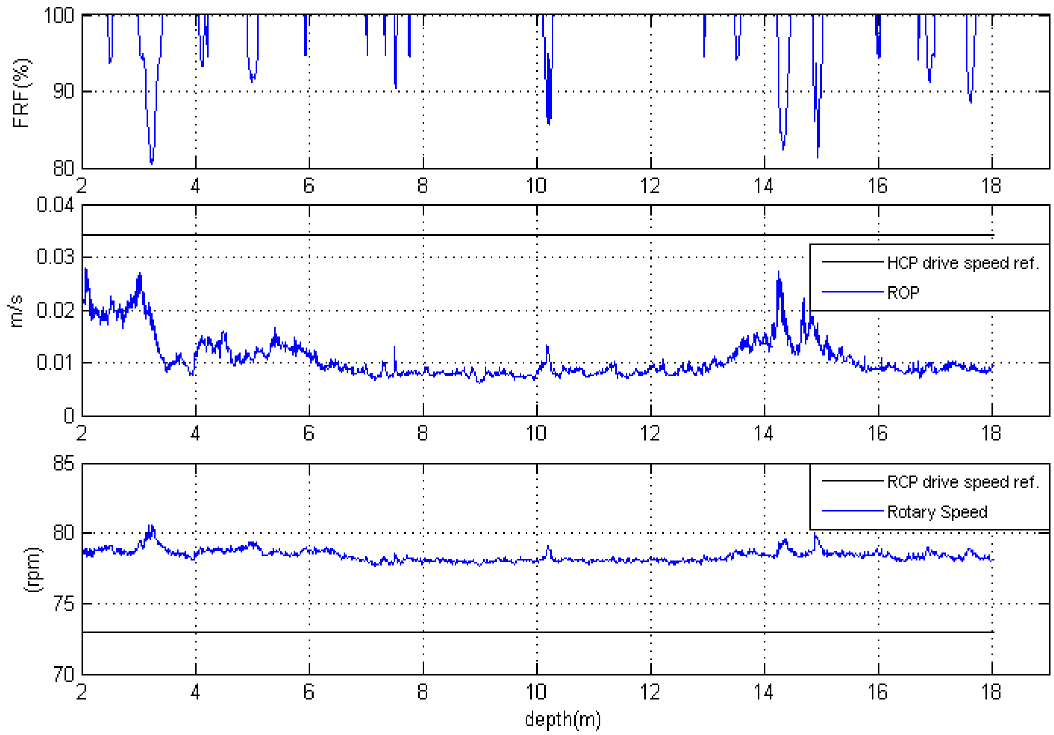

Figure 5.9 shows that the reference signals are constant and they have no effect on the results for drill13.

Regarding Hole18, in addition to the high dip fractures, Figure 5.10 shows a big jump in the depth after the depth reset jump set by the operator at the beginning of drilling.

Figure 5.10, Original depth signal from DataQ for Hole18

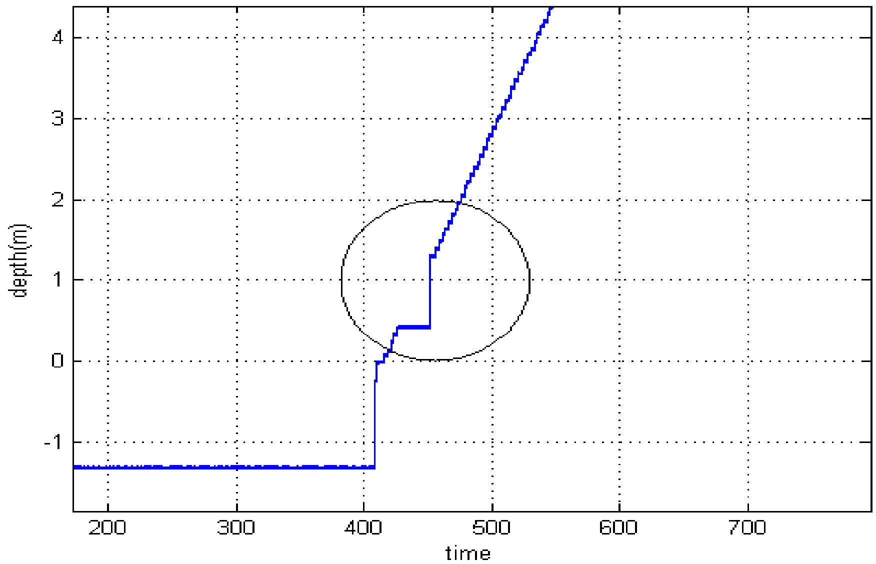

A long length of step prior to the highlighted big jump from 237 to 262 seconds is observed where the drill is rotating (drilling) during this period. The 25 seconds elapsed period can be because of PLC delay or mechanical stickiness and it can be one of the reason for mismatches between FRF values(Fracture Logs) and geophysical logs for this hole since their depth are not matched. The solution for this problem is beyond this thesis and a black box solution will demand improvements in the bit position feed to solve this issue.

Finally in addition to FMI Logs, as discussed in Section 4.1 for the portions of the hole where FMI Logs were not taken, neutron, sonic and density porosity [9]are plotted to compare them with FRF values. For instance Figure 5.11 compares these logs with algorithm FRF log for Hole28.

[9] These logs also do not cover the full length of hole – they can only partially fill in the area where FMI does not exist.

Figure 5.11, FRF log and sonic, neutron and density porosity logs for Hole28

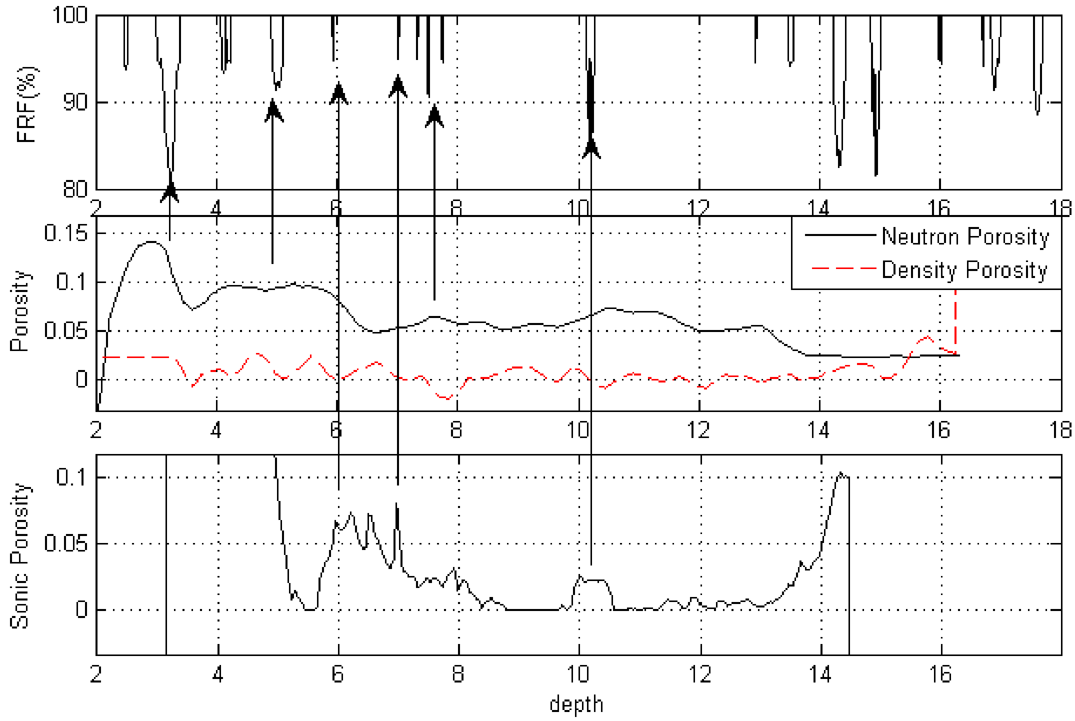

As previously discussed sonic, neutron and density porosity spikes can locate large fractures. Arrows in Figure 5.11 show that in comparison with sonic and neutron porosity spikes, FRF log can determine the place of large fractures over the portions of the blasthole that FMI logging was unable to cover.

In addition to open and partially open fractures, a set of closed fracture logs is derived from FMI logging though based on the CBI Algorithm properties it is not expected to detect them. To verify this closed (restrictive) fracture logs were compared to the FRF log for all the holes and no correlation between FRF spikes and closed (restrictive) fracture occurrence was obvious. An example this comparison for Hole28 is shown in the Figure 5.12.

Figure 5.12, Closed fractures for Hole28

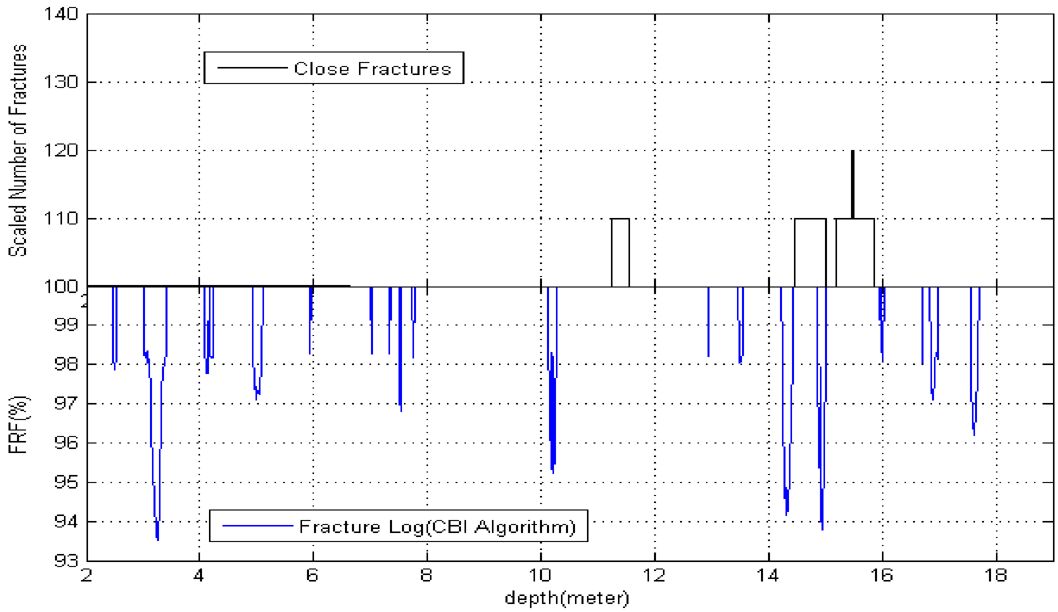

5.2.Drill 11 Test-Holes

Figures 5.13, 5.14, 5.15, 5.16 and 5.17 present the results for holes 22,30,31,32 and 44 respectively.

Figure 5.13, CBI algorithm results for Hole22

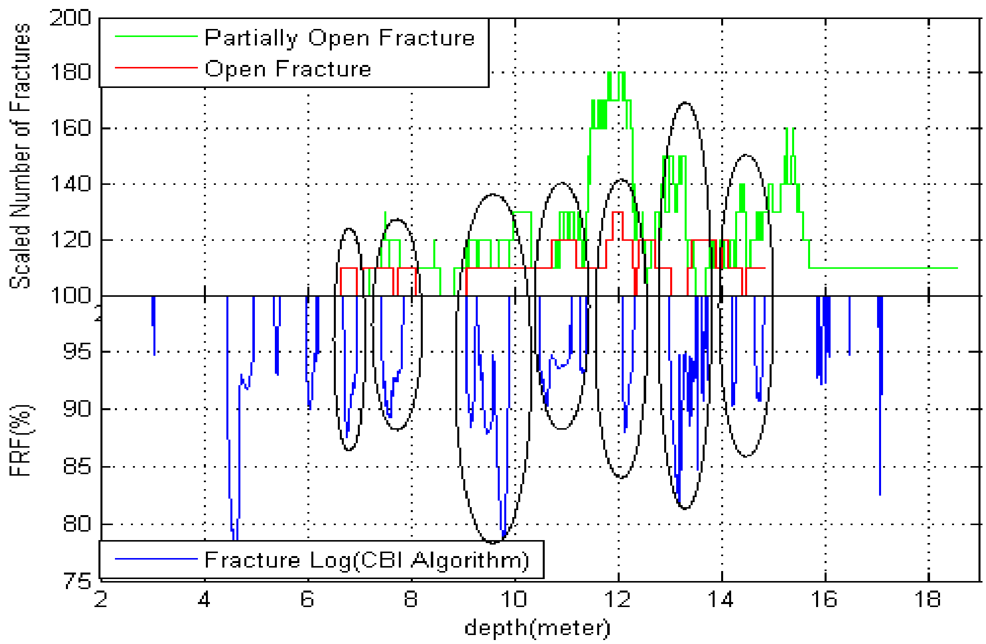

Figure 5.14, CBI algorithm results for Hole30

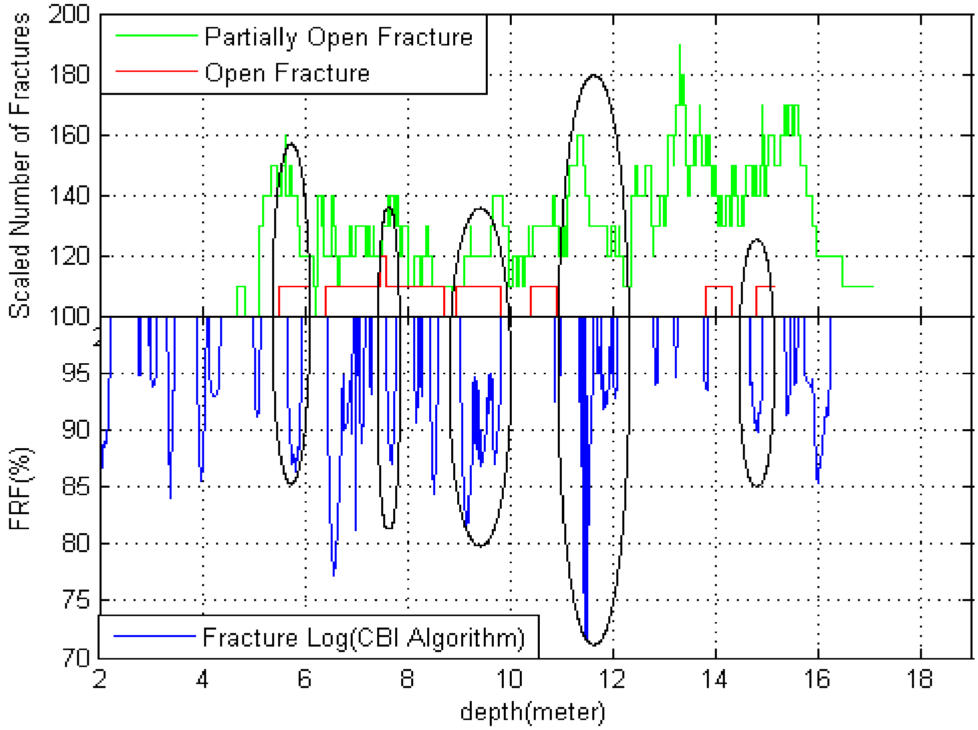

Figure 5.15, CBI algorithm results for Hole31

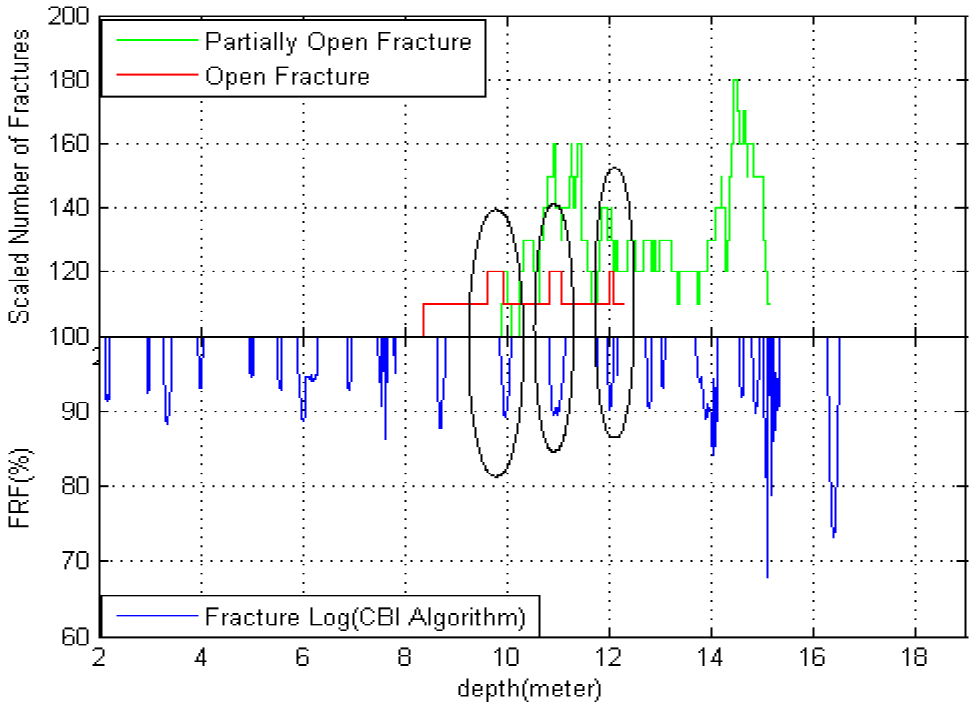

Figure 5.16, CBI algorithm results for Hole32

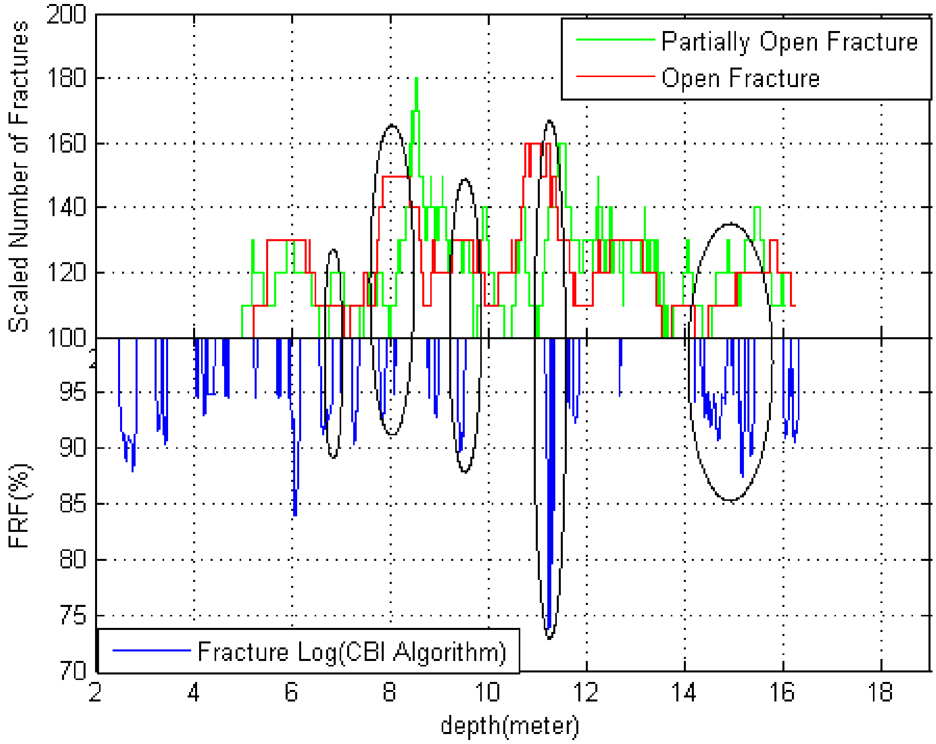

Figure 5.17, CBI algorithm results for Hole44

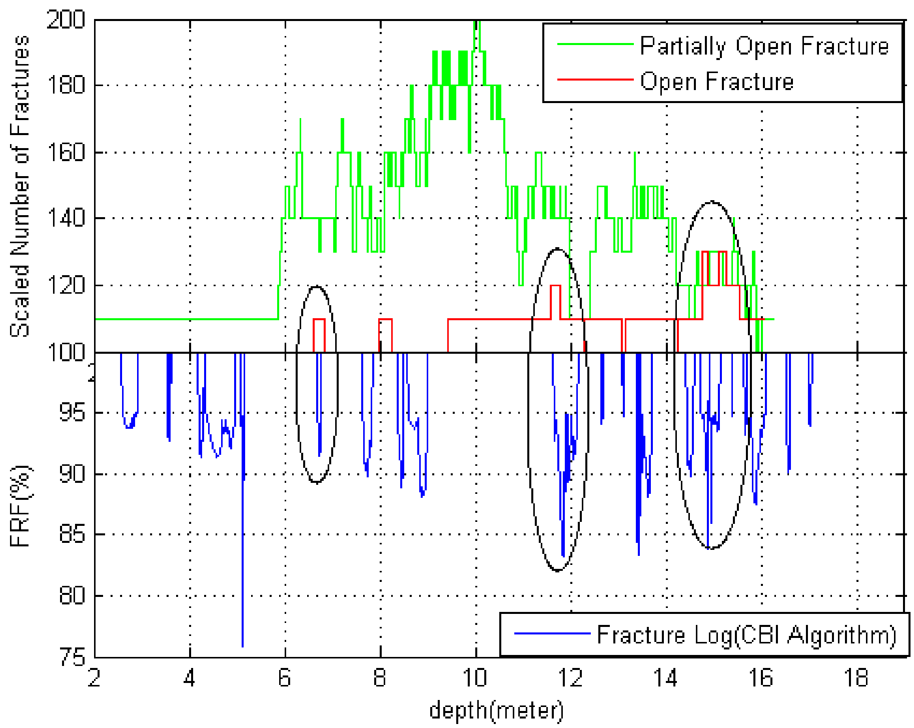

These Figures demonstrate that CBI algorithm is relatively successful in identifying the occurrence of open fractures and a few of partially open fractures for drill11 test-holes as well. However the visually observed correlation between CBI fracture logs and geophysical logs for drill 11 test-holes is weaker than that for drill13 test-holes. Above Figures show that at some points the FRF spikes seem non-smooth. As described in the Section 4.3, these non-smoothed spikes can be related to auto control spikes occurring in the motor drive speed reference signals as a response to high vibrations. To investigate this hypothesis, the FRF values (Fracture Log from CBI) and speed reference signals are plotted to compare them as shown in Figure 5.18 for hole32.

Figure 5.18, Invalid results for Hole32

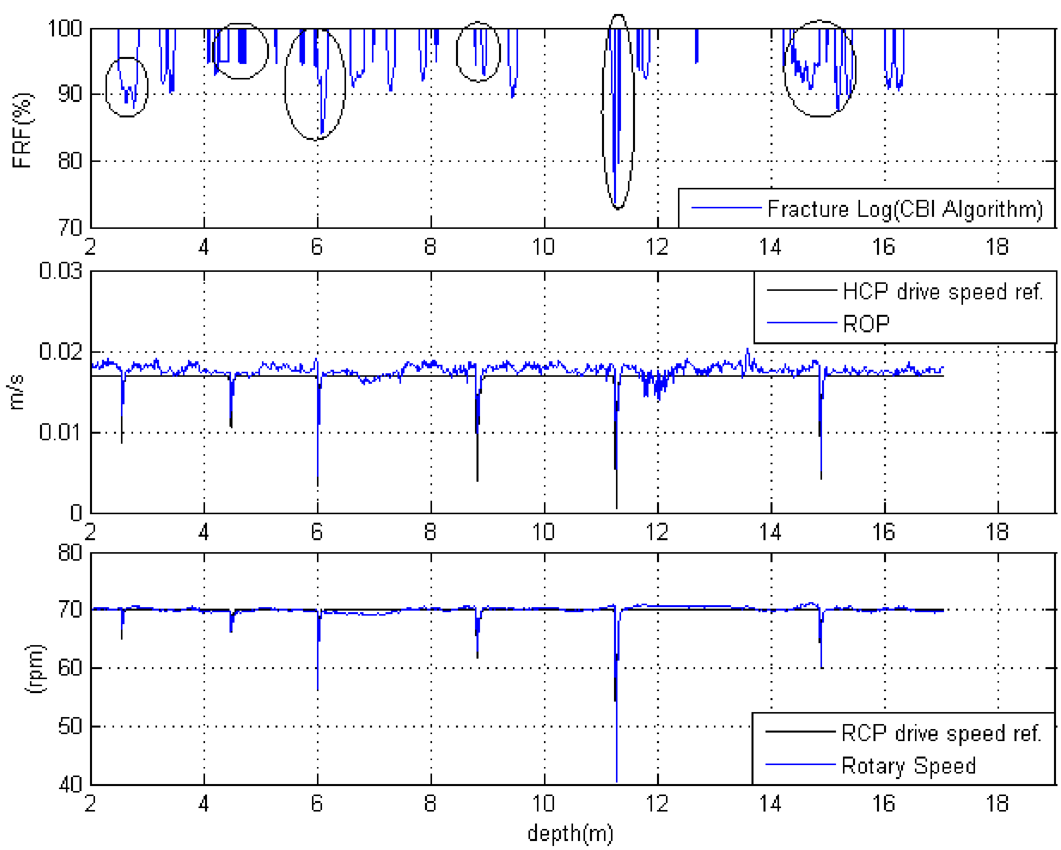

As Figure 5.18 shows, the FRF non-smoothed spikes correspond to speed reference signal perturbations. The speed reference spikes cannot be filtered in the pre-processing algorithm because the bit is drilling during these spikes. Some of these spikes are about 10 sec intervals which with assumption of 0.02m/s rate of penetration will be about 20cm (at least two depth increments). To remove them the penetrated depth during each spike could be subtracted from the steps coming after the spike but this makes the results unrealistic. Similar to Figure 5.18, the invalid results of other holes are shown in Appendix F.

In addition to reference signals issue, dip angle of both open and partially open fractures should be considered. The analysis for all the holes shows that more than 50 percent of open fractures on the bench V115 are high dip fractures. As an example, for Hole32 cumulative probability distributions for both open and partially open fractures in the Figures 5.19 and 5.20 are respectively plotted.

Figure 5.19, Open fracture dip angle distribution for Hole32

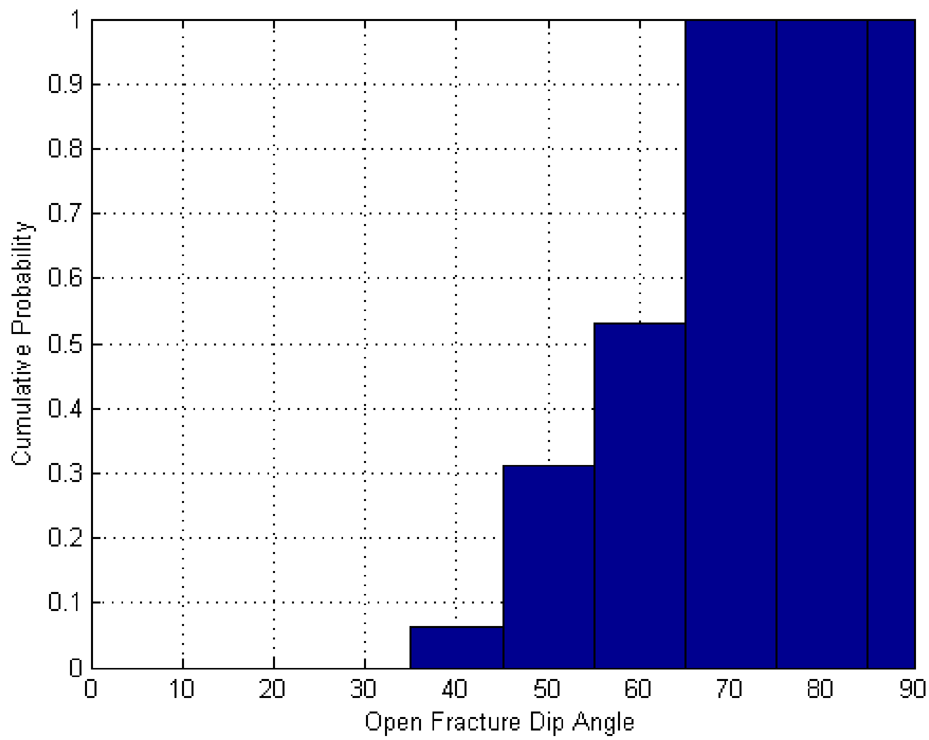

Figure 5.20, Partially open fracture dip angle distribution for Hole32

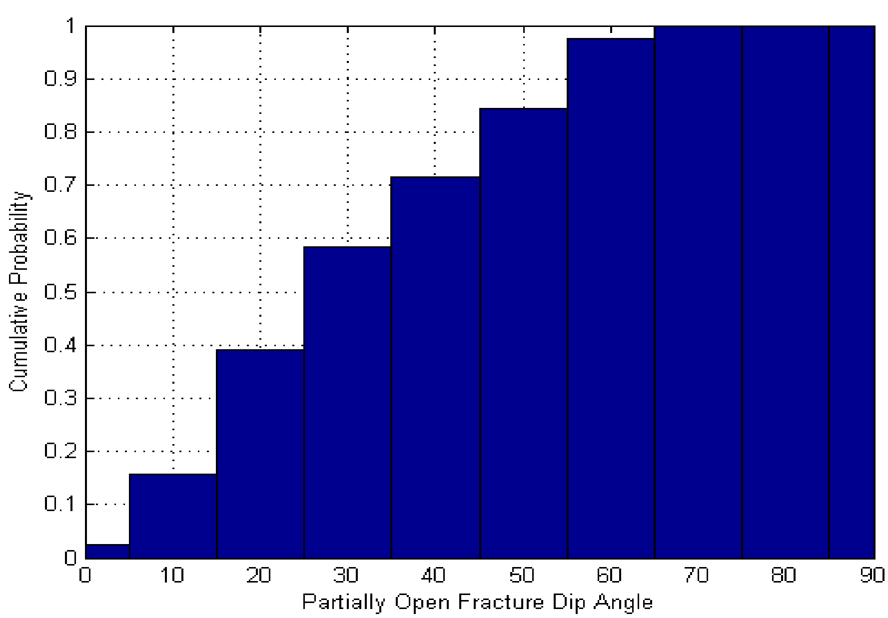

Assuming that the center of each bin in these Figures is the representative of bin, about 70 percent of open fractures for Hole32 are high dip fracture while more than 50 percent of partially open fractures are low dip fractures.

The fracture logs and dip angles for Hole32 are plotted in the Figure 5.21 to observe the relationship between CBI Algorithm results and fractures dip angles.

Figure 5.21, FRF values and fractures dip angles for Hole32

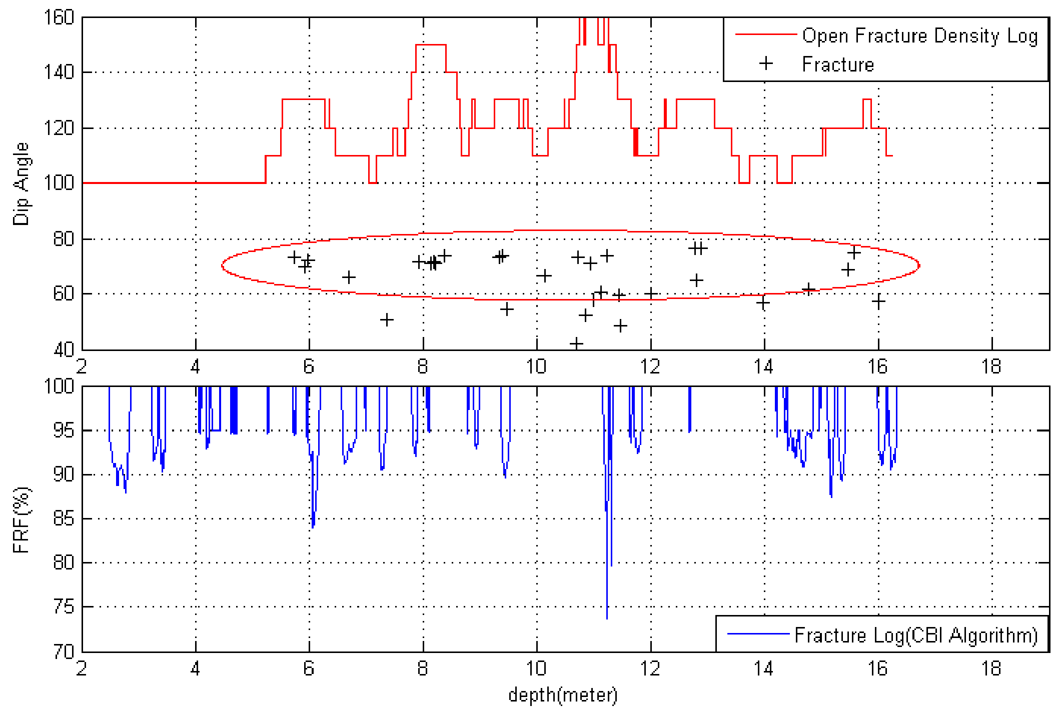

The red ellipse in Figure 5.21 shows the zone of high dip fractures. Table 5.1 shows the percentage of detected open fractures by CBI Algorithm based on visual comparison with fracture density logs from the FMI Logs. In this approach the fracture depth from FMI log is compared with FRF peaks from the CBI Algorithm. It is assumed that the fracture depth presents fracture and the priority is given to open fractures which means first open fractures are compared to FRF values then if there is no overlap between them, FRF values are compared to Partially Open Fractures.

Table 5.1, CBI algorithm results based on open fracture dip angle

	CBI Algorithm % detections		
Hole ID	**Low Dip**	**Moderate Dip**	**High Dip**
13	100	66.67	0
18[10]			
28	100	100	0
22	NA[11]	50	0
30	NA	33.33	50
31	NA	NA	0
32	NA	25	12.5
44	NA	50	0

Table 5.1 demonstrates that the CBI algorithm cannot detect high dip open fractures. For holes 32 and 30 due to high density of partially open fractures in some cases it is difficult to check whether the detected fracture by CBI Algorithm is representative of an open or partially open fracture. Therefore it can cause an error in the presented percentages in Table 5.1 for high dip fractures.

[10] As discussed in section 5.1, page109-111, Hole18 has data processing problem and the results are not valid.
[11] NA – Not Applicable – no fractures fall in this range

Response of MWD to fractures, in addition to fractures dips depends on their filling. If they are filled with soft materials it is easier to detect them rather than if they are filled with hard materials (Lear, 2013). Also in addition to open and partially open fractures, as previously discussed, FMI log can locate the place of closed fractures. This thesis has not focused on closed fractures because they have the lowest probability of being detected from MWD (by CBI Algorithm).

To determine which kind of partially open and closed fracture can be detected by the CBI Algorithm or generally MWD, in addition to their dip angles, the relationship between CBI Algorithm and fracture filling as well as fracture aperture needs to be investigated.

When the CBI results from monitored blastholes are spatially combined within an appropriate software package for a complete pattern, a blast design that more accurately reflects the spatial presence of fractures can be developed. More specifically knowing the location of fractures within individual blastholes can guide the proper placement of explosives in unfractured/intact zones. The resulting outcomes from such a capability should be reflected by a muckpile that has a more even fragmentation size distribution as well as improved looseness. The result will be better digging conditions that lead to higher excavator productivity, lower machine wear as well as a reduced need for secondary blasting. In addition, as a result of more efficient use of explosive energy, there is also a potential to enable improved slope stability and wall control through a reduction in blast induced vibration damage.

6. Conclusion and Future Work

Based on the presented results under certain operational conditions the developed CBI algorithm is capable of accurately identifying the presence of open fractures intersecting a blasthole at near orthogonal angles. However, the fracture identification accuracy of the defined algorithm is highly dependent on the bit depth, monitored penetration/feed rate measurement accuracy as well as the levels of rotary speed and pulldown force settings (autodrilling) at the particular point in time.

6.1. Research Contributions

The conducted research has provided a further investigation of the relationship between monitored performance parameters from a blasthole drill and known fracture zones. The results have led to the development of an approach to modify a standard blastability index when the presences of fractures are detected. The following points summarize some of the key outcomes and thus contributions of the research:

1. The value of MWD data from blasthole drills for rock mass characterization purposes is highly dependent on the processing methods used in its collection. The data needs to be properly processed which includes data segmentation, filtering and interpolation methods to enable the proper processing of acquired MWD data;
2. In the entire formulization of CBI Algorithm, it is necessary to properly use engineering units for the various drill variables used in the CBI calculation. In this case all the electrical signals were converted to their physical units and term D (bit diameter) was introduced onto calculations to make a dimensionless group of parameters;

3. Rate of penetration (ROP) was seen to be the most important monitored drill variable for use in rock mass characterization. In this research, an approach for the proper calculation of a true ROP was also identified for use in calculating CBI values;
4. To filter out noise in the monitored bit position data, a revised moving window technique was defined to provide a more continuous and smooth response. This technique helps to remove steps in some of the recorded signals that may limit the ability to identify fractures;
5. The importance of specific energy (SE) as the basis for the calculation of the CBI data has been further supported. The current work proposed two approaches to calculate SE. Also it was shown that if the depth and ROP can be accurately derived, an accurate SE, WORON and WOSE can be derived by using Electrical SE. This eliminates the need for mechanical variables in physical units;
6. A relationship between acquired MWD data and the presence of fractures determined by geophysical logging was undertaken. This analysis showed that fractures were generally present when increases in ROP along with associated decreases in torque and slight decreases in bailing air pressure were seen;
7. An algorithm was developed and coded in MATLAB to automatically process MWD data to calculate SE values and subsequently detect the locations of fractures that intersect the blasthole. The presence of fractures were then used to derive a compensated blastability index or CBI;
8. To validate the developed CBI algorithm, a geometrical approach was used to extract fracture density logs from associated geophysical (FMI) logs based on the relationship between fractures sinusoids and planes that intersect a blasthole. This method was used to determine the extent of fractures over a borehole and the dip of the fractures that were present. The

fractures determined by this method were then categorized based on their angle of incidence to the blasthole as low (perpendicular), moderate and high (parallel). It was also shown that MWD data does not respond to fractures with an angle of incidence to the blasthole of greater than 60 degrees.

6.2. Future Work

The following points summarize some of the main recommendations for future work to build on the outcomes of the current research:

1. Gather, process and analyze CBI values and trends (contours) for large bench areas and over extended periods of time at a site and correlate these to known blast domains (very poor, poor, good, excellent), powder factor as well as mill rates for the same regions. This will further serve to understand the validity of the calculated CBI data to know rock mass characteristics for a particular site geology and known blasthole drill configuration and operational conditions;
2. Further examination of the influence of variations in pulldown pressure and rotary speed (due to manual operator changes or due to auto-drill systems) as well as bit wear on calculated CBI values;
3. The algorithm developed in the current work is based on drill data generated using Rotocan tricone bits with 12.25 inch diameters. Additional work using bits of varying diameter and from different suppliers may be necessary to further understand the sensitivity of the developed CBI algorithm to these factors;
4. Similarly the assessment of the influence on the CBI algorithm when MWD data acquired from different types of blasthole drills as well as from geological environments other than homogeneous granodiorite ore-bodies (for example, coal mines) are used;

5. Using a simulation approach, examine the feasibility of predicting CBI values (and thus blastability and mill rates) for a selected bench are based on historical data determined using MWD data acquired when drilling the benches above. This information could be used to provide better short range planning accuracy;
6. Using calculated CBI values to predict what type of ore is coming into the mill. For this purpose the relationship between CBI values and grindability can be studied which helps to reduce the energy consumed by grinding operation.

References

- Ashby,J.P.,1982."Production blasting and the development of open pit slope".Proceeding: Third International Conference on Stability in Surface Mining, Vancouver,B.C.,AIME
- Atlas Copco,2009."Blasthole Drilling in Open Pit Mining".Ulf Linder,p.16
- Australian Drilling Industry training Committee Limited,1997,"Drilling,The Manual of Methods,Applications and Management".Lewis Publishers,New York, pp.1-4
- Azimi,Y.,Osanloo,M.,Aakbarpour-shirazi,M., and Aghajani Bazzazi.A.,2010."Prediction of the blastability designation of rock masses using fuzzy sets".International Journal of Rock Mechanics and Mining Sciences, 47(7):pp.1126−1140.
- Barton,N.,Lien,R., and Lunde,J.,1974."Engineering classification of rock masses for the design of rock support".Rock Mechanics 6, pp.189 – 236
- Bhalchandra,V.G.,2011."Rotary Drilling and Blasting in large Surface Mines".Taylor and Frances group,London,UK, Chapters 26, pp.553-560
- Bieniawski,Z.T.,1973."Engineering classification of jointed rock masses".Trans. S. African Instn. Civ. Engrs., Vol 15, No 12, pp.335 - 344.
- Branscombe,E.A.,2010."Investigation of Vibration Related Signals for Monitoring of Large Open-Pit Rotary Electric Blasthole Drills".Master’s Thesis, Queen’s University
- Casselman,M.J.,McMillan,W.J., and Newman,K.M.,2000."Highland Valley Porphyry Copper Deposits near Kamloops, British Columbia: A review & Update with Emphasis on the Valley Deposit", Porphyry Deposits of the Northwestern Cordillera of North America, p.161;
- DataQ Instruments,2007. "DI-718BX DATA Logger Manual"

- Deere,D.U.,1963."Technical description of rock cores for engineering purposes". Felsmechanik und Ingenieurgeologie, Vol. 1, No 1, pp.16 - 22.
- Dey,K., and Sey,Ph.,2003."Concept of Blastability-An update".Indian Mining and Engineering Journal,Vol-42,No-8&9,pp24-31
- Feng,X.,1995."A neural network approach to comprehensive classification of rock stability, blastability and drillability",International Journal of Surface Mining, Reclamation and Environment,Vol9,Issue2,pp.57-92
- Fraenkel,K.,1954."Handbook in rock blasting technique".Part-1. Stockholm: Esselte AB
- Gaillot,P.,Brewer,T.,Pezard,P., and Yeh,En.,2007. "Borehole Imaging Tools - Principles and Applications".Scientific Drilling,No.5
- Hansen,D.W.,1968."Drilling and Blasting Techniques for Morrow Point Power Plant". Proceedings Ninth Symposium of Rock Mechanics, Golden, Colorado, pp.347-360.
- Hino,K.,1959."Theory and Practice of Blasting". Nippon Kayaku Co. Ltd. Japan.
- Kadkhodaei-Ilkchi,A.,Ramos,F., and Hatherly,P.,2010."Rock recognition from MWD:A comparative study of Boosting, Neural Networks and Fuzzy Logics".IEE Geoscience and remote sensing letter, Vol.7,No.4
- Lear,C.D., 2013."Joint Probability of Detection". Internal Communications.Peck Tech
- Leighton, J.,1982."Development of a Correlation between Rotary Drill Performance and Controlled Blasting Powder Factors".M.Sc. Thesis, Department of Mining and Mineral Process Engineering, University of British Columbia.
- Lilly,P.,1986."An Empirical Method of Assessing Rockmass blastability".Large Open Pit Mine Conference, Newman, Australia, October, pp.89-92.

- Liu,H., and Yin,K.K.,2001."Analysis and interpretation of monitored rotary blast hole drill data".International Journal of Mining Reclamation and Environment. 15 (3): pp.177 – 203.
- Liu,H., and Yin,K.K.,2001."Using information extracted from drill data to improve blasting design and fragmentation". Fragblast. 5 (3): pp.157 – 179.
- Lopez,C.,Lopez,E., and Javier,F.,1995."Drilling and Blasting of Rocks".p.53
- Lucifora,D.J.,2012."Comparative Modeling,Simulation and Control of Rotary Blasthole Drills for Surface Mining ".Master's Thesis, Queen's University
- Lutz,J.,1982. "Automatic Recording of Drilling Parameters - General Presentation". Jurançon, France.
- Mohanty,B.,1996."Rock Fragmentation by Blasting".Proceedings of the Fifth International Symposium on Rock Fragmentation by Blasting--Fragblast-5, Montreal, Quebec, Canada,
- Mozaffari,Sh.,2007."Measurement While Drilling System in Aitik Mine".MSc thesis,Lulea University of Technology,Sweden
- Peck Tech,2009."Functional Requirements Definition for the Compensated Blastability Index (CBI) Algorithm".Internal Technical Document. Peck Tech Consulting
- Peck Tech,2011."Data Capture Configuration".Internal Communications.Peck Tech Consulting Ltd
- Peck Tech,2011."Specific Energy Equations & Calculation from Drill PLC Data".Internal Technical Document.Peck Tech Consulting Ltd

- Peng,S.S,Sasaok,T.,Tang,X.D,Luo,Y., and Wilson,G.,2005."A method for quantitative void/fracture detection and estimation of rock strength for underground mine roof".Roof Bolting,pp.44-49
- Phelps Dodge Mining Company, Aquila MS, University of Arizona, Lawrence Berkeley Laboratory, and Julius Kruttschnitt Mineral Research Centre,2002."On Measurement While Drilling at Sierrita Phelps Dodge".Phelps Dodge Sierrita Mine, AZ, United States Of America
- Schunnesson,H.,1996."RQD Prediction Based on Drill Performance".Tunneling and Underground Space Technology".Vol.11,No.3,pp. 345-351
- Schunnesson,H.,1998."Rock Characterization using percussive drilling".International Journal of Rock Mechanics and Mining Science, Vol.35(6), pp.711-725
- Schwartz,B.C.,2006."Fracture Pattern Characterization of Tensleep Formation,Teapot Dome,Wyoming".Master Thesis, West Virginia University
- Scoble,M.J., and Peck,J.,1987."A Technique for ground characterization using automated production drill monitoring".Int. Journal of Surface Mining1:pp.41-54
- Scoble.M.J.,Peck.J, and Hendricks.C,1989."Correlation between rotary drill performance parameters and borehole geophysical logging".Mining Science and Technology.8: pp.301 – 312
- Serra,O.,1988."Fundamental of Well-Log Interpretation: The Acquisition of Logging Data".Elsevier Science,pp.269-301
- Teale,R.,1965."The concept of specific energy in rock drilling".International Journal of Rock Mechanics & Mining Sciences. 2: pp.57 – 73

- Wonik,T., and Olea,A.P.,2007."Borehole Logging, Environmental Geology".Springer, pp.431-474

Appendices

Appendix A- CBI Algorithm MATLAB Code

```
%CBI Algorithm
clc
% Data Q file consists of n x 17 channels of data viz:
% 1  rel.time
% 2  Bit Position
% 3  RCP Armature Voltage
% 4  RCP ArmatureAmps
% 5  RCP Field Current
% 6  RCP Speed Refernce
% 7  HCP Armature Voltage
% 8  HCP ArmatureAmps
% 9  HCP Field Current
% 10 HCP Speed Refernce
% 11 HCP Pulldown Current Limit
% 12 Water Inj. Motor Speed
% 13 Rotary Master Switch Input
% 14 Hoist Pulldown Master Switch
% 15 Raw Vert. Vibration
% 16 Raw Horiz. Vibration
% 17 Main Air Pressure

%i j T are the global counters in the algorithm
%St is the number of desired step edges

%*************************************************%
% Define known parameters for drilling & conversion

bitDia = 12.25;  % Inches
headMass = 14982;   % mass of drill assembly in kg (motors, gearbox, shock sub, drill rod & stabilizer)
encStep = 0.08267; % step interval for 9 bit head position encoder
% DataQ to Drill scaling constants
D = [1 3.048 60 75 5 10 60 75 5 1.6764 10 10 10 10 10 10 68.7];
% Motor characteristic factors imported as 'rcpMotor' & 'hcpMotor' arrays
% Gearbox conversion factors imported as 'rcpFactor' & 'hcpFactor' arrays
% Output units from conversion rcp[rpm, N.m] & hcp[mpm, N]

% Necessary calculations
D = bitDia * 0.0254; % Bit diameter in m
area = pi*(bitDia/2)^2;   % Bit area m^2
stWgt = headMass * 9.81;        % Weight of drill assembly N

%>>>>>>>>>>>>>>>>>>>>>>>>>>>>>>>>>>>>>>>>>>>>>>>>>>>>>
% Assumes relevant DataQ file is imported as array 'A'

[n,signals] = size(A);       % No samples, signal channels
samprate = 1/A(2,1);      % Sampling rate - can be calculated based on the DataQ has regular sampling rate
% Detrend the vibration channels (15,16) of their offsets
for i = 15:16;
   tmp = detrend(A(:,i));
   A(:,i) = tmp;
end
```

```
% Scale the data to physical/electrical units (DataQ volts to Drill Motors Amps/Volts and other physical units)
ident = eye(signals);
for i = 1:signals;
    ident(i,i) = D(i);
end
tmp = A * ident;
A = tmp;
% Add & initialise two columns to the data array
% 18 Drilling(It can be an indicator of end of drilling)
% 19 Interpolated depth            m
tmp1 = ones(n,1);
tmp2 = zeros(n,1);
A = [A tmp1 tmp2];
clear tmp tmp1 tmp2
Astar=A;%a backup of A

%>>>>>>>>>>>>>>>>>>>>>>>>>>>>>>>>>>>>>>>>>>>>>>>>>>>>>
%remove non-drilling events

B=zeros(n,19);%A temporary substitution for A
T=0;
tmp=0;
for i = 1:n
  if (A(i,3) > 0)&&(A(i,4) > 0)&&(A(i,7) < 0)&&(A(i,2) > 0)&&(A(i,2)-tmp)>-0.025
       T=T+1;
       B(T,:)=A(i,:);
       tmp=A(i,2);
   end
end
A=B(1:T,:);
figure(1);plot(Astar(:,1),Astar(:,3),'b',A(:,1),A(:,3),'k');grid
%Relative Drilling Time recalculation
A(1:T,1) = Astar(1:T,1);
clear i j  m B

%>>>>>>>>>>>>>>>>>>>>>>>>>>>>>>>>>>>>>>>>>>>>>>>>>>>>>>
%Determine depth step occurrences and true magnitude

MD=max(A(:,2));%maximum depth
a=find(A(:,2)==MD);%indices of maximum depth
MiT=A(a,1);
MiT=min(MiT);%time of first occurance of maximum depth
%number of samples=samplerate*MiT,
M=(0.005*samprate*MiT/MD);%window size=number of samples at 0.005m depth interval
if mod(M,2)==0
    M=M+1;
end
m=fix(M/2);% half of window
mp = zeros(T, 2);
for i = 1:T
    mp(i,1) = i; %indices
    j=max(1,i-m);
    k=min(i+m,T);
    mp(i,2) = mode(A(j:k,2)) ;
end
```

```
time=zeros(T,1);
for i=1:T
    time(i)=A(mp(i,1),1);%relevant time to each index
end

%depth of each step
C=zeros(500,2);%Depth Matrix
C(:,3)=ones(500,1);
C(:,4)=zeros(500,1);
St=1;
for i=2:T
  if (mp(i,2)-mp(i-1,2)>0.0475)&&(mp(i,2)>0)%Depth matrix should be in ascending order and positive
      St=St+1;
      C(St,4)=C(St-1,4)+encStep;
      C(St,3)=i;%index of each step change
    C(St,2)=mp(i,2);%Depth
     C(St,1)=time(i,1);%Time
  end
end

%>>>>>>>>>>>>>>>>>>>>>>>>>>>>>>>>>>>>>>>>>>>>>>>>>>>>>>
% Interpolate depth between depth step changes

Rtm=0;%Temporary ROP
SumHcpV=zeros(St-1,1);%Sigma ROP over each step %if we have n depth points we need n-1 ROP
X=zeros(St-1,1);%Number of samples at each step
for i = 2:St
    S=0;
    for j = 1:T;
        if A(j,1) >= C((i-1),1) && A(j,1) < C(i,1)
            Rtm=Rtm+A(j,7);%A(j,7) is Hoist Motor Voltage
            S=S+1;
        end
    end
    SumHcpV(i-1,1)=Rtm;
  Rtm = 0;

end
clear i j
for i=2:St
    A(C(i,3),19)=C(i,4);%substitute C in A(:,19)
    interval = C(i,4)-C(i-1,4);
    for j=2:T
        if (A(j,1) >= C((i-1),1)) && (A(j,1) < C(i,1))
            A(j,19)=A(j-1,19)+(A(j,7)/SumHcpV(i-1))*(interval);
            %A(j,20)=A(j-1,19)+interval*0.0025/(C(i,1)-C(i-1,1));%for
            %linear interpolation
        end
    end
end
Z=find(A(:,19));
B=zeros(max(Z),19);
for i=1:max(Z)
  B(i,:)=A(i,:);
end
```

```
clear i A
n=length(B);

%>>>>>>>>>>>>>>>>>>>>>>>>>>>>>>>>>>>>>>>>>>>>>>>>>>>>>>>>>>>>>>>>>>>>>>
% Run Motor Calculator
% Rotary Motor -> RPM & TRQ
[mRS, mRT] = motorCalc(B(:,3), B(:,4), B(:,5), rcpMotor);
RS = mRS * rcpFactor(1) ;
RT = mRT * rcpFactor(2) ;

% Hoist Motor -> ROP & WOB
[mRS, mRT] = motorCalc(B(:,3), B(:,4), B(:,5), rcpMotor);
ROP = mRS * hcpFactor(1) ;
% Apply Inertia Adjustment
mRF = inertiaCalc(mRT, B(:,4), B(:,5))
PF = mRF * hcpFactor(2);
WOB = PF + stWgt ;

% cleanup
clear mRS mRT hcpFactor hcpMotor rcpFactor rcpMotor
%>>>>>>>>>>>>>>>>>>>>>>>>>>>>>>>>>>>>>>>>>>>>>>>>>>>>>>>>>>>>>>>>>>>>>>

%Generating 1cm signal resolution
Chunk = input('Chunk size (m) ? : ');%desired depth interval
maxdepth = max(B(:,19));
maxD = maxdepth - mod(maxdepth,Chunk);t = maxD/Chunk;
t=round(t);
avgsig=zeros(t,25);
%j and k are counters for a given depth interval marking beginning and end
j=1;
k=2;
h=1;
for m = 1:length(B);
    if h <= t;
        if  B(m,19) > (Chunk*h);
            avgsig(h,1)=B(m,1);%Time
            avgsig(h,2)=mean(B(j:k,2));%Depth
            avgsig(h,3)=mean(B(j:k,3));
            avgsig(h,4)=mean(B(j:k,4));
            avgsig(h,5)=mean(B(j:k,5));
            avgsig(h,6)=mean(B(j:k,6));
            avgsig(h,7)=mean(B(j:k,7));
            avgsig(h,8)=mean(B(j:k,8));
            avgsig(h,9)=mean(B(j:k,9));
            avgsig(h,10)=mean(B(j:k,10));
            avgsig(h,11)=mean(B(j:k,11));
            avgsig(h,12)=mean(B(j:k,12));
            avgsig(h,13)=mean(B(j:k,13));
            avgsig(h,14)=mean(B(j:k,14));
            avgsig(h,15)=mean(B(j:k,15));
            avgsig(h,16)=mean(B(j:k,16));
            avgsig(h,17)=mean(B(j:k,17));
            avgsig(h,18)=mean(B(j:k,18));%it can be used as the indicator of end of drilling
            avgsig(h,19)=mean(B(j:k,19));%interpolated Depth
            avgsig(h,20)=mean(ROP(j:k,1));%avgMechROP
```

```
            avgsig(h,21)=mean(PF(j:k,1));%avgPulldown
            avgsig(h,22)=mean(RS(j:k,1));%avgSpeed
            avgsig(h,23)=mean(RT(j:k,1));%avgTorque
            avgsig(h,24)=(B(k,19)-B(j,19))/((k-j)*(1/samprate));%average depth based ROP
            avgsig(h,25)=mean(WOB(j:k,1));%aveWOB
            j=m;
            k=m;
            h=h+1;
        else
            k=m;
        end
    end
end
clear i j T

%>>>>>>>>>>>>>>>>>>>>>>>>>>>>>>>>>>>>>>>>>>>>>>>>>>>>>>>>>>>>>>>>>>>>>>>
%SE calculations

w=length(avgsig);
CarriageNewtons = stWgt; Depth(:,1)=avgsig(:,19);
Time(:,1) = avgsig(:,1);
RotI(:,1) = avgsig(:,4);
RotV(:,1) = avgsig(:,3);
HoistI(:,1) = avgsig(:,8);
HoistV(:,1) = avgsig(:,7);

%Converted SE
SFERotCon=zeros(w,1);%Rotary component of Converted SE
SFEFeedCon=zeros(w,1);%Axial Component of Converted SE
SFECon=zeros(w,1);%Converted SE(Physical)
i=1;
while i<= w
   SFEFeedCon(i,1)=(avgsig(i,25)/Area);
   SFERotCon(i,1)=(2*pi*avgsig(i,23)*avgsig(i,22))/(Area*avgsig(i,24)*60);
   SFECon(i,1)=SFERotCon(i,1)+SFEFeedCon(i,1);
   i=i+1;
end
clear i

%Electrical SE
SFERotElec=zeros(w,1);%Rotary component of Electrical SE
SFEFeedElec=zeros(w,1);%Axial component of Electrical SE
SFEElec=zeros(w,1);%Electrical SE
i=1;
while i<= w
   SFERotElec(i,1)=RotI(i,1)*RotV(i,1)/(Area*avgsig(i,24));
   SFEFeedElec(i,1)=HoistI(i,1)*HoistV(i,1)/(Area*avgsig(i,24)) + CarriageNewtons/Area;
   SFEElec(i,1)=SFERotElec(i,1)+SFEFeedElec(i,1);
   i=i+1;
end
%>>>>>>>>>>>>>>>>>>>>>>>>>>>>>>>>>>>>>>>>>>>>>>>>>>>>>>>>>>>>>>>>>>>>>>>>>>>>
%WORON and WOSE signals generation

woron=zeros(t,1);
wose=zeros(t,1);
```

```
for i=1:t
  woron(i,1)=(avgsig(i,25)/(avgsig(i,24))/avgsig(i,22));

  wose(i,1)=woron(i,1)/(D*SFECon(i,1));

end
clear i
%>>>>>>>>>>>>>>>>>>>>>>>>>>>>>>>>>>>>>>>>>>>>>>>>>>>>>>>>>>>>>>>>>>>>>>>>>>
% CBI Calculation
%Below is the code to calculate fractures and determine a new BI index.

%Moving Average for windows of varying size
%MA is a moving average function written in MATLAB
%Size of window1=4cm
Dummy1=MA(wose,4);
%Size of window2=10cm
Dummy2=MA(wose,10);
%Size of window3=80cm
Dummy3=MA(wose,80);
%Size of window4=150cm
Dummy4=MA(wose,150);
%FRF,BI and CBI Calculation
fractable=ones(t,3);
fractotal=zeros(t,1);
OldBI=zeros(t,1);
NewSFE=zeros(t,1);
NewBI=zeros(t,1);
BIconv = 135*(10^6);%Mpa
for i=1:t;
   if Dummy1(i) < 0.95*Dummy2(i);
      fractable(i,1) = Dummy1(i)/Dummy2(i);
   elseif Dummy2(i) < 0.95*Dummy3(i);
      fractable(i,2) = Dummy2(i)/Dummy3(i);
   elseif (Dummy3(i)) < 0.95*(Dummy4(i));
      fractable(i,3) = Dummy3(i)/Dummy4(i);
   end
   fractotal(i) = fractable(i,1)*fractable(i,2)*fractable(i,3);
   NewSFE(i)= SFECon(i,1)*fractotal(i);
   NewBI(i)=NewSFE(i)*100/BIconv;
   OldBI(i) = SFECon(i,1)*100/BIconv;
end
```

Appendix B- Alpha CBI Algorithm Results

Hole18

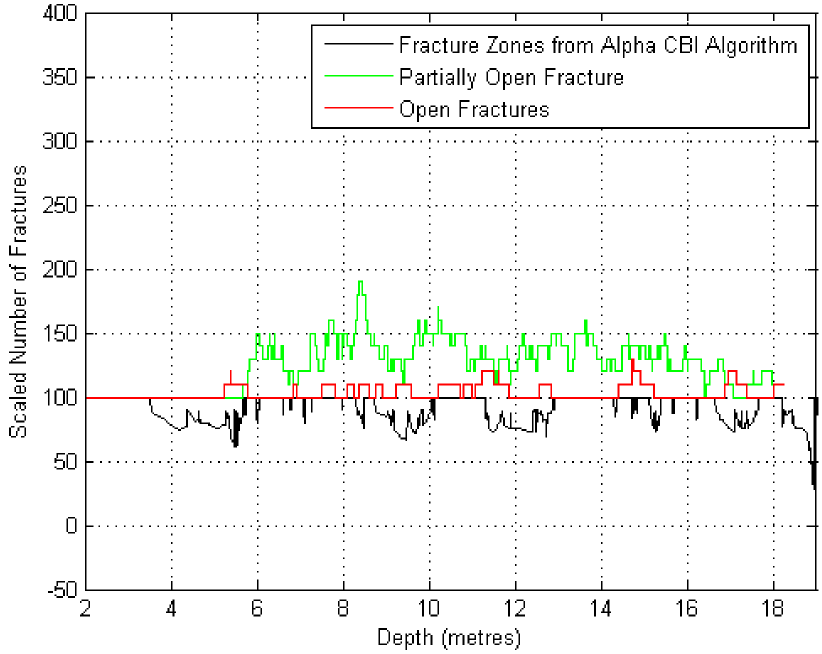

Hole28

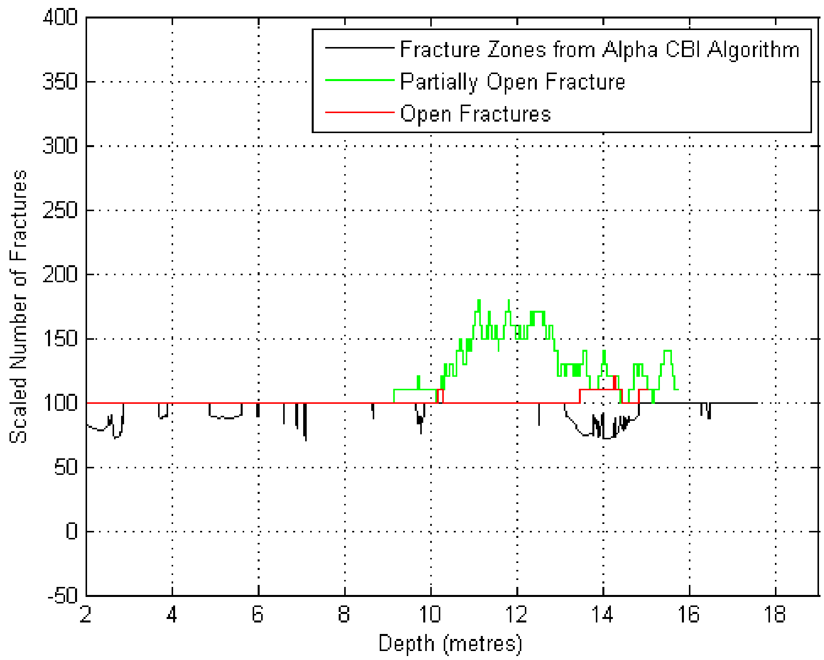

Hole22

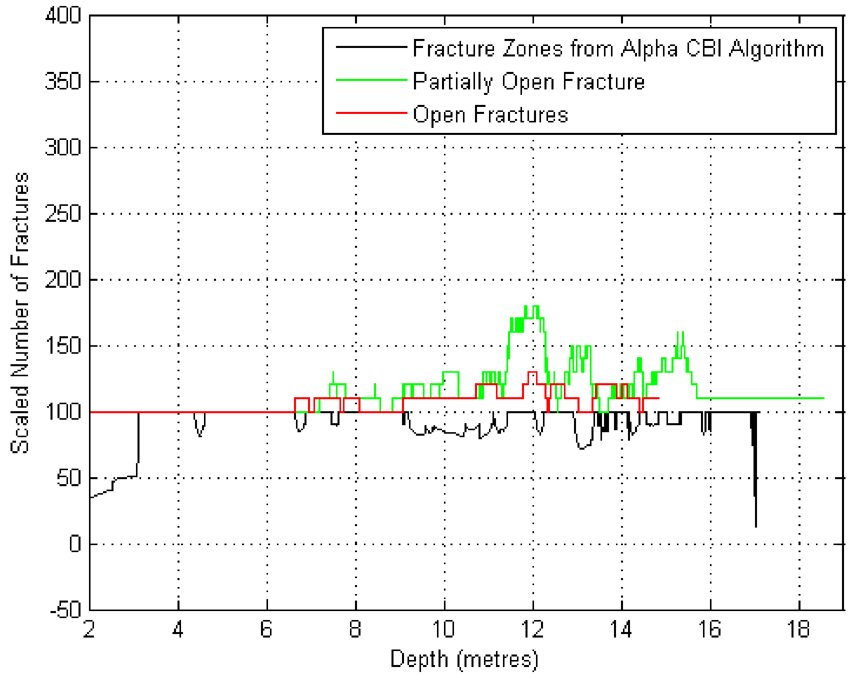

Hole30

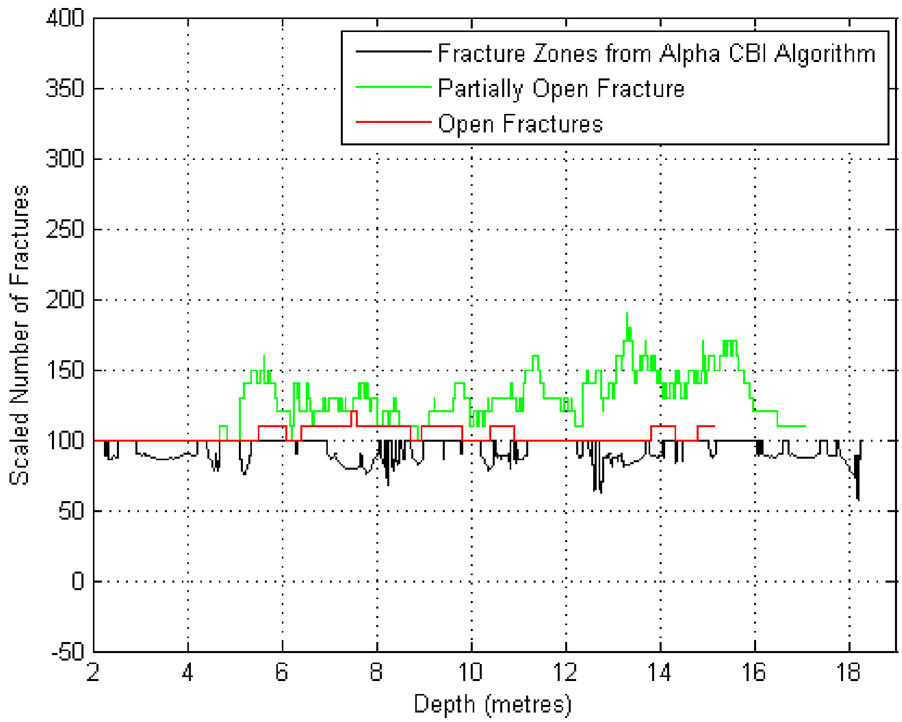

Hole31

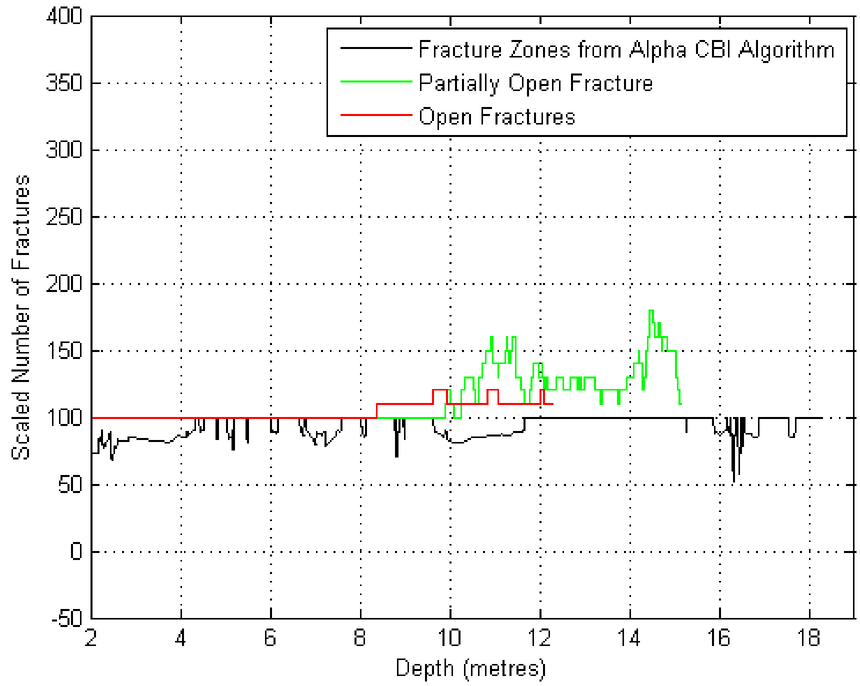

Hole44

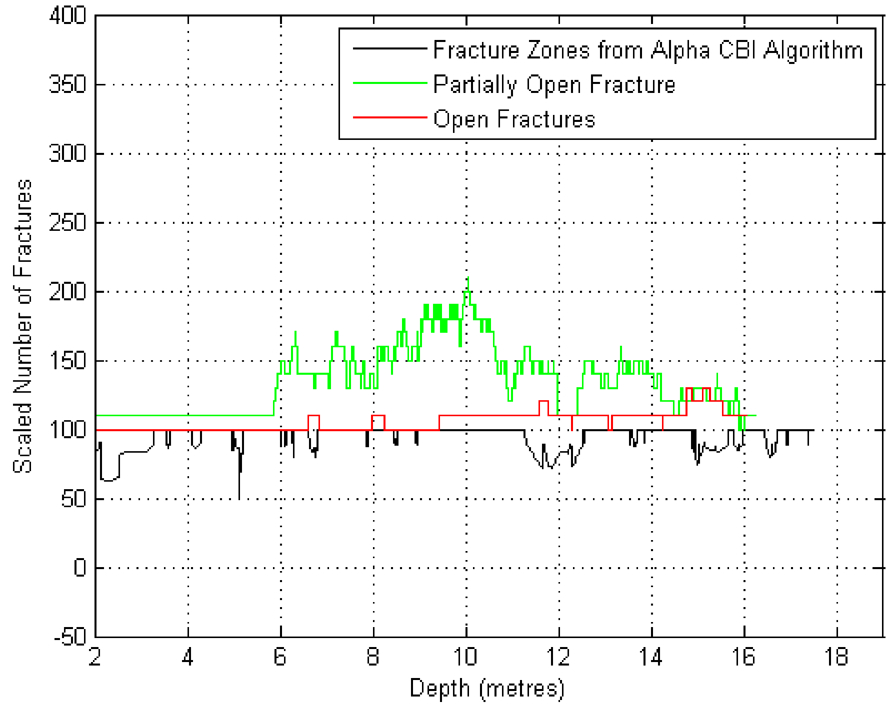

Appendix C- CBI and BI Values

Hole18

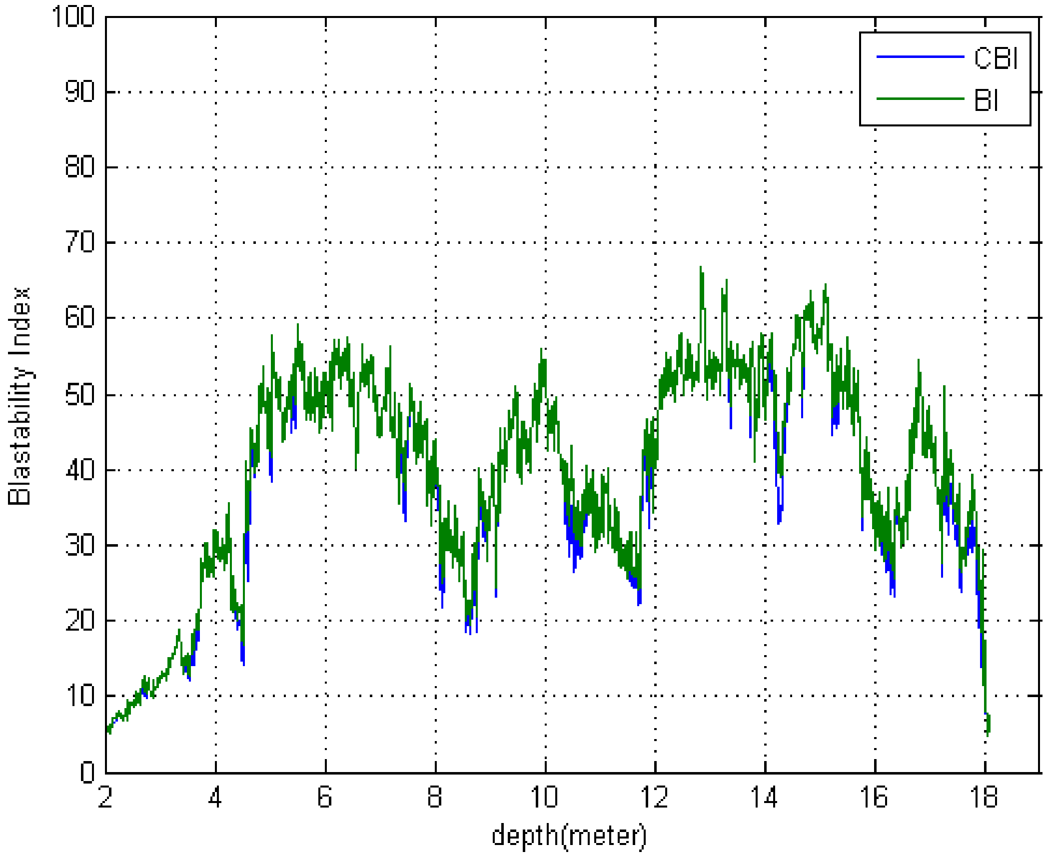

Hole28

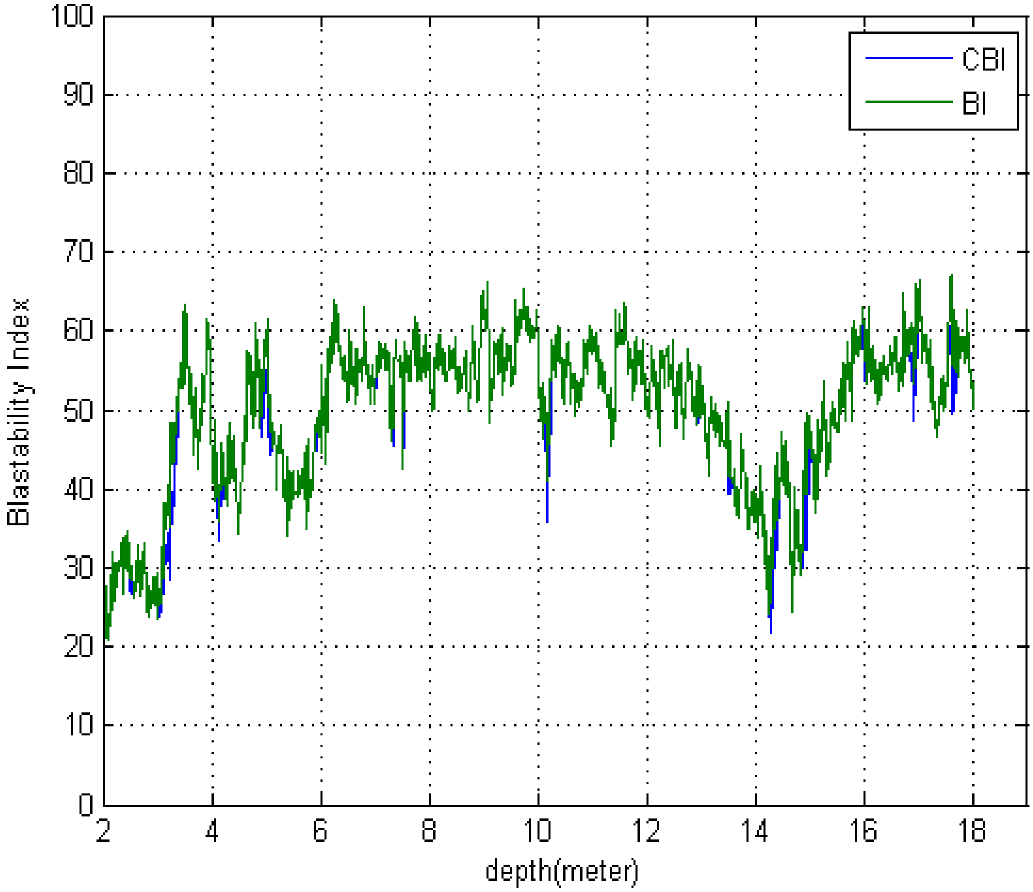

CBI
BI
Blastability Index
depth(meter)
100
90
80
70
60
50
40
30
20
10
0
2
4
6
8
10
12
14
16
18

Hole22

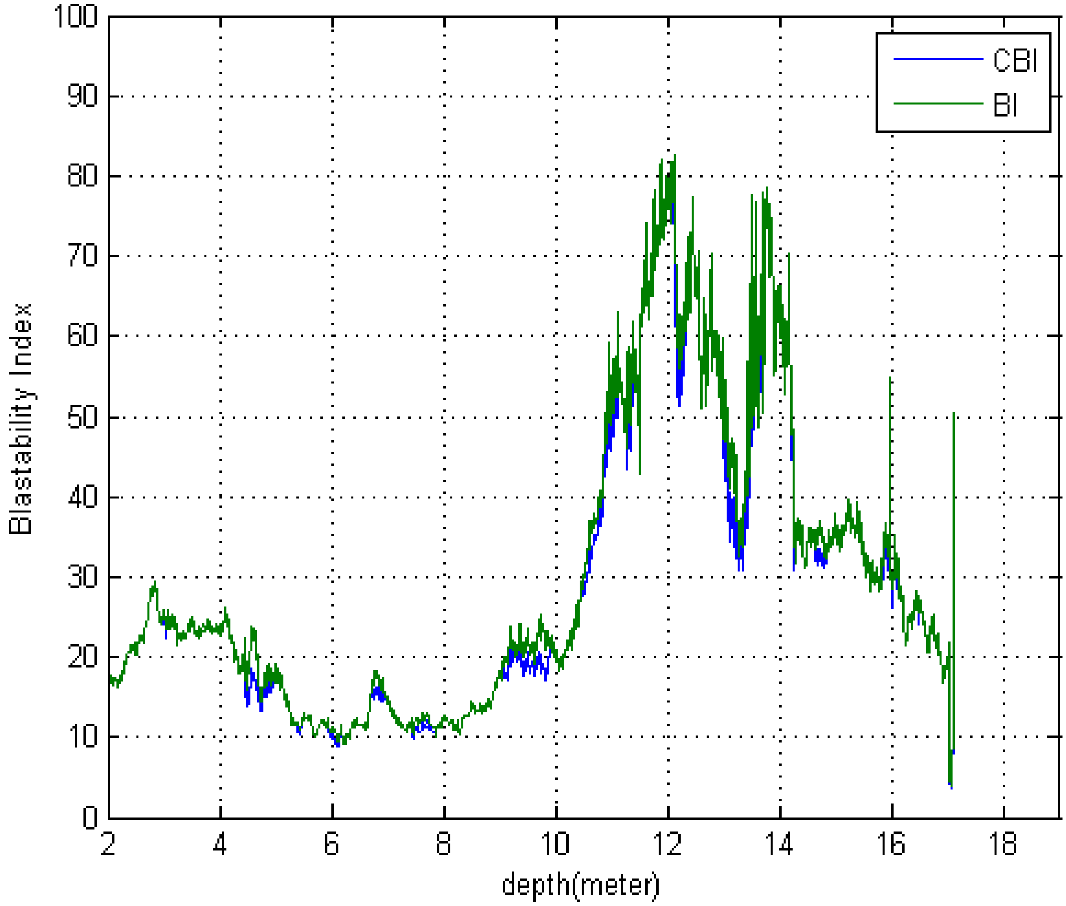

100
90
80
70
60
50
40
30
20
10
0
2
4
6
8
10
12
14
16
18
Blastability Index
depth(meter)
CBI
BI

Hole30

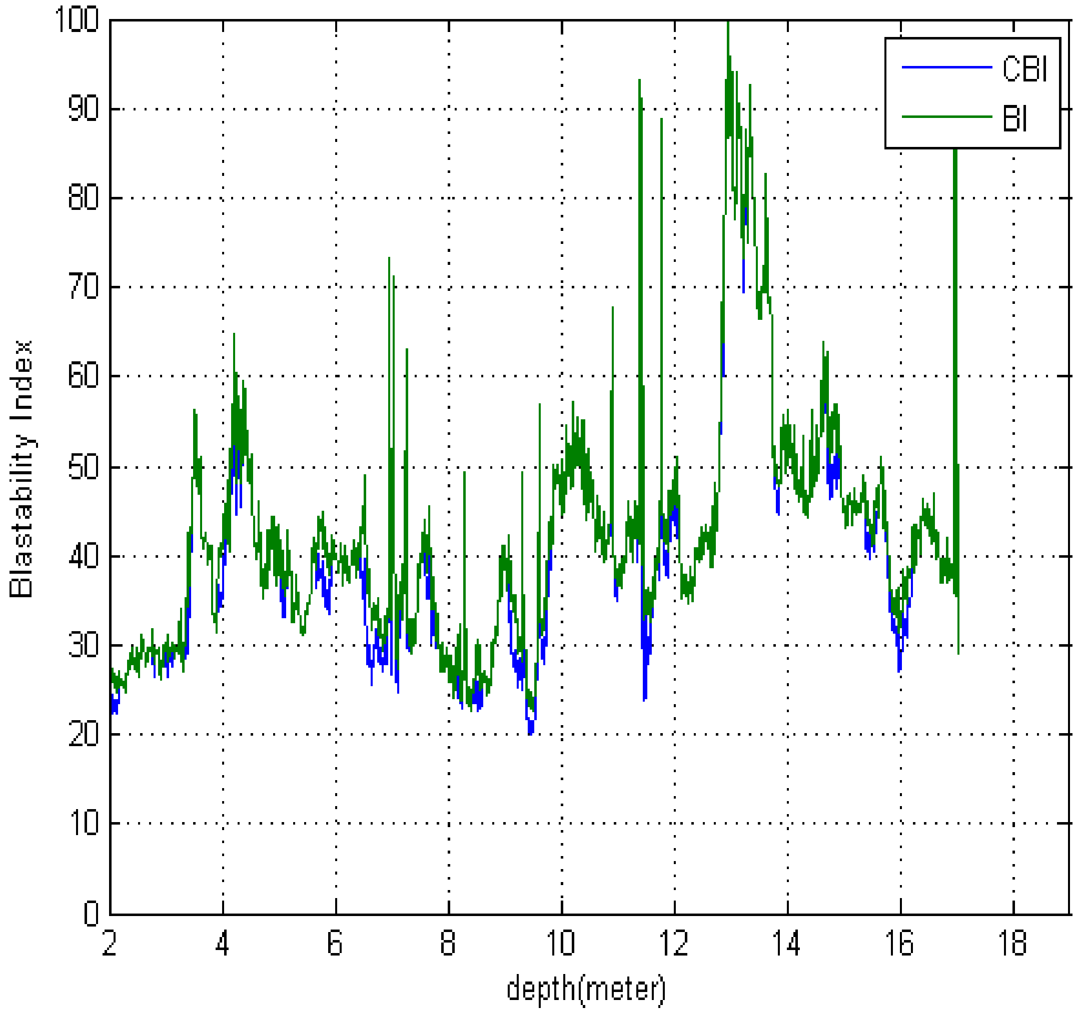

100
90
80
70
60
50
40
30
20
10
0
2
4
6
8
10
12
14
16
18
Blastability Index
depth(meter)
CBI
BI

Hole31

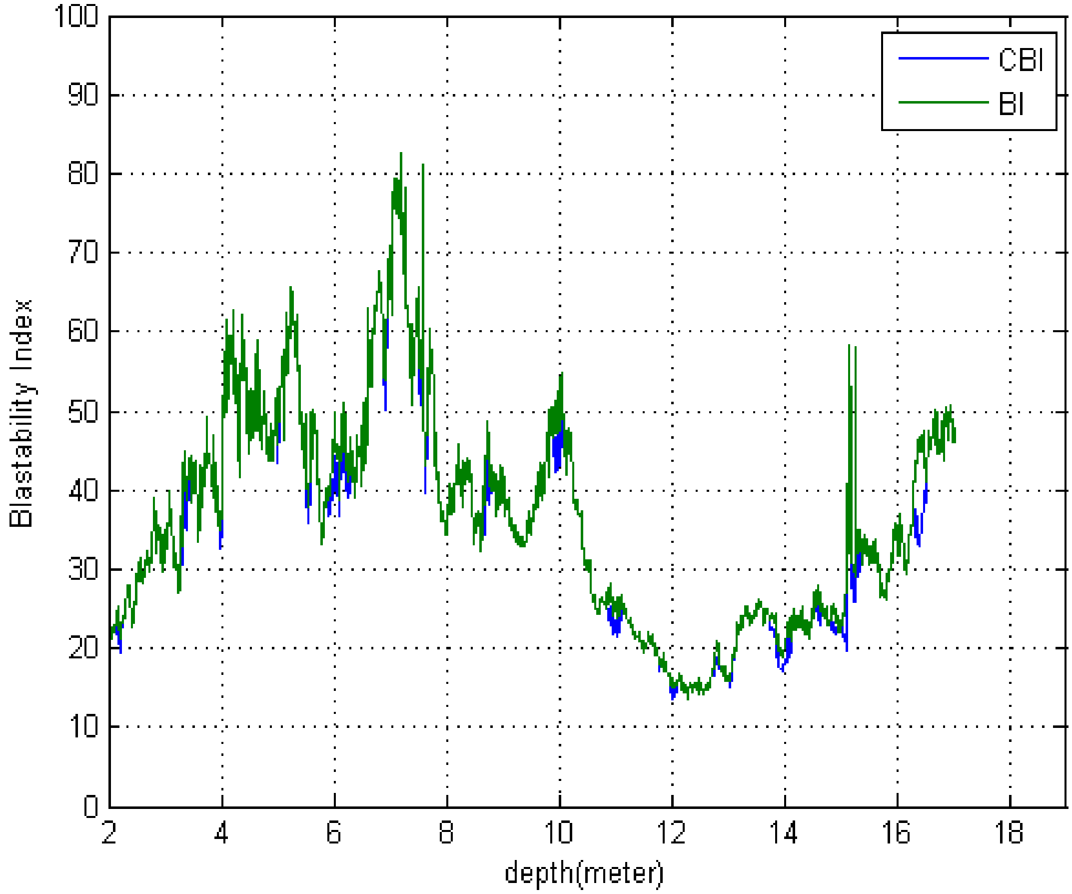

Hole32

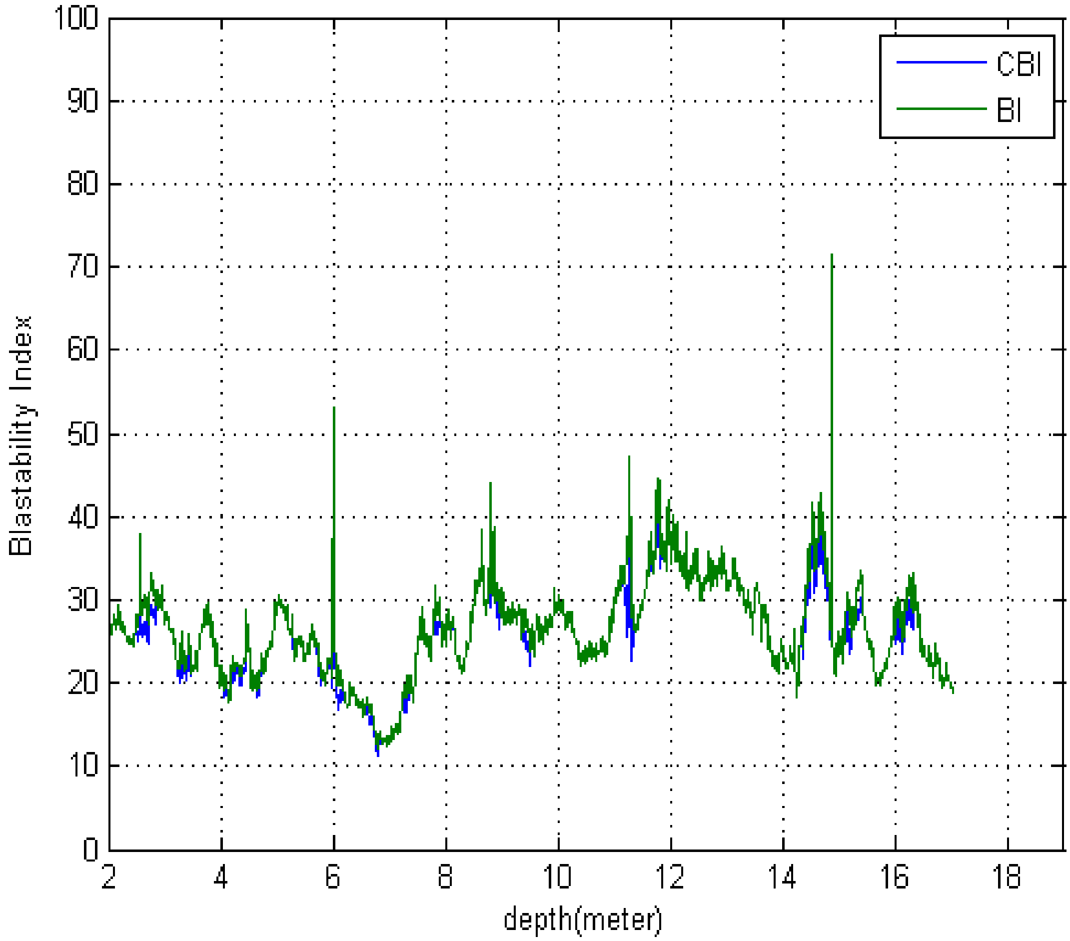

CBI
BI
Blastability Index
depth(meter)
100
90
80
70
60
50
40
30
20
10
0
2
4
6
8
10
12
14
16
18

Hole44

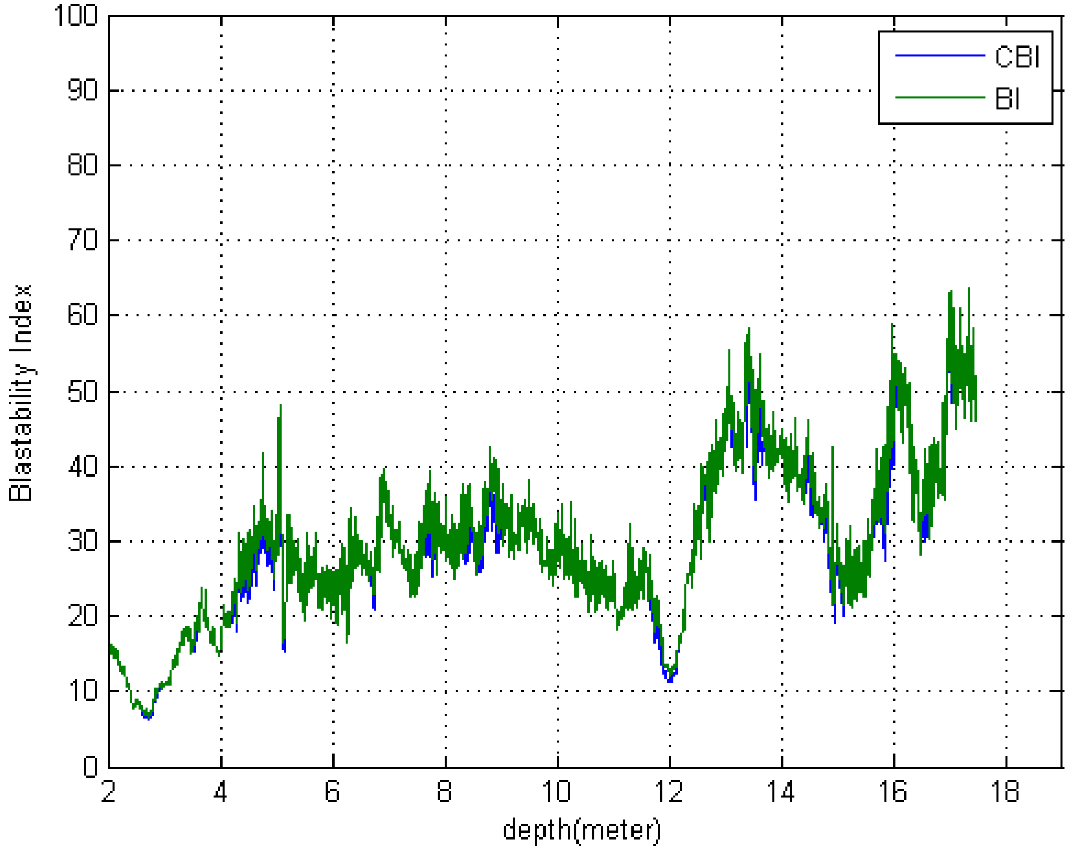

100
90
80
70
60
50
40
30
20
10
0
2
4
6
8
10
12
14
16
18
Blastability Index
depth(meter)
CBI
BI

Appendix D- Open Fractures Dip Angles/FRF

Hole18

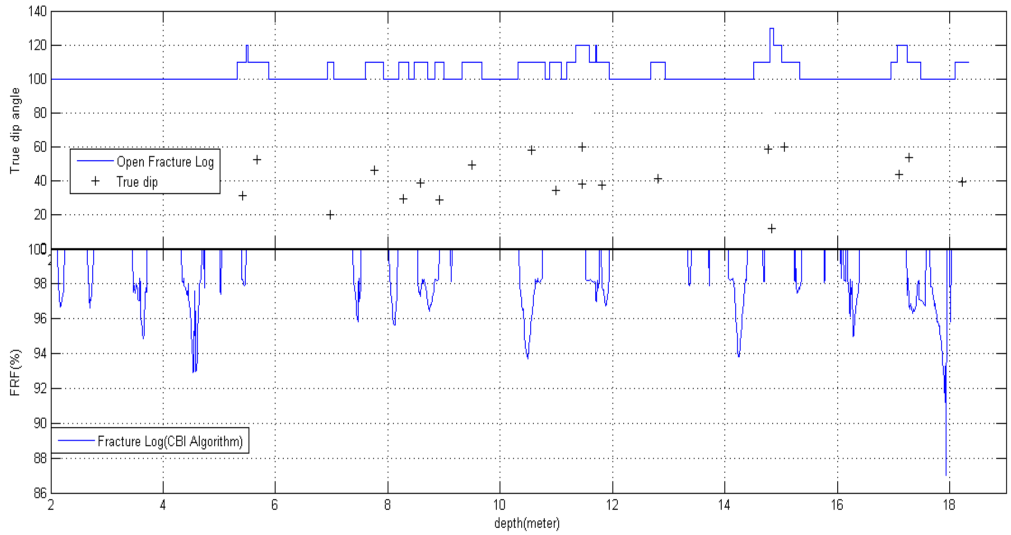

Hole22

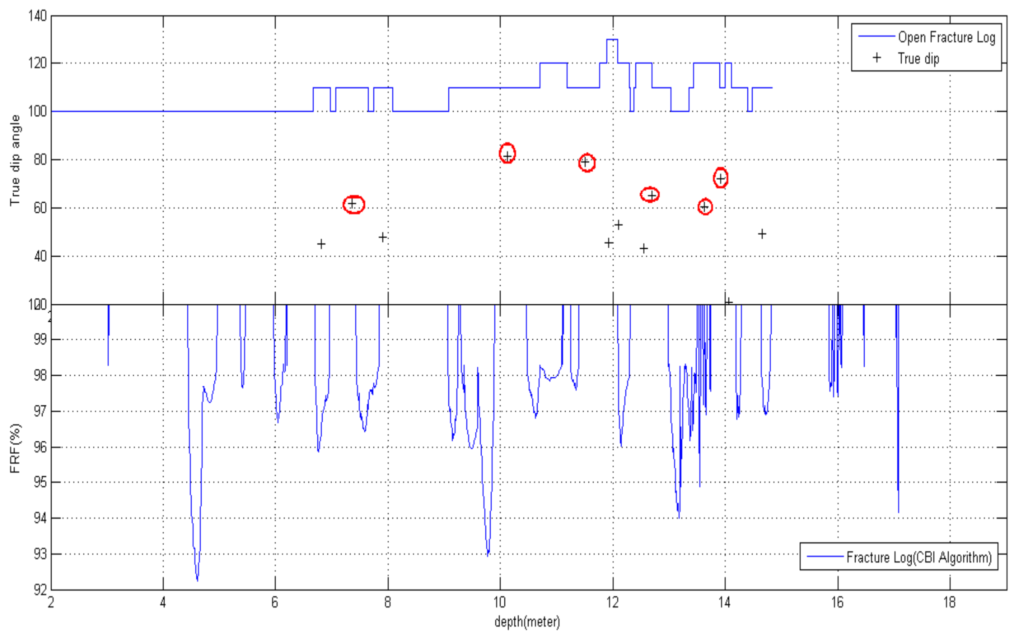

Hole30

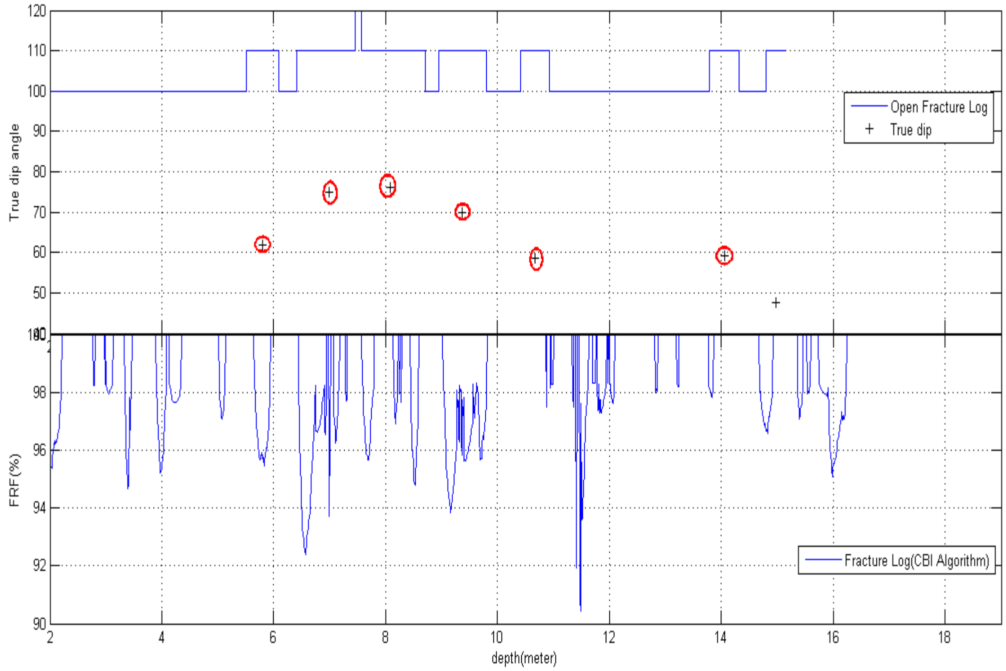

Hole31

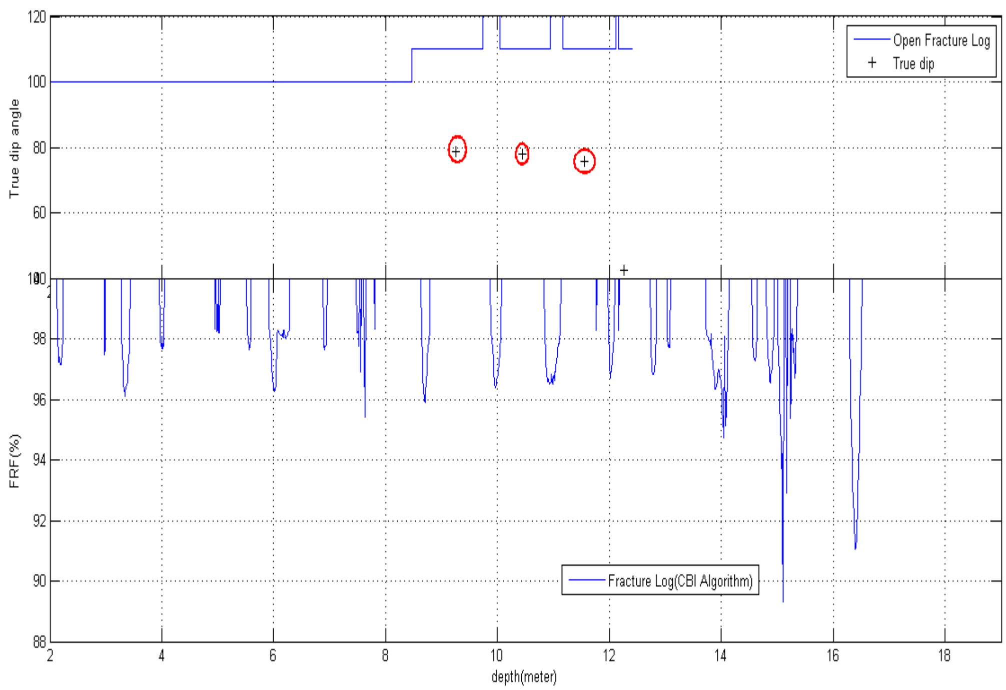

Hole44

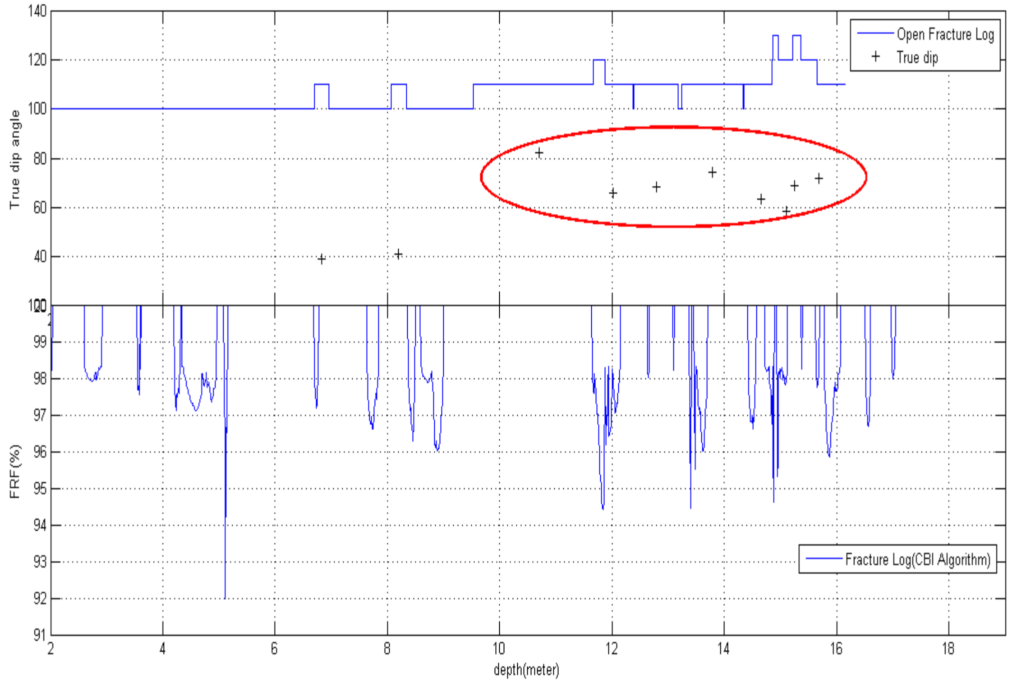

Open Fracture Log
True dip
True dip angle
FRF(%)
Fracture Log(CBI Algorithm)
depth(meter)

Appendix E- Partially Open Fractures Dip Angles/FRF

Hole13

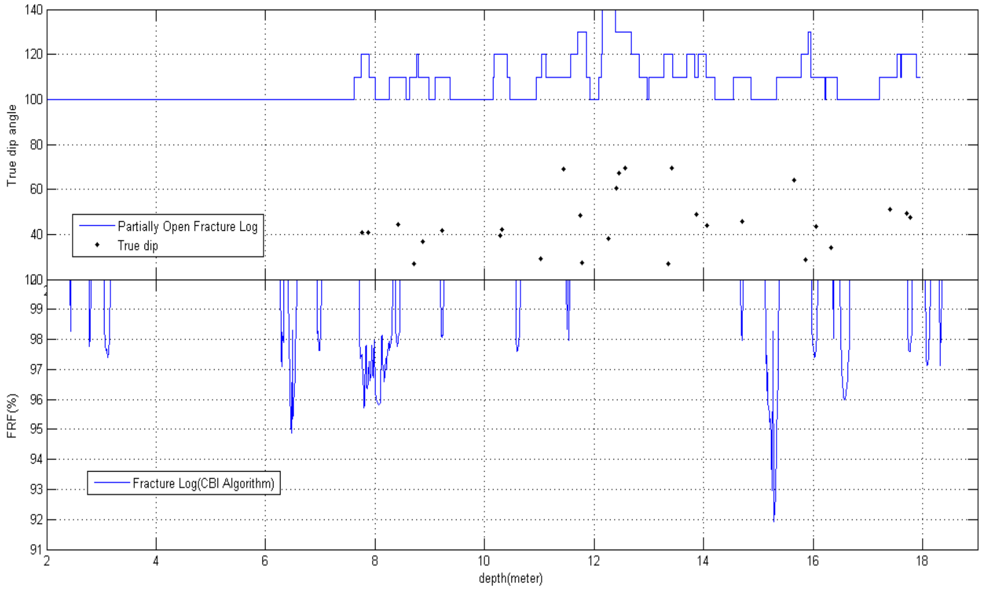

Hole18

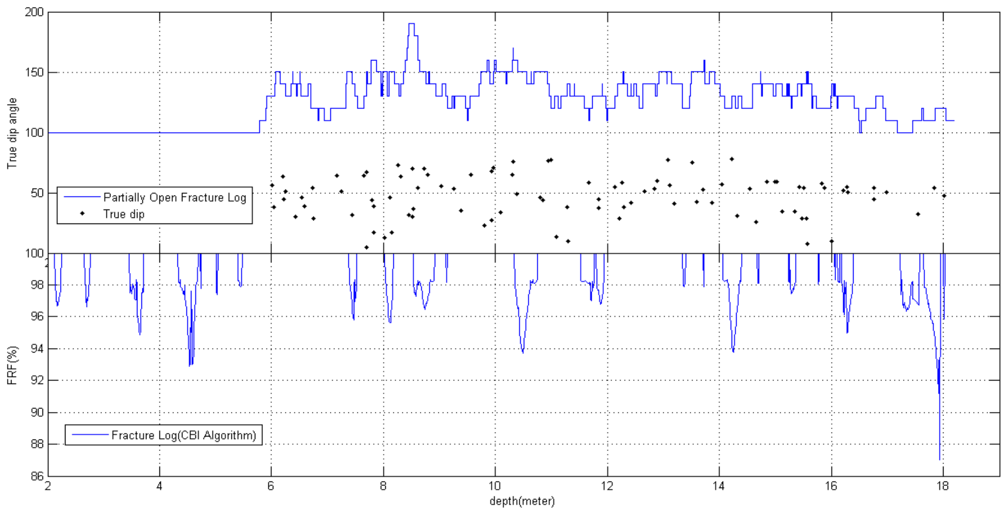

Hole28

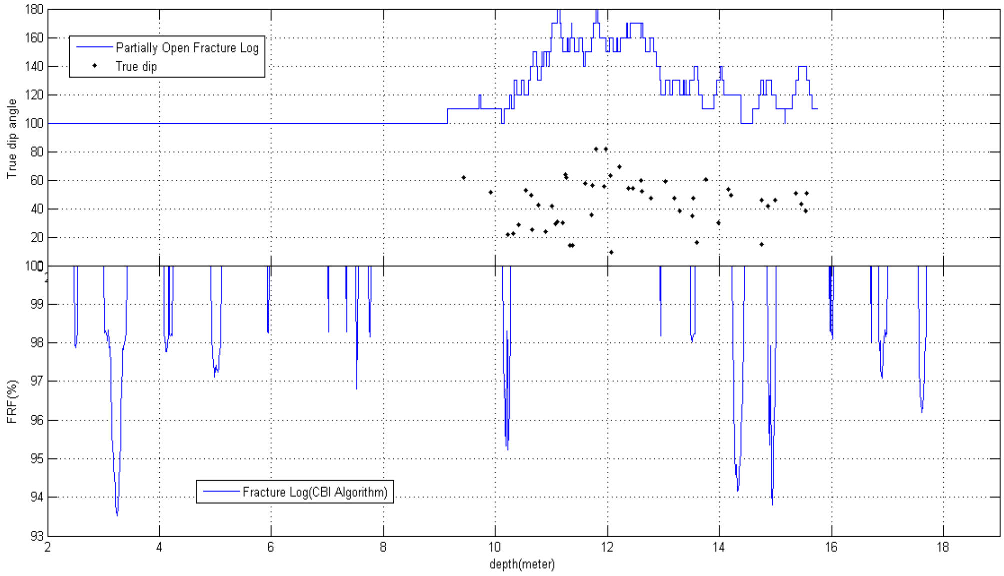

Hole22

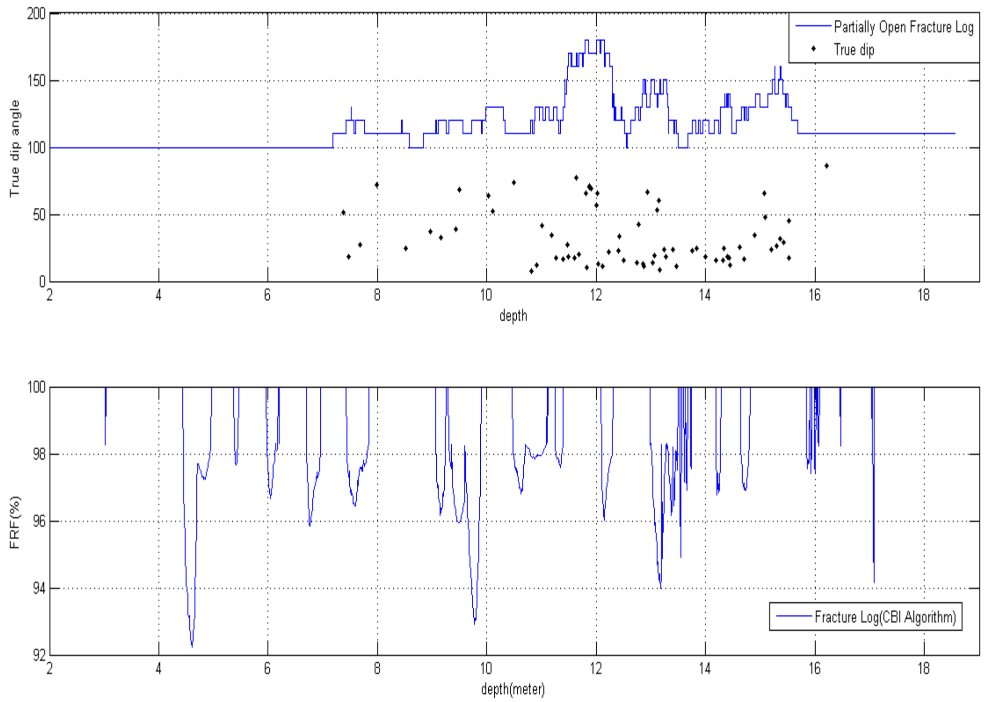

Hole30

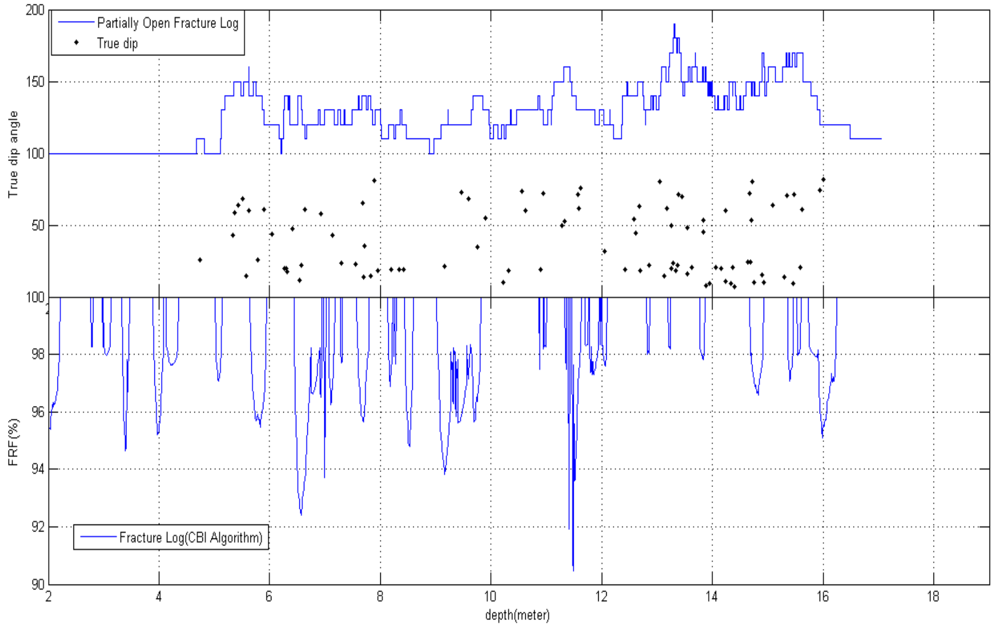

Hole31

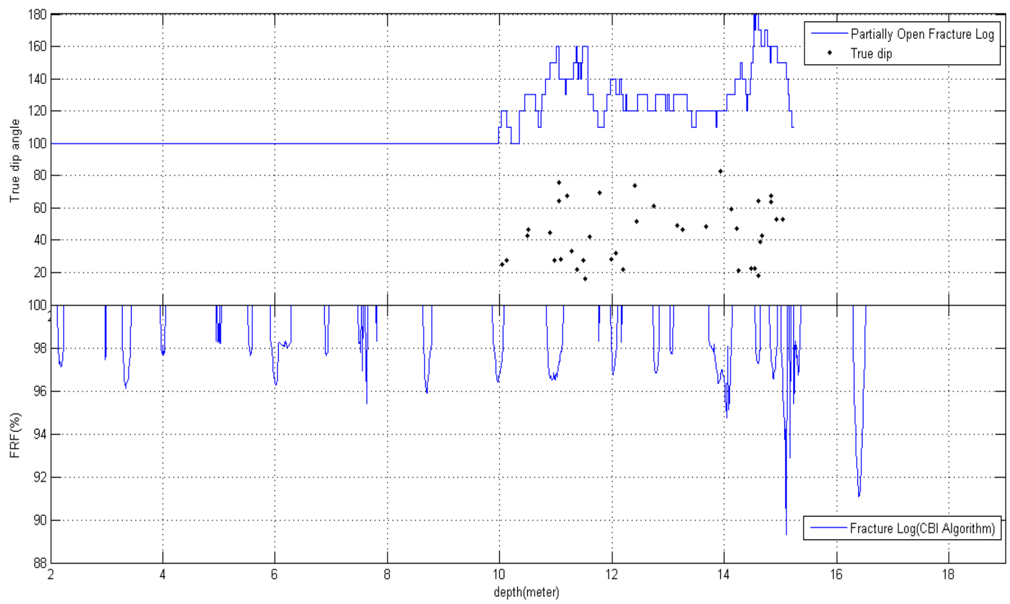

Hole32

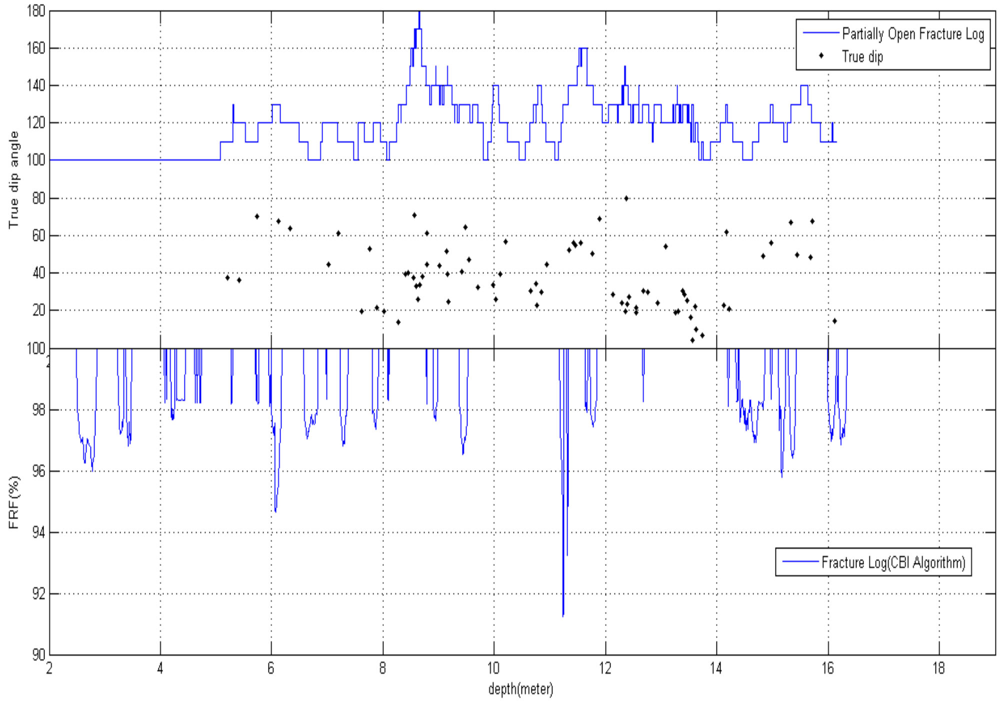

Hole44

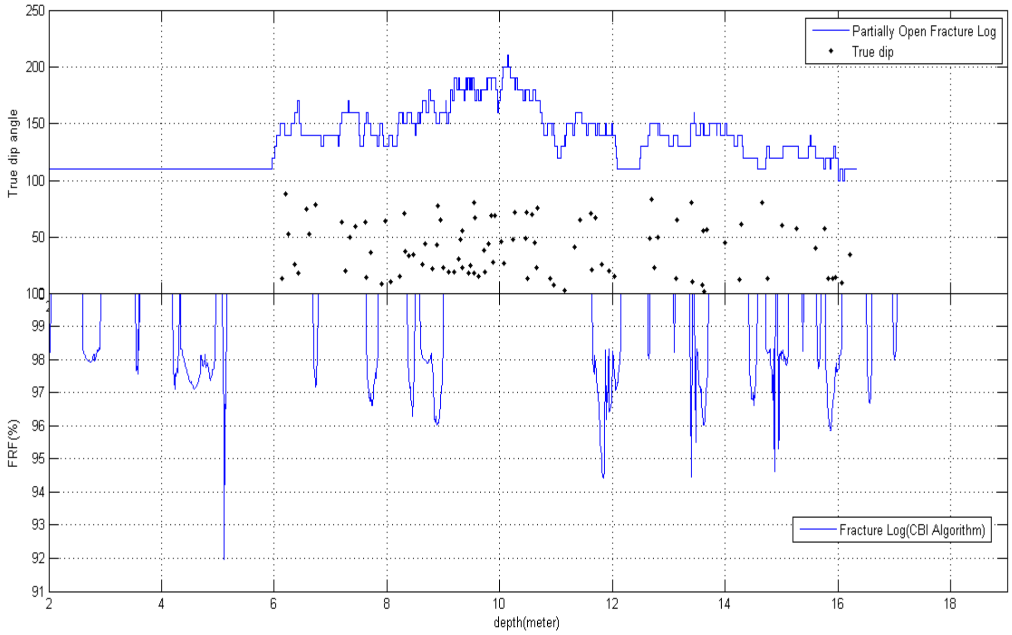

Appendix F- Reference Signals Perturbations for Drill 11

Hole22

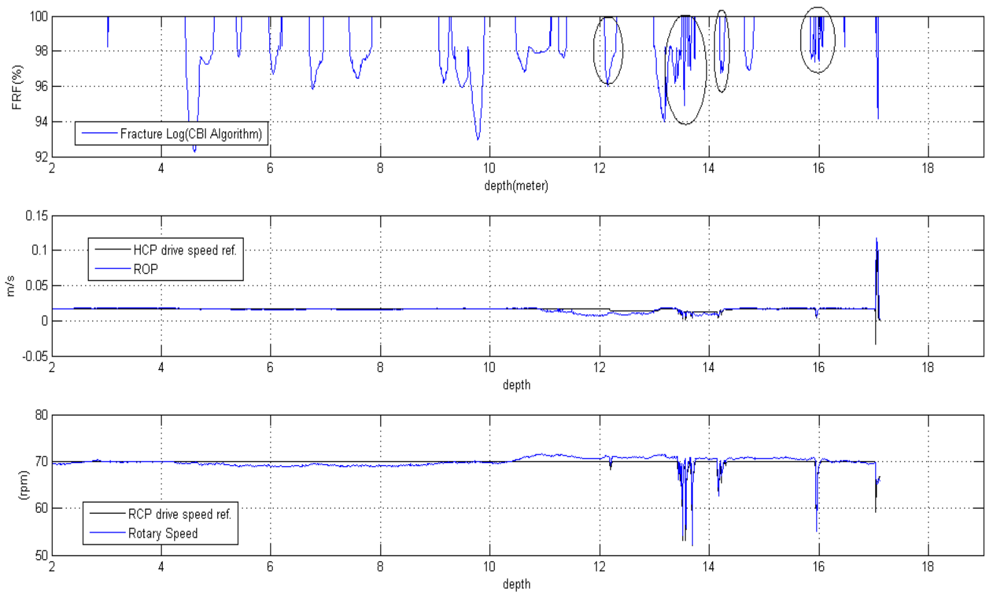

Hole30

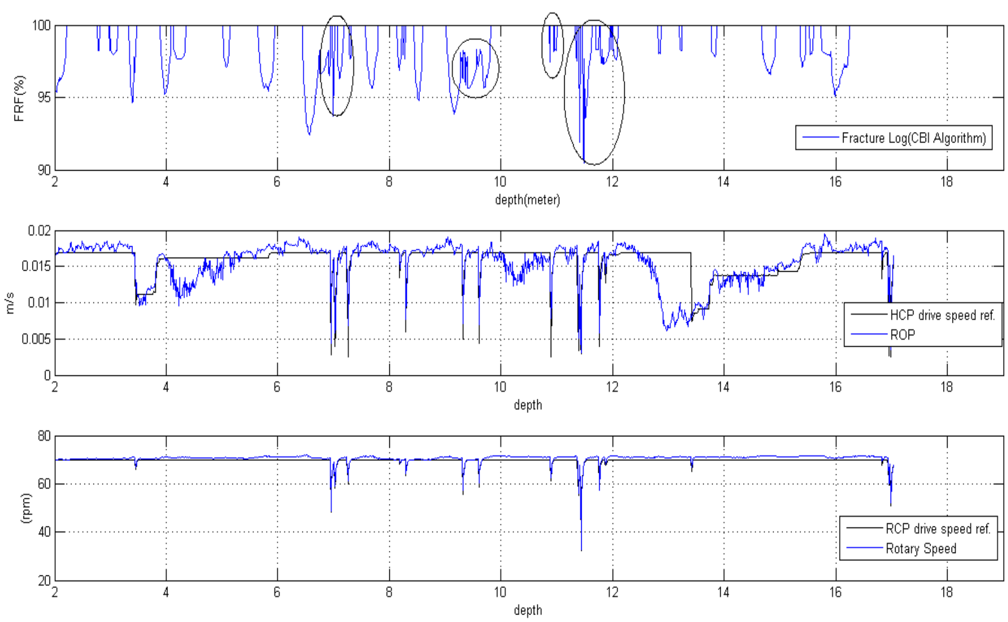

Hole31

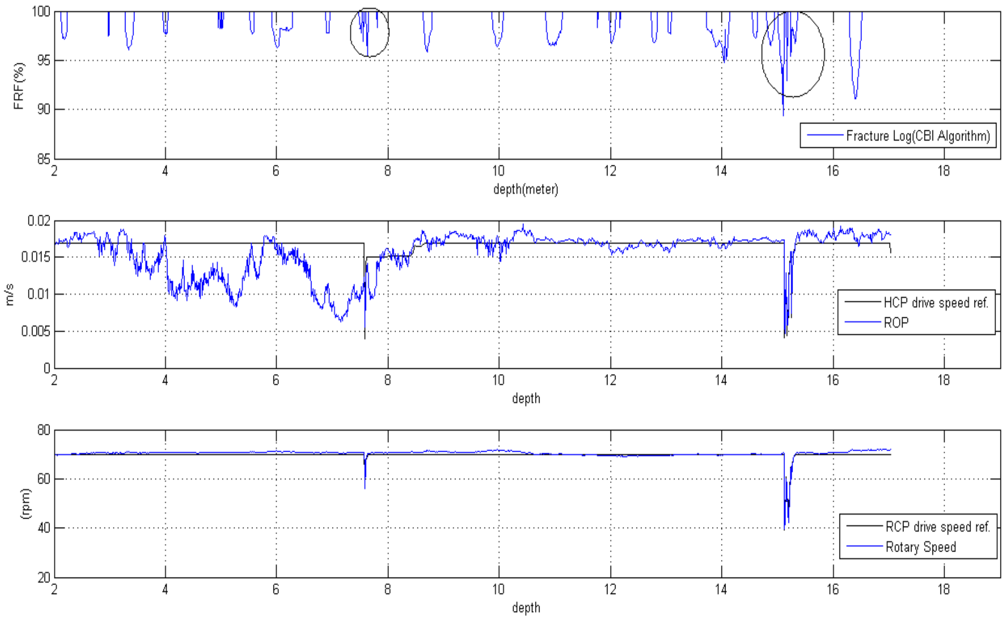

Hole44